Experimental Detection of Dark Matter

Astro Physics Meeting, Pune
25 February, 2018

Satyaki Bhattacharya
Saha Institute of Nuclear Physics
Kolkata, India

Avenues of Dark Matter Searches

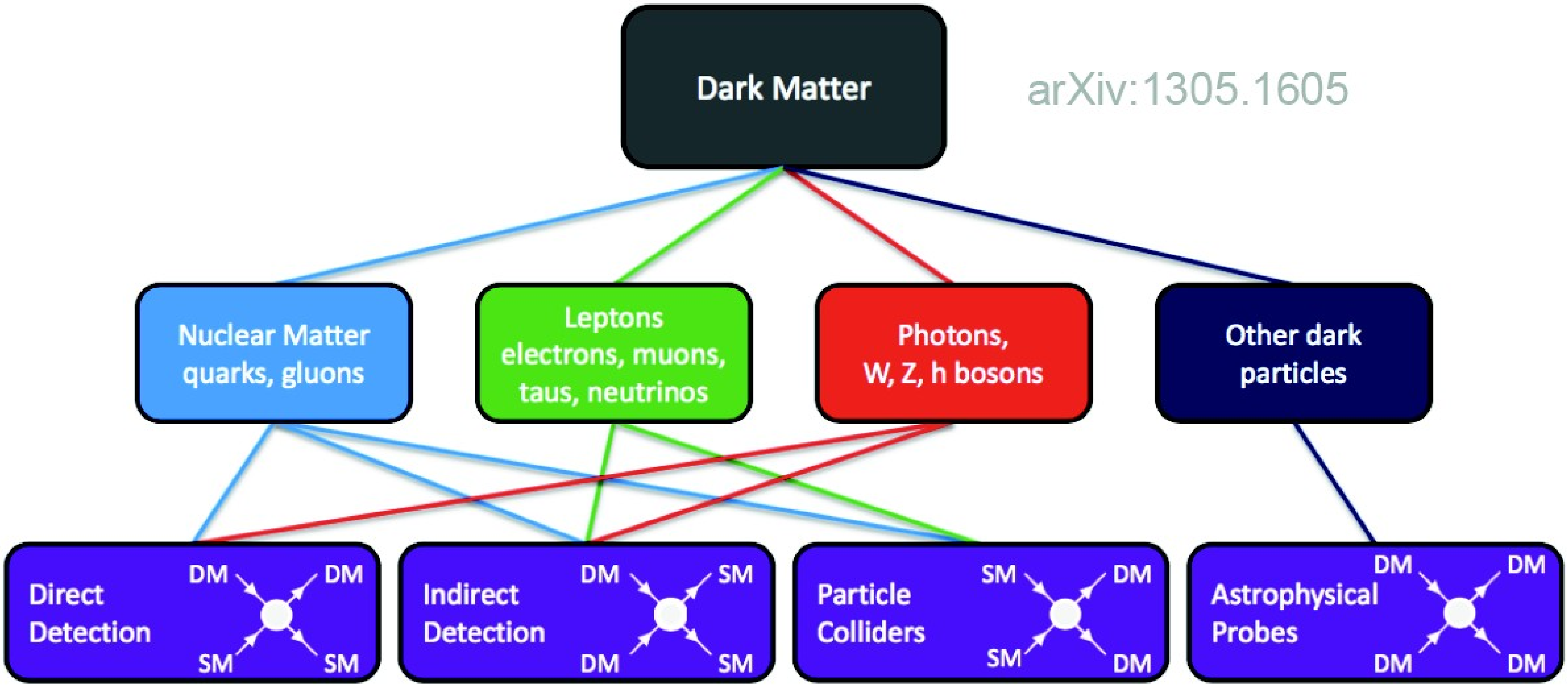

Direct Detection (DD)

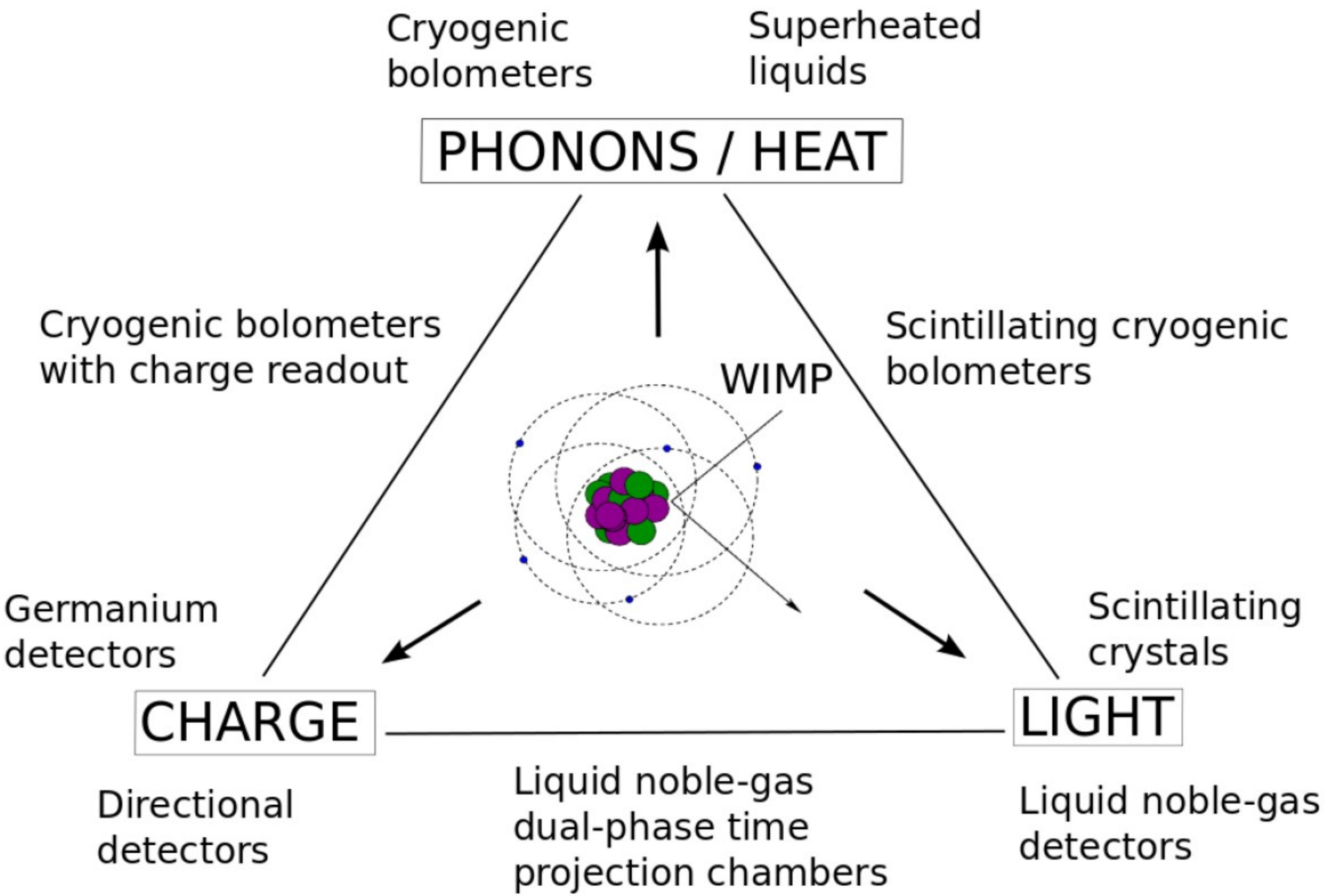

Backgrounds

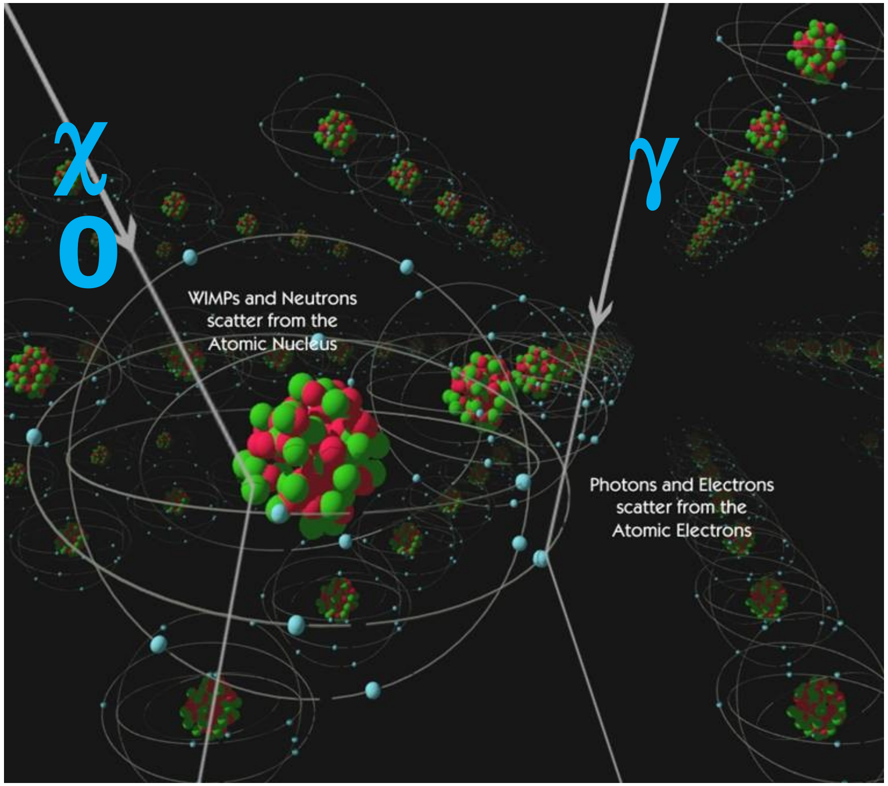

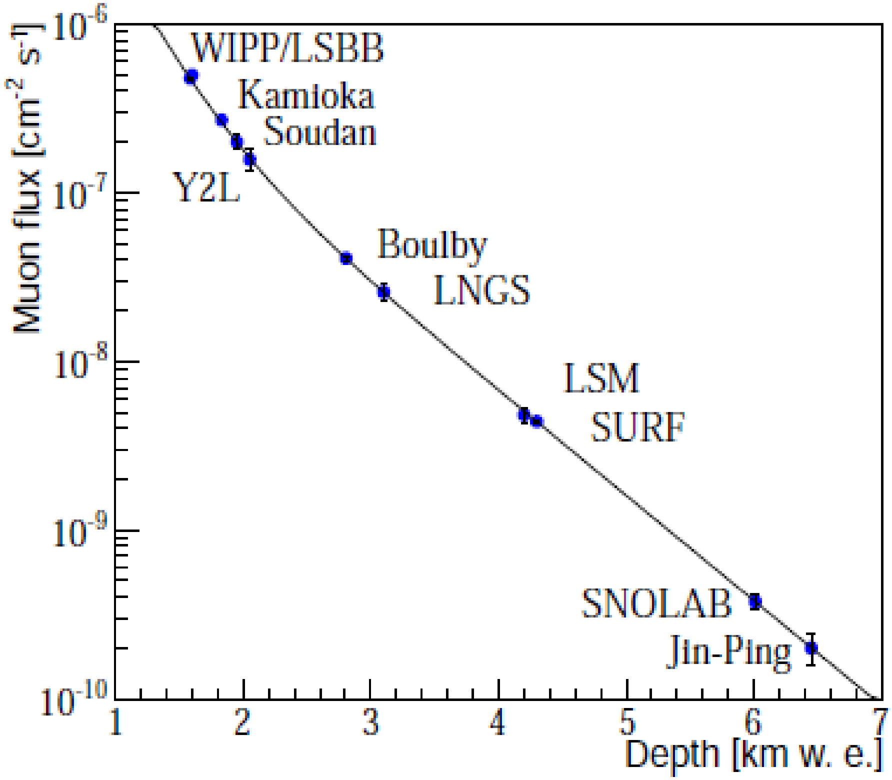

- Cosmogenic, radiogenic, intrinsic
- Discriminate between electron recoil (ER) and nuclear recoil (NR)

Scintillators at room temperature

- NaI(Tl), CsI(Tl)
- Scintillation light in suitable range for photosensors (415,580 nm for NaI, CsI)
- Large stopping power (3.5, 4.5 gm/cc density)
- Resolution 8% at 1 MeV
- No particle discrimination possible
- Aim for ultra radio pure crystal

DAMA@LGNS

- Ultra radio pure NaI(Tl)
- DAMA + DAMA/LIBRA collected 1.33 ton.Year
- Annual modulated rate in the range (2-6) KeVee
- Maximum is compatible with June 2nd, within 2σ
- 9.3σ significance over 14 annual cycles

DAMA: annual variation

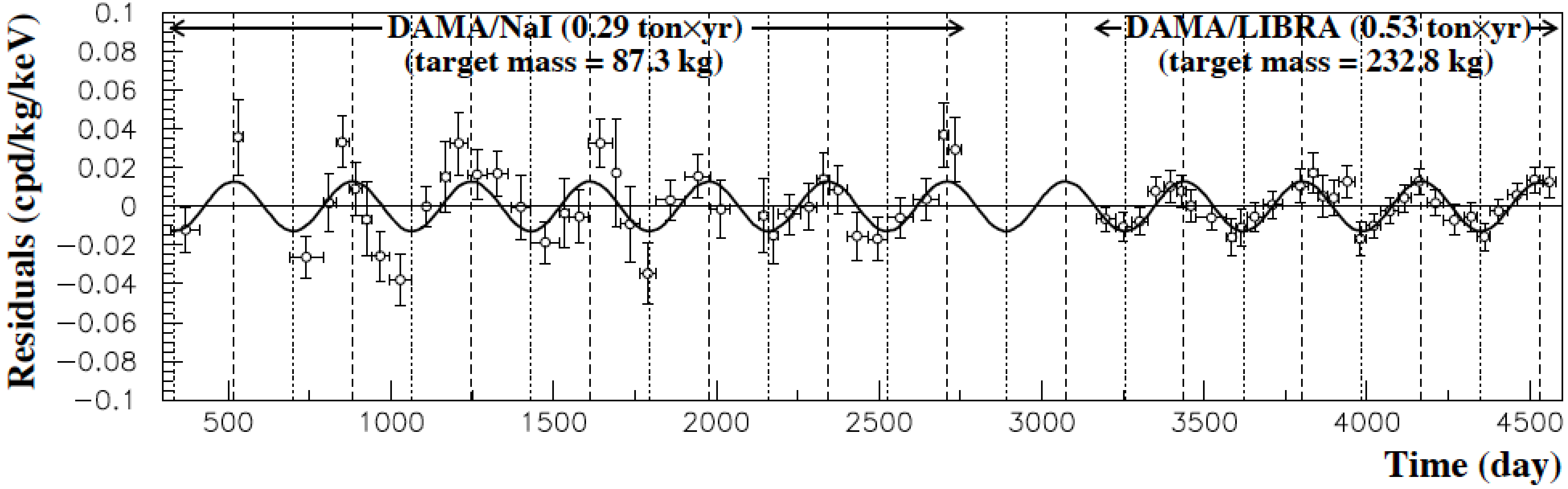

Cryogenic Bolometers

- Operating at milli Kelvin (mK)
- Very low threshold, excellent resolution
- Phonon (+ scintillation/charge)
- Can discriminate electron and nuclear recoils
- Applied electric field for charge can enhance phonon signal generated by drifting electron-hole pairs (Neganov Luke phonons)

Cryogenic Bolometers

- Weakly coupled to thermal bath at 10 – 100 mK
- $\Delta T = (E/C(T))*\exp(t/\tau)$ is measured
- Small heat capacity C(T) at low temp (T^3 dependence) gives large ΔT
- Ge shows a rise of 1 μK at 20mK for few keV recoil
- Read out with transition edge sensors (TES) or neutron transition doped (NTD) Ge sensors

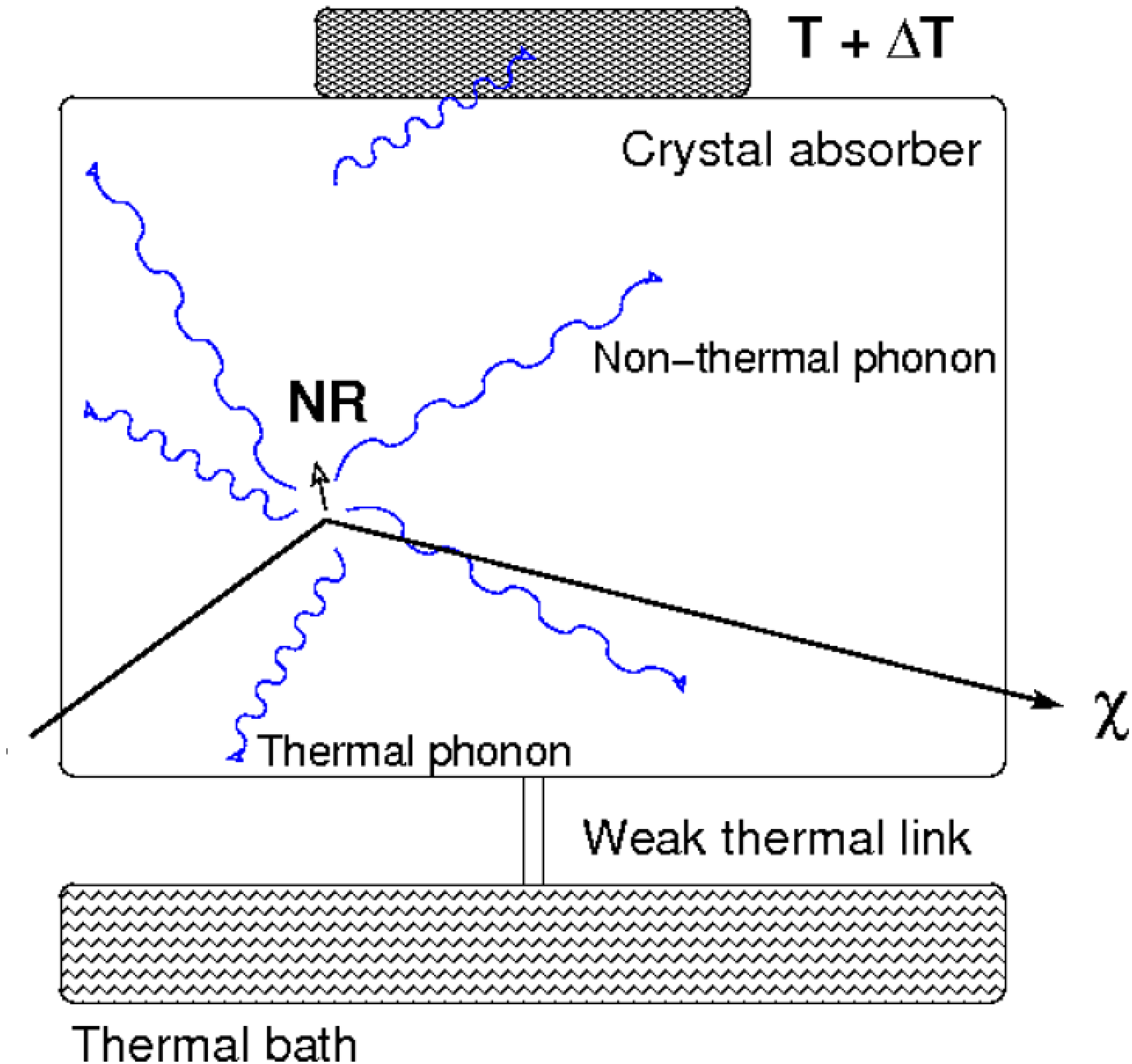
T + ΔT
Crystal absorber
Non−thermal phonon
NR
χ
Thermal phonon
Weak thermal link
Thermal bath

CDMS: Cryogenic Dark Matter Search

- CDMS, CDMS II used Ge, Si bolometers
  - Upto 11 Ge detectors (230 gms) and 9 Si detectors (100 gms)
- Z sensitive Ionization phonon radiation detectors (ZIP)
- Main background: misidentified electron recoil from surface
  - Controlled by pulse shape discrimination
  - 1 in 10^6 mis-id rate

CDMS results

- $\sigma < 3.8 \times 10^{-44}$ cm^2 for $M_\chi = 70$ GeVfrom combined CDMS II
- Best threshold (3-14) keV gives:
- σ of 10^{-41} cm^2 at $M_\chi = 7$ GeV
- Si with 23.4 kg.d, E_{recoil} in (7-100) keV_{nr}, excess was observed at σ of 1.9×10^{-41} cm^2 for $M_\chi = 8.6$ GeV (in the range of DAMA, CoGent)
- Later results do not confirm the excess
- No evidence of annual modulation (contradicts CoGent)

SuperCDMS

- Successor of CDMS-II
- Interleaved ZIP – interleaved structure of phonon and ionization electrodes
- 15 Ge crystals with 0.6kg each
- Sensitive to NR in (1.6 – 10)keVnr
- Target mass range M_χ < 30 GeV
- Recorded exposure 577 kg.d
- Limit: $\sigma < 1.2 \times 10^{-42}$ cm^2 for M_χ = 8 GeV

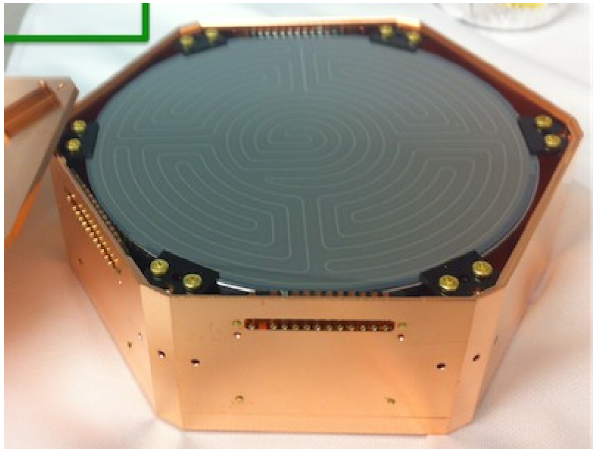

CDMSlite

- Low Ionization Threshold
- Single crystal exploiting Neganov-Luke effect
- Improved threshold, resolution
- No discrimination between NR and ER
- Best limits in the low WIMP mass region from superCDMS, CDMSlite

EDELWEISS@LSN

- Measures thermalised phonons with NTDs
- Interleaved structure for charge readout
- EDELWEISS-III exposure 582 kg.d (24 Ge detector 0.8 kg each)
- Search range (2.5 – 20) keVnr

Plans to improve detector to reach lower mass

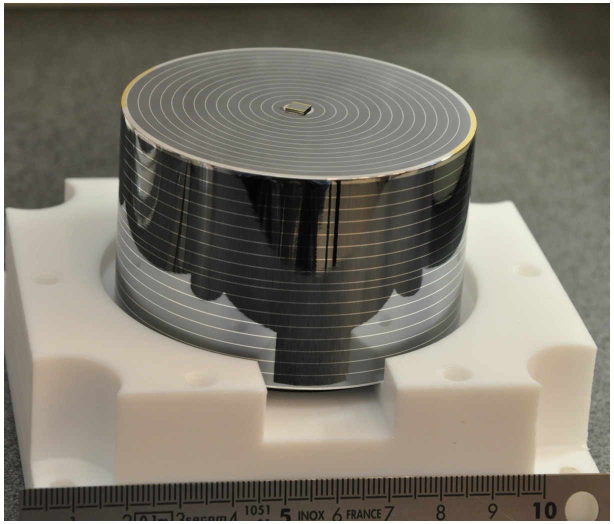

EDELWEISS-III

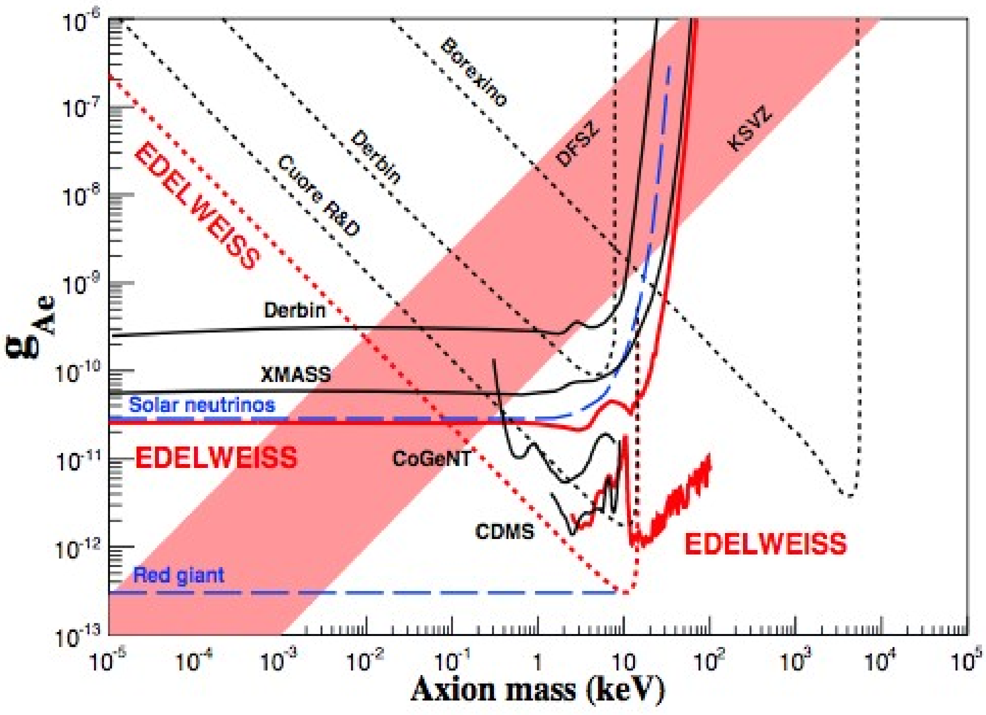

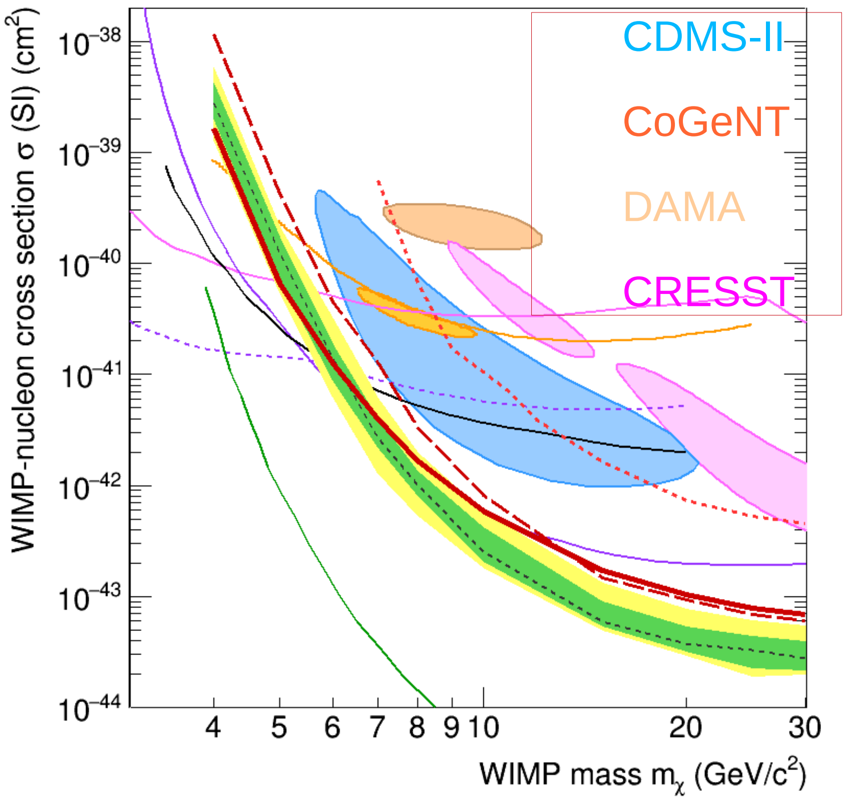

10^{-40} cm^2 reached at 5 GeV

7 times Improvement with likelihood analysis at 4 GeV

CRESST-II @ Gran Sasso(LNGS)

- CaWO4 with TES readout
- Phonon + scintillation (particle discrimination)
- Exposure 730 kg.d with 8 detectors
- Energy thresholds in range (10.2 – 19.0) keVnr
- Observes excess at
  - σ 3.7 x 10^{-41} cm^2 , M_χ = 11.6 GeV (4.2 sigma)
  - σ 1.6 x 10^{-42} cm^2 , M_χ = 25.3 GeV (4.7 sigma)

CRESST-II

- Main background is collision of Pb nucleus with crystal(from α decay of ^{210}Po, α is undetected)
- With an improved detector – higher alpha detection and phonon, photon efficiency was achieved.
  - 600 eVnr threshold!
- Signal could not be confirmed with 29.35 kg.d
- Limit: $\sigma < 8 \times 10^{-40}$ cm^2 for $M_\chi = 3$ GeV
- With lowest threshold of 307 eV, 52 kg.d first bolometer to be sensitive in sub-GeV range at $\sigma \sim 10^{-37}$ cm^2 !

EURECA

- A joint effort of EDELWEISS, CRESST, ROSEBUD
- EURECA aims to operate 1000 kg detectors
- Scintillators and Ge
- Would be located in LSM
- Sensitivity goal 3×10^{-46} cm^2

Noble Gas Detectors

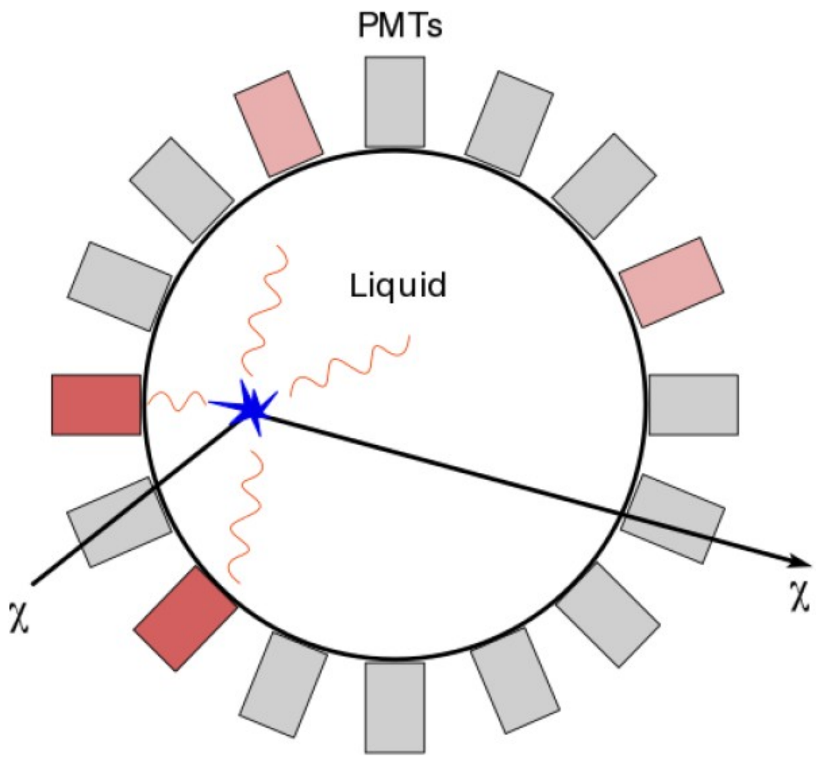

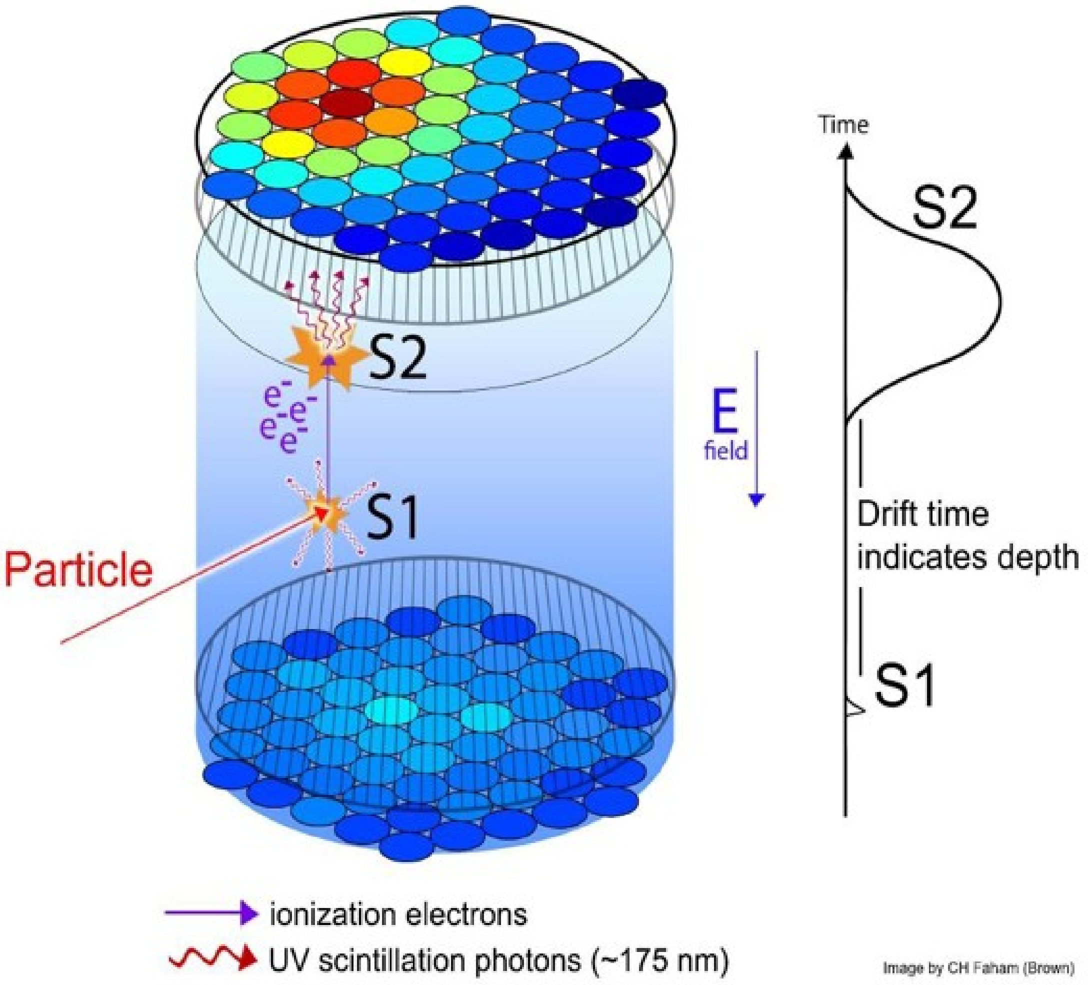

Noble Gas Detectors

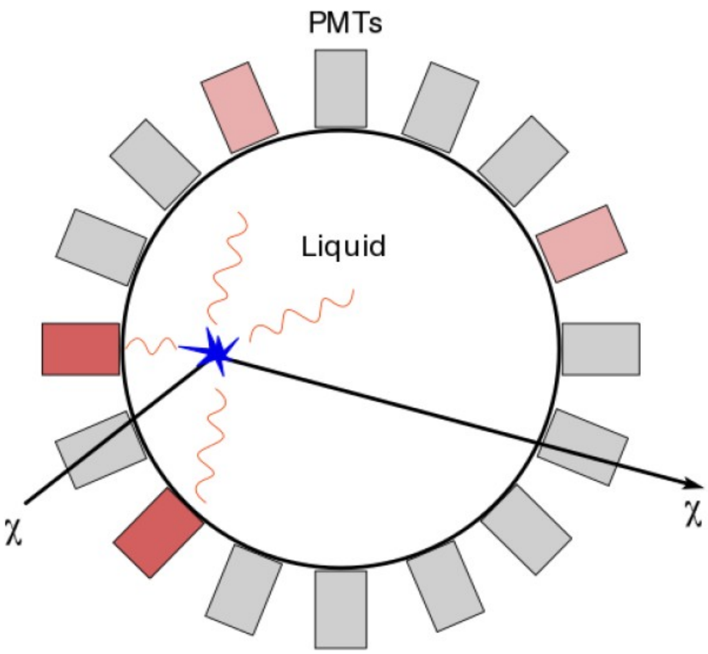

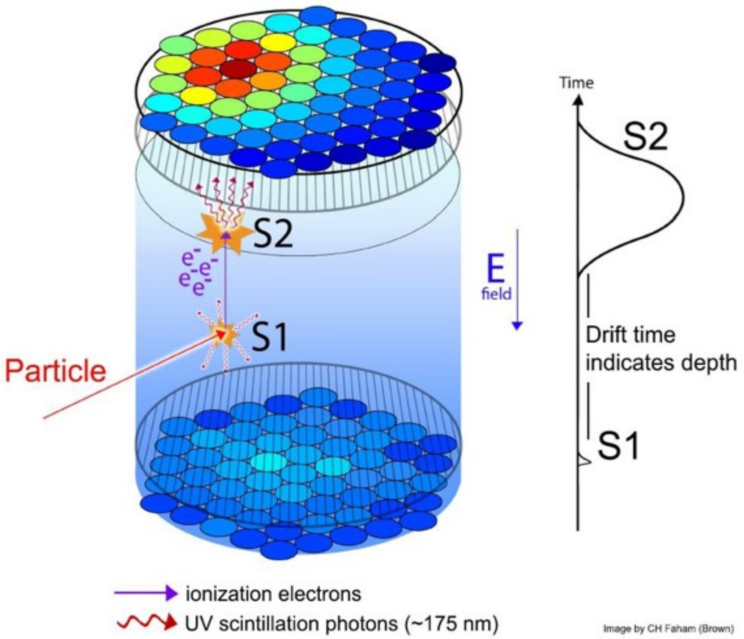

- 4π coverage
- Position resolution ~ cm

- Z from time of S1-S2, X-Y from hit pattern
- Position resolution ~ mm

Noble Gas Detectors

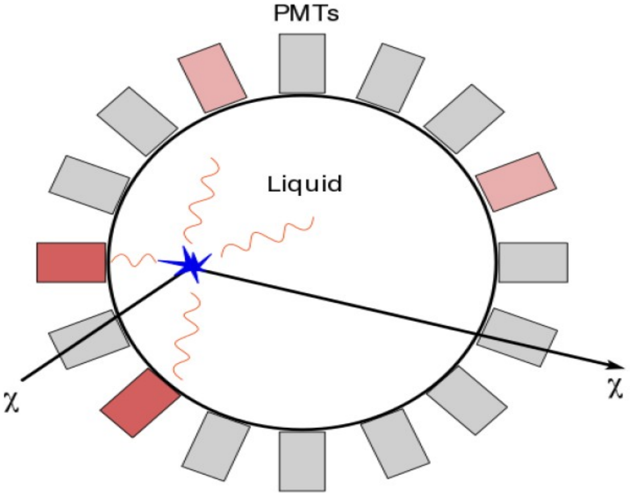

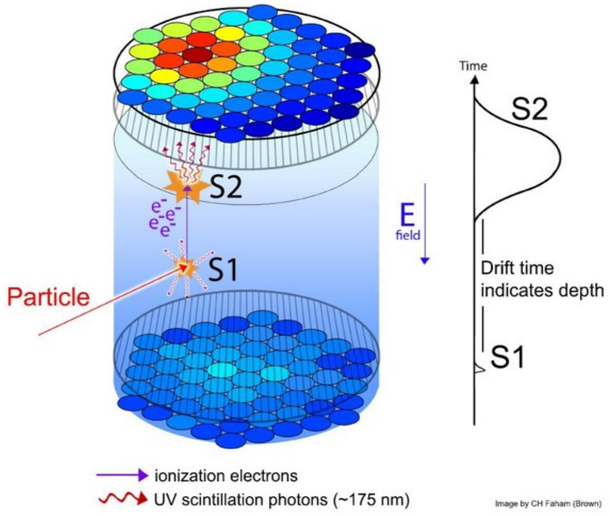

- DEAP,CLEAN, XMASS with LAr

- DarkSide with LAr
- ZEPELIN, XENON, Lux, LZ with Xe

Noble gas detectors

- Main background : gamma/electron
- The detectors can separate between NR and ER
- Ar has large separation power due to different ratio of singlet and triplet states of excitation for different particles
- Xe sensitive to SD scattering due to about 50% ^{129}Xe and ^{131}Xe isotopes

Xenon @ LNGS

- XENON, ZEPLIN showed the effectiveness of LXe TPC
- 2009 – 2016 XENON100 (60 kg TPC mass)
- Combined exposure 1.75 X 10^4 kg.d
- Limit: $\sigma < 1.1 \times 10^{-45}$ cm^2 for $M_\chi = 50$ GeV
  - Also performed Axion search
  - **excludes DAMA results @ 5.7 σ**
- From 2016 XENON1T taking data
- XENONnT: Upgrade from 3T to 7T in future

Xenon @ LNGS

- XENON, ZEPLIN showed the effectiveness of LXe TPC
- 2009 – 2016 XENON100 (60 kg TPC mass)
- Combined exposure 1.75 X 10^4 kg.d
- Limit: $\sigma < 1.1 \times 10^{-45}$ cm^2 for $M_\chi = 50$ GeV
  - Also performed Axion search
  - **excludes DAMA results @ 5.7 σ**
- From 2016 XENON1T taking data
- XENONnT: Upgrade from 3T to 7T in future

LUX @ Sanford

- 250 kg active mass
- Threshold of 1.1 keVnr
- Provides best limit

Limit: $\sigma < 1.1 \times 10^{-46}$ cm^2 for $M_\chi = 50$GeV, an order of magnitude below XENON

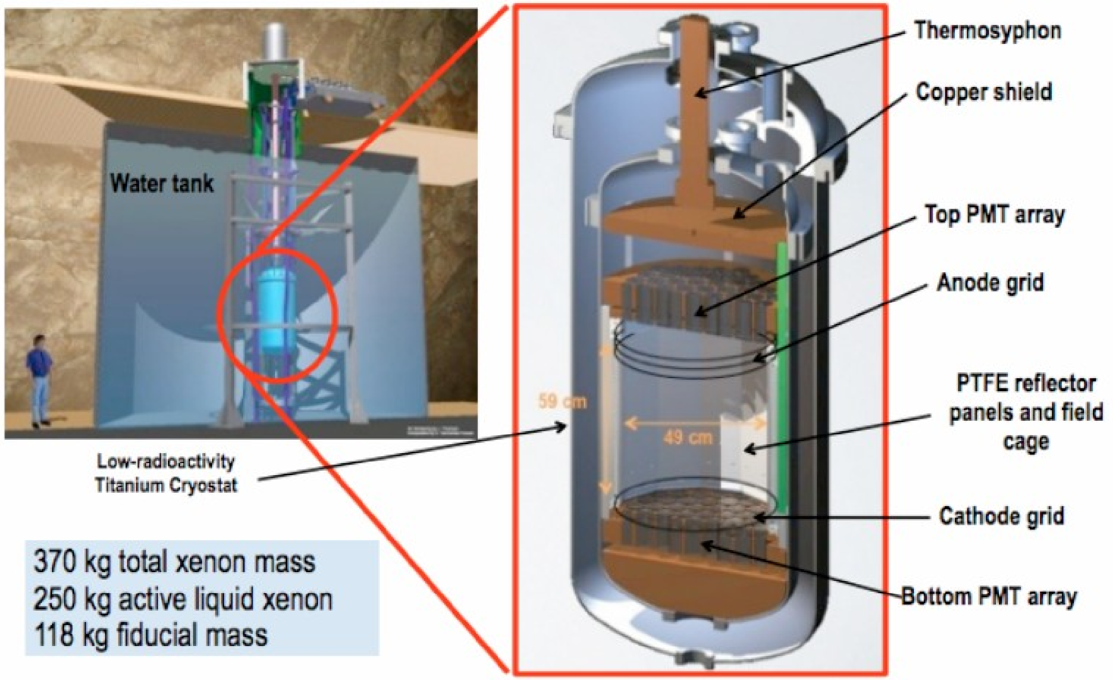

Superheated liquid detectors

- Bubble Chambers
  - COUPP
  - PICO (PICASSO + COUPP)
- Droplet Detectors
- Suspended droplets
  - PICASSO
  - SIMPLE
- Accoustic signals from mini explosions
- Free from gamma X-ray, beta backgrounds
- Alpha is the main background

PICO @ SNOLAB

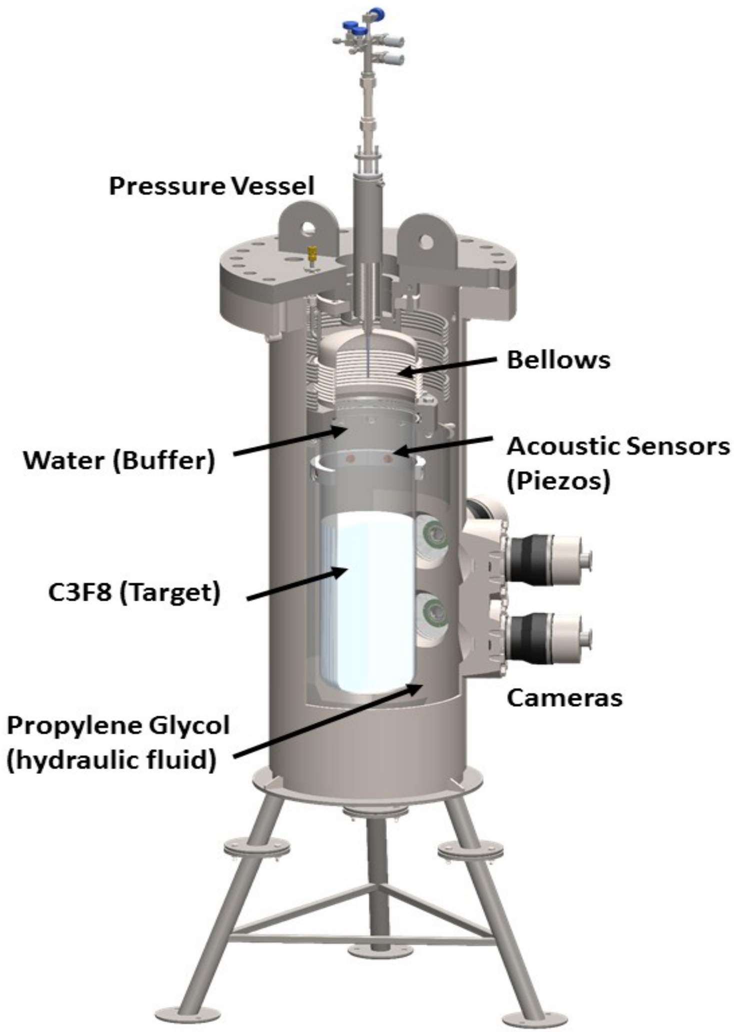

- C_3F_8 droplets of average size 200 micron
  - Accoustic signal read by Pizo crystals 2.5 MHz
- 3.3 keV threshold
- PICO 60 and PICO-2L
- Flourine – sensitive to SD proton coupling interaction
- Latest result from 52 kg detector with 1167 kg.d

PICO: spin dependent analysis

- Most stringent bound on SD proton-WIMP cross section

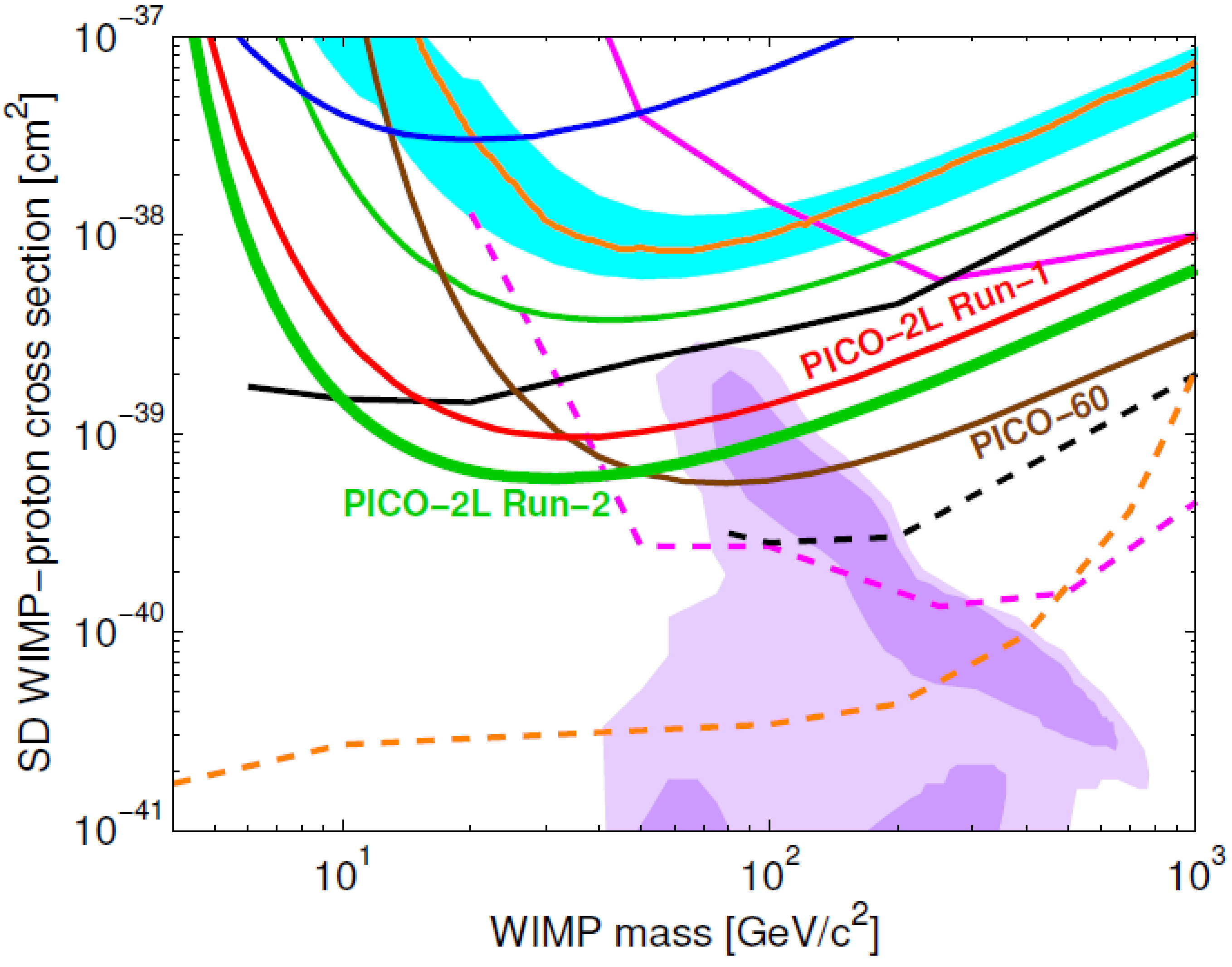

Evolution of Sensitivity

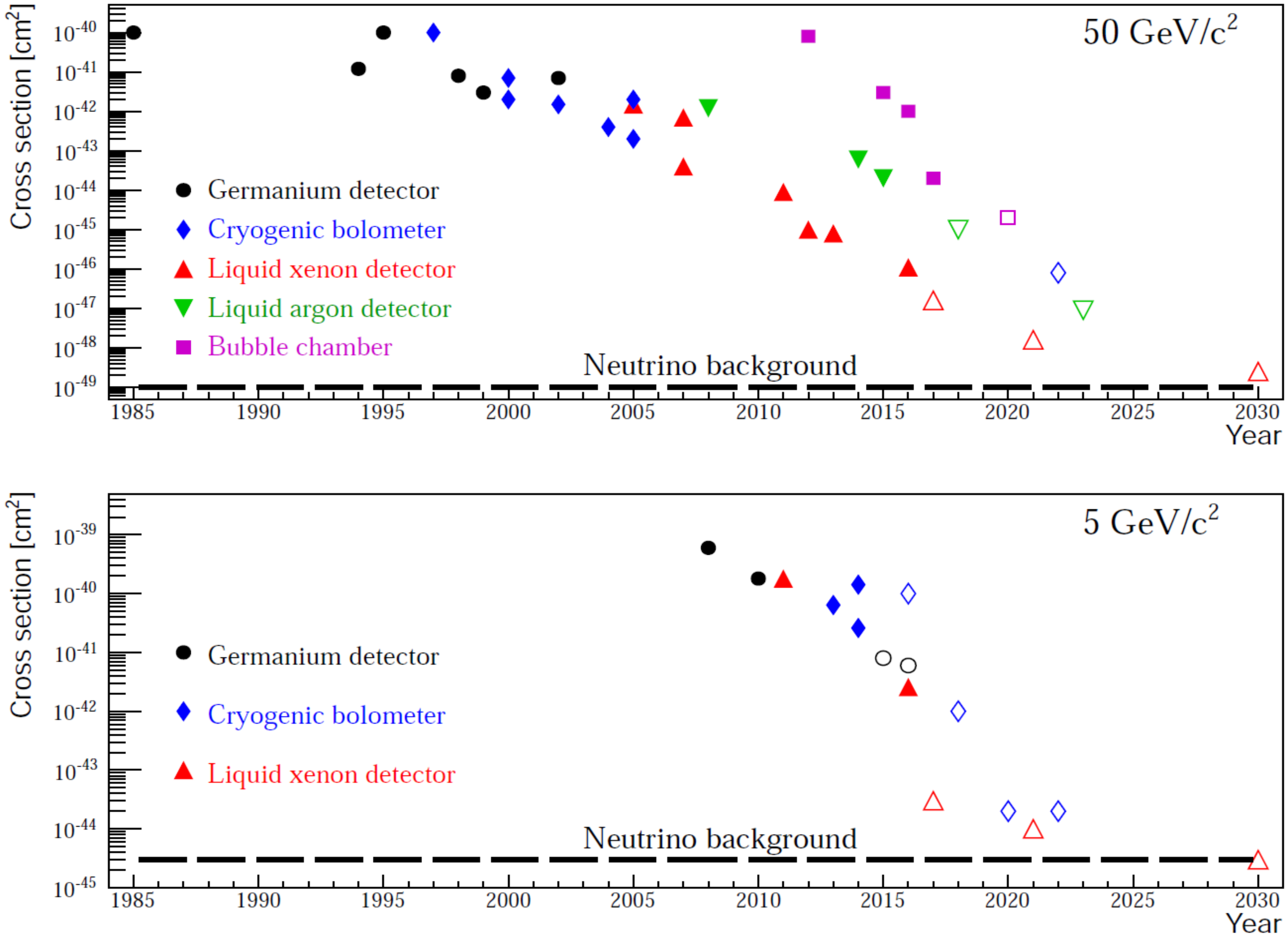

Astro
2018

SI interactions summary

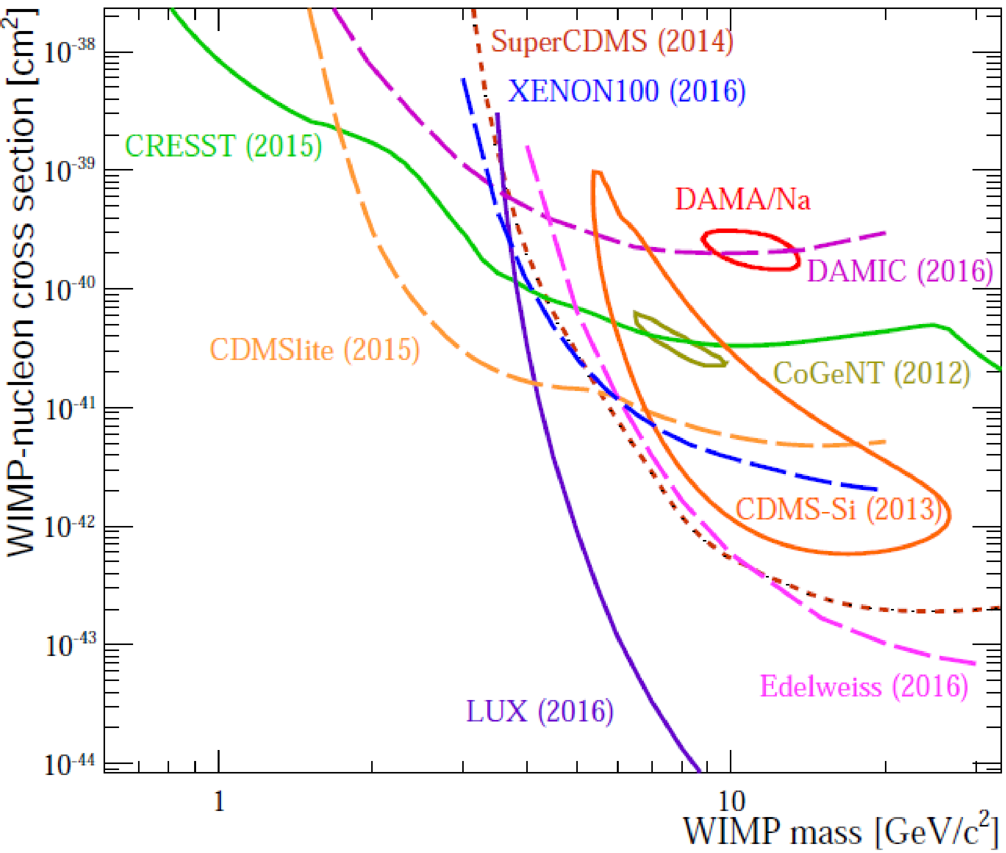

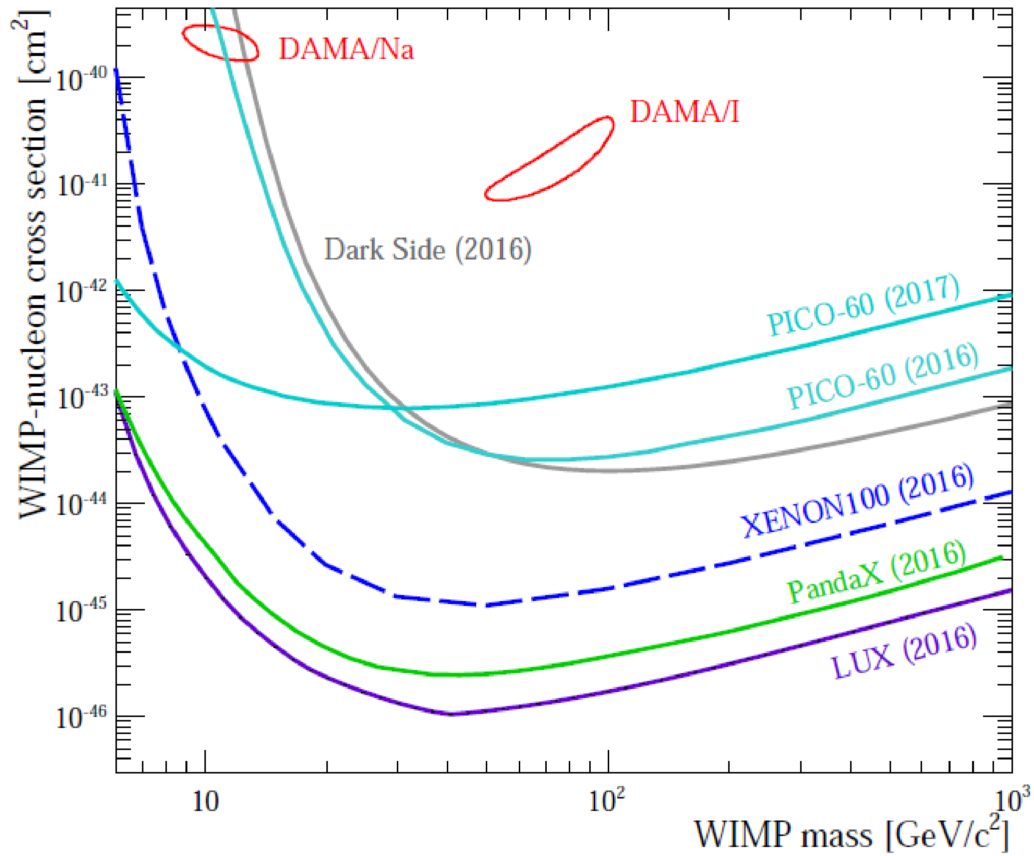

SD limits summary

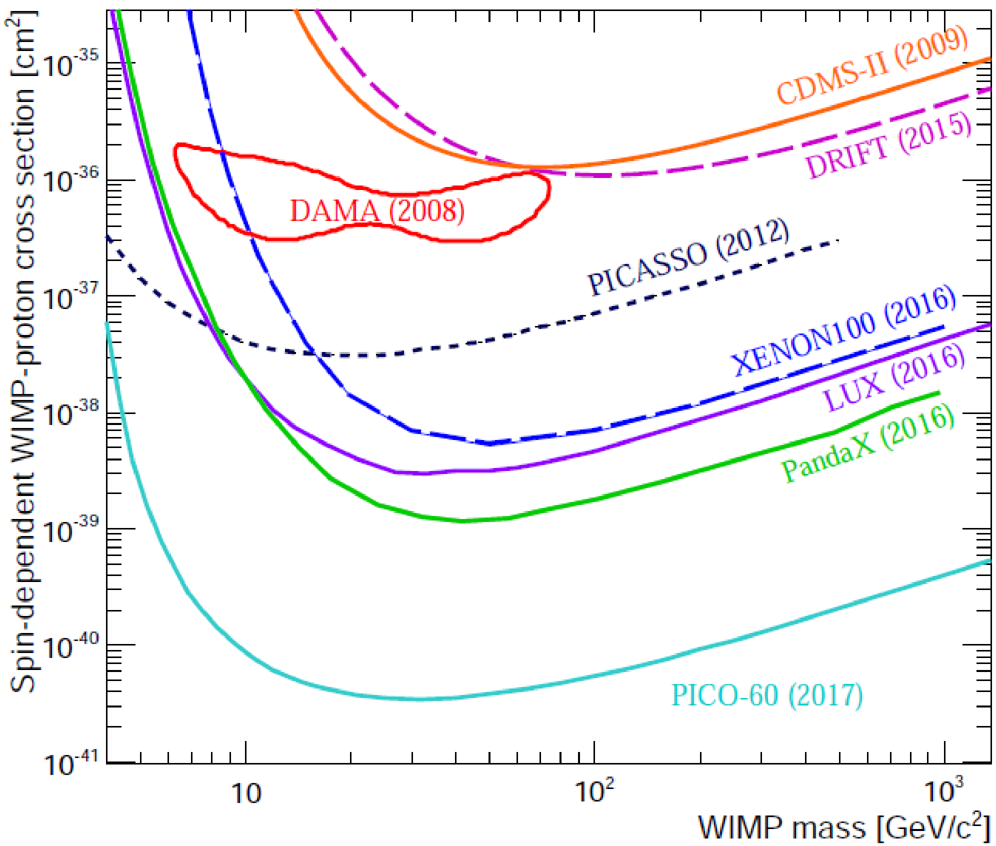

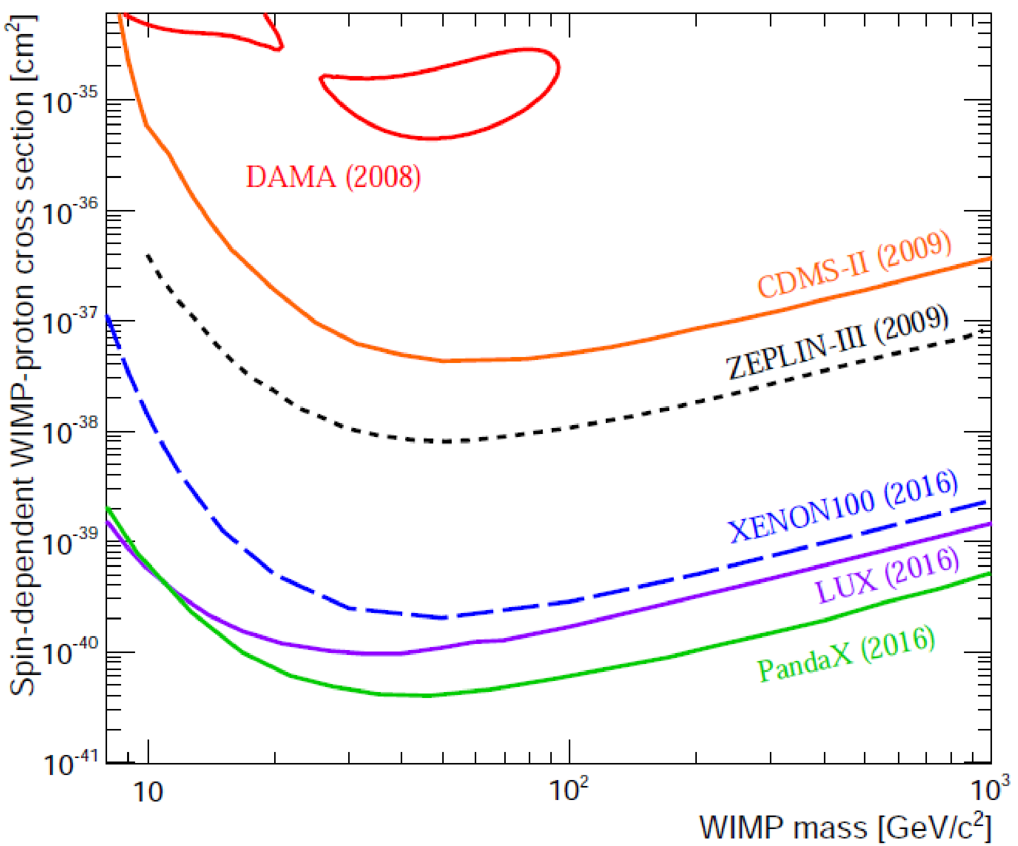

Summary and future

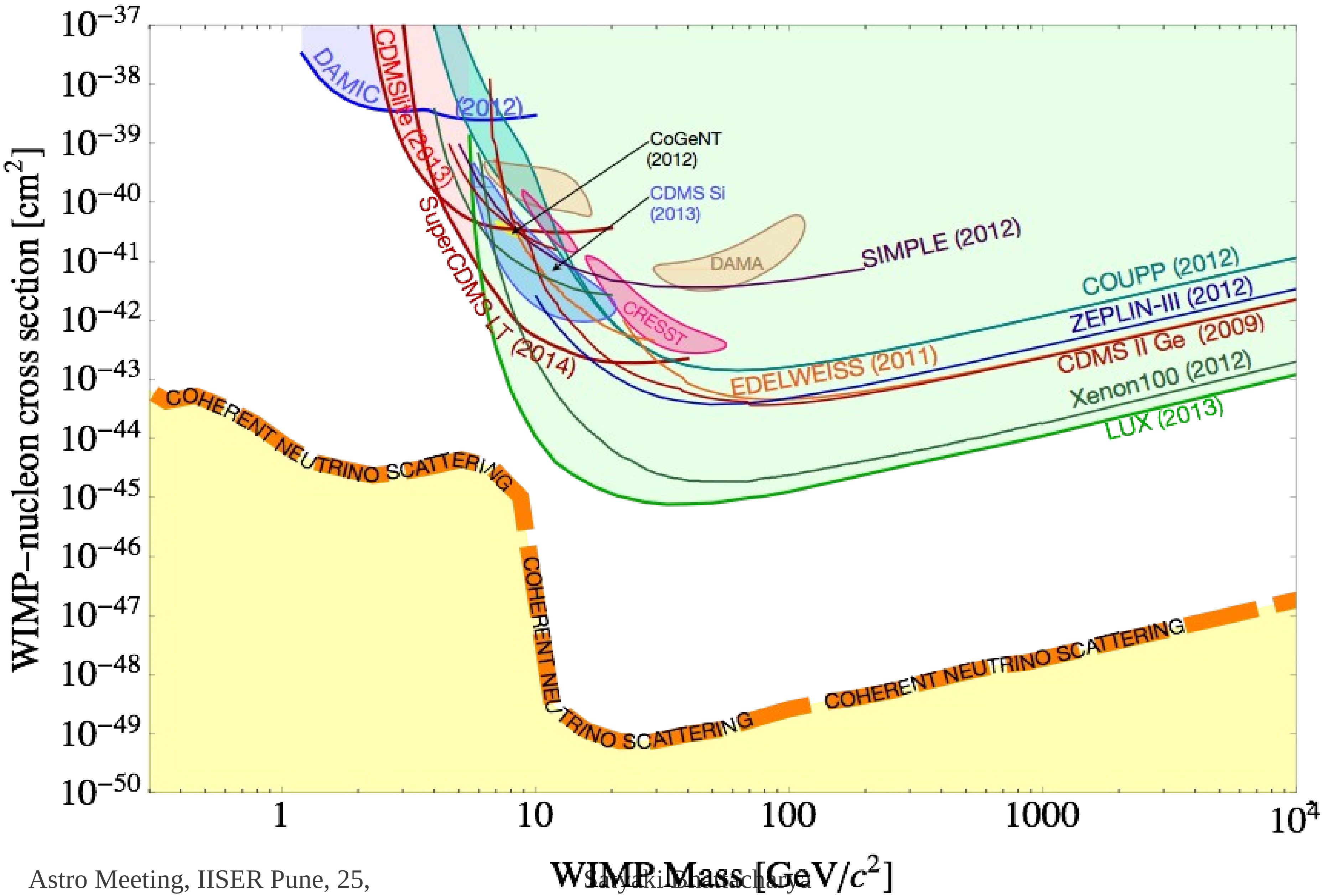

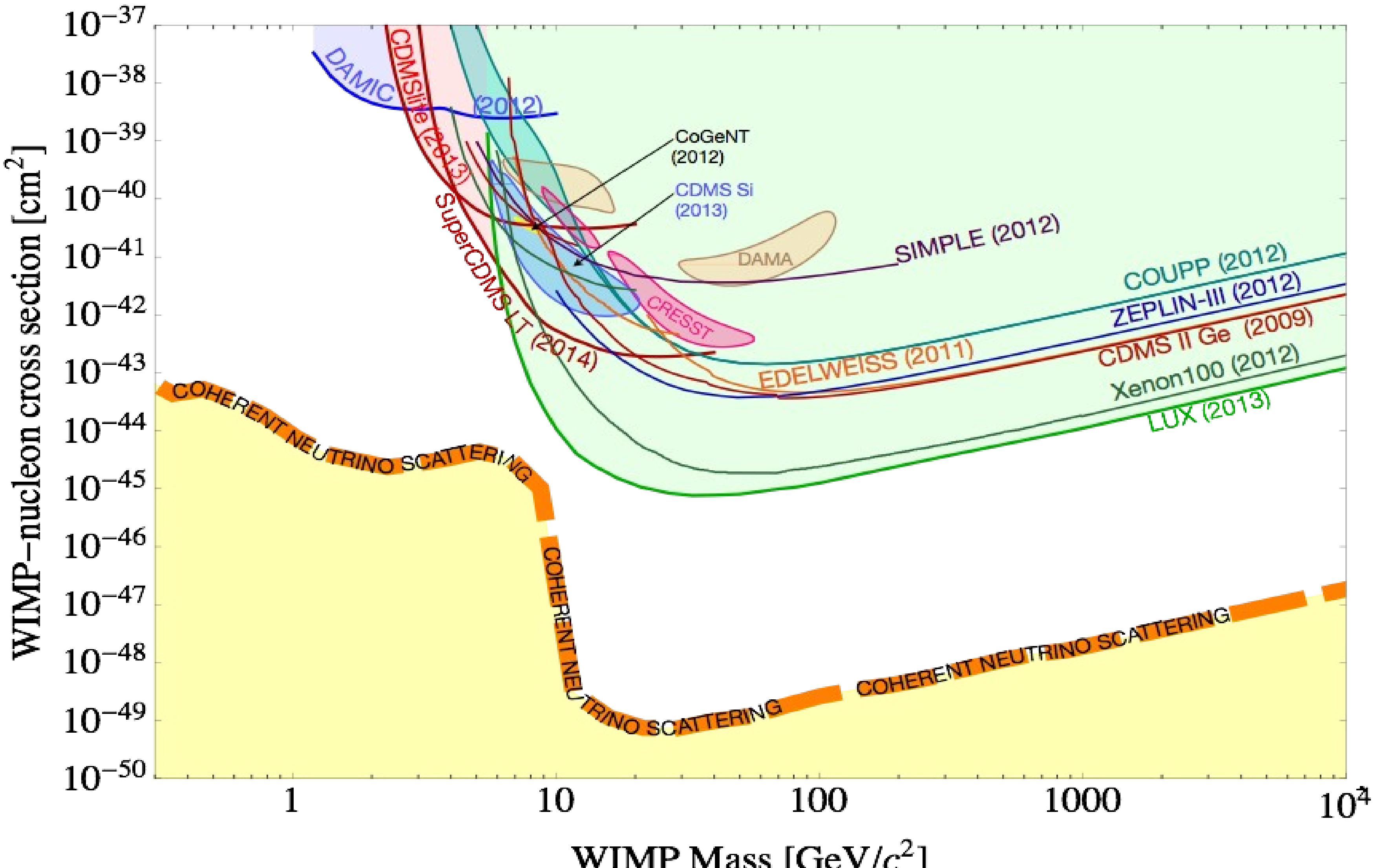

- Present generaion expeimens probing weak cross sections
- Next generation aims to reach neutrino floor --> at low mass lower thresholds, at high mass higher detector mass

Dark Matter Search at LHC

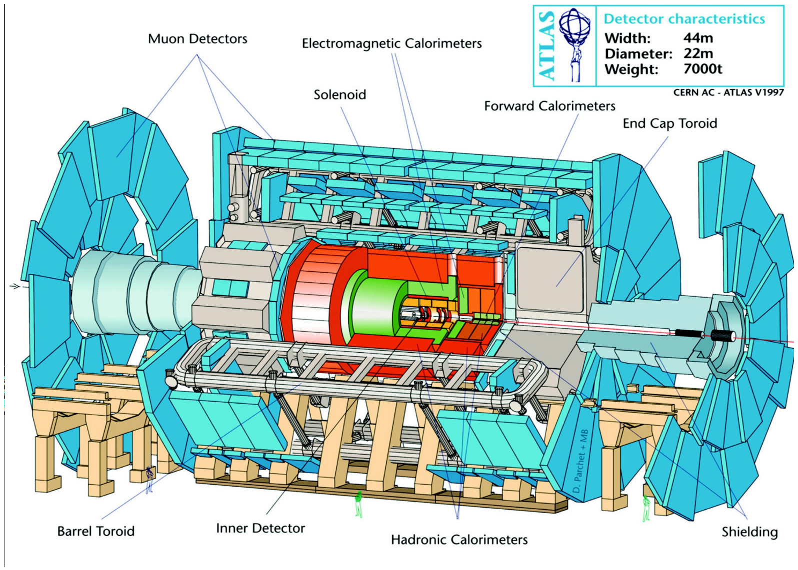

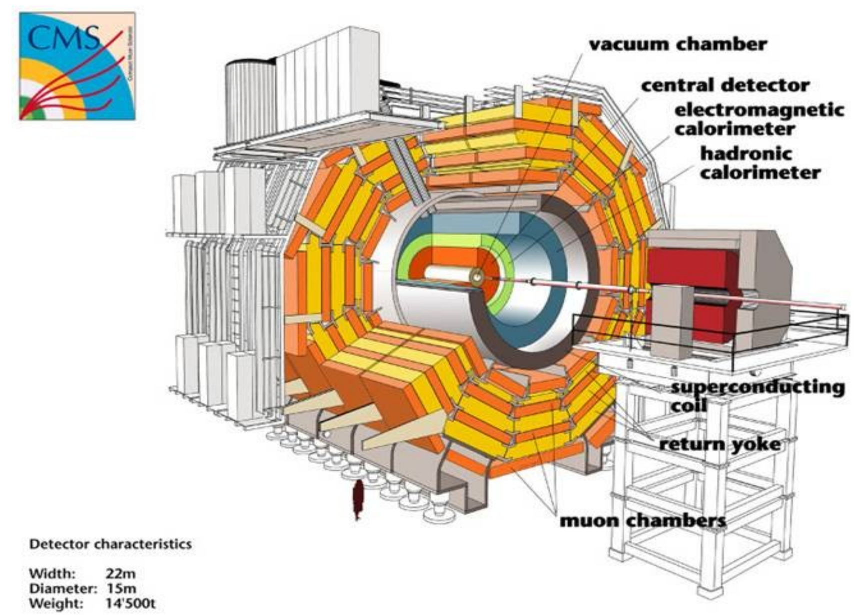

- ATLAS and CMS at the LHC are capable of probing DM direct production in the range ~ 1GeV – 1 TeV

Mono-X at LHC

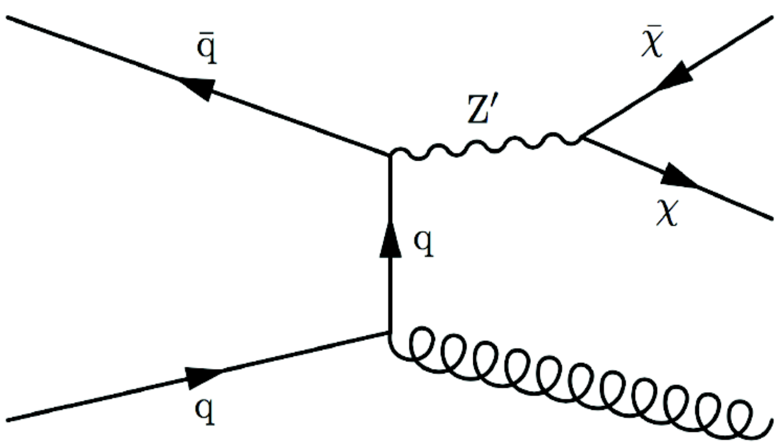

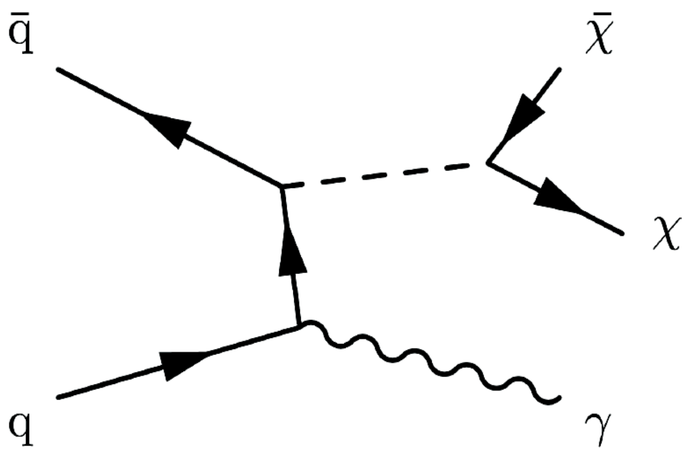

Mono-jet

Mono-photon

Mono-X at LHC

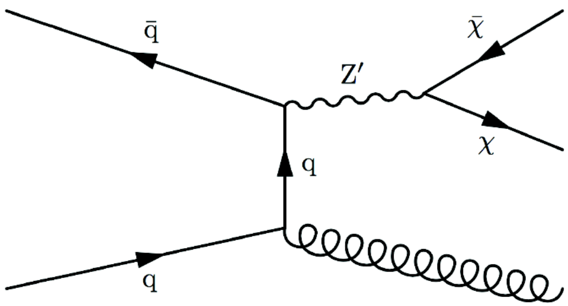

Mono-jet

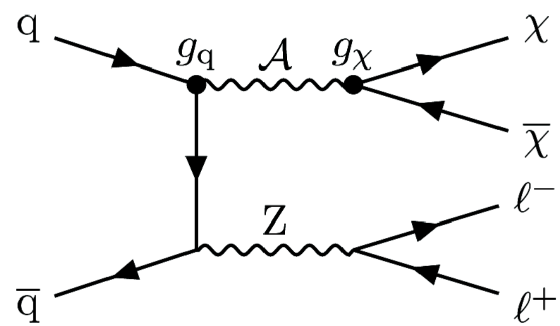

Mono-Z(leptonic)

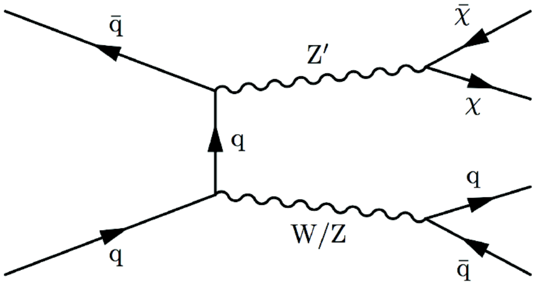

Mono-W/Z(hadronic)

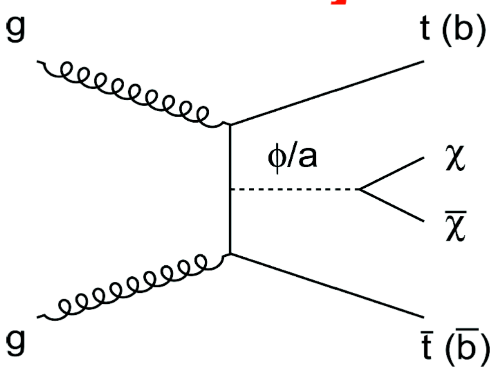

tt/bb

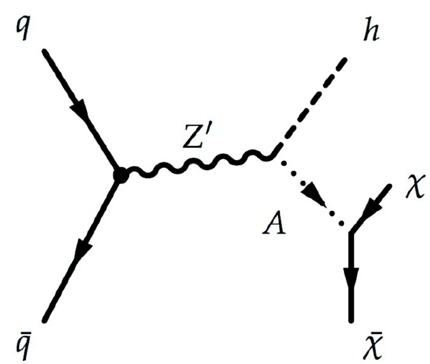

Mono-h (bb, $\gamma\gamma$)

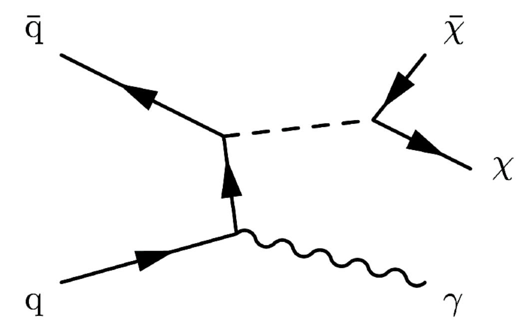

Mono-photon

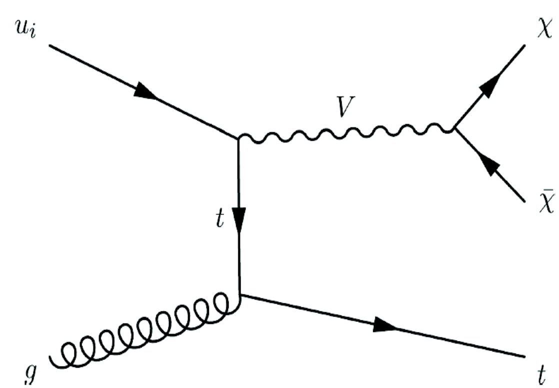

Mono-top

Mono-X + MET : Simplified model and EFT

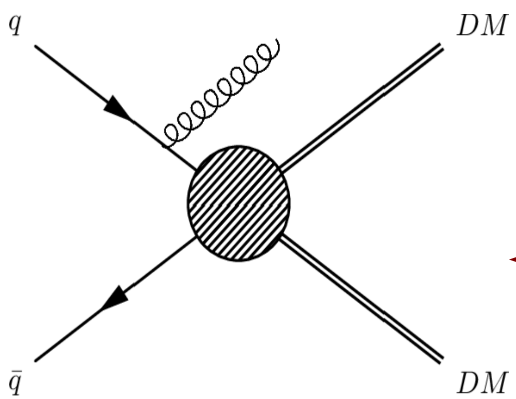

DM EFT

$$\Lambda = M/\sqrt{g_q g_\chi}$$
$$Q_{tr} < M$$

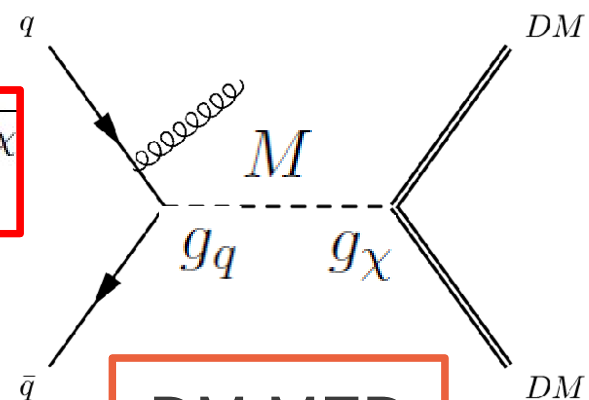

DM MED

perturbative

$$g_{q,\chi} < 4\pi$$
$$\Lambda > \frac{Q_{tr}}{\sqrt{g_q g_\chi}} > \frac{Q_{tr}}{4\pi}$$

s-channel

$$\Lambda > \frac{m_{DM}}{2\pi}$$

	spin 0	spin 1
Charge Q	Q_{med} = 0 for s-channel	
Mass m	unknown	
Dark sector bosons similar to	H [1609.09079]	γ, Z, Z'
Lorentz structure	scalar 1 pseudosc. γ_5	vector γ^μ axial v. $\gamma^\mu \gamma_5$
Coupling "g"	∝ mass	∝ charge

Tae Min Hong, LHCP 2017

LHC in 2016 and future

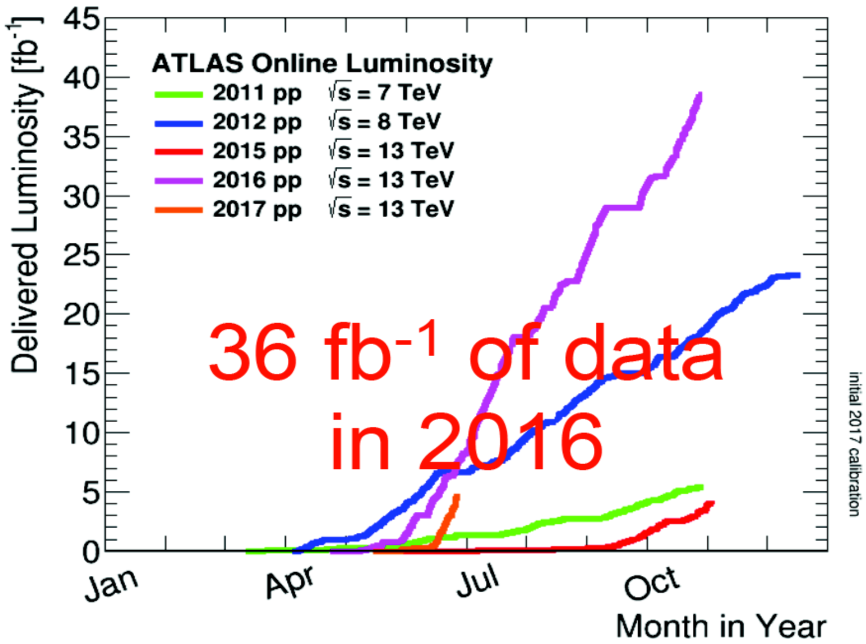

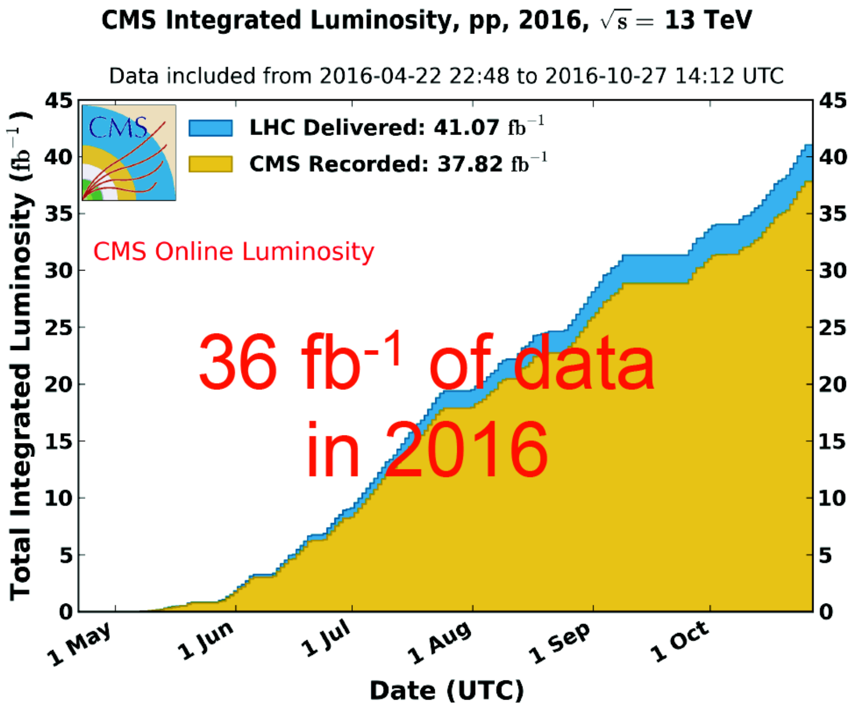

<u>expected luminosity</u>

now:	36 fb^{-1}
end of 2018:	100 fb^{-1}
end of 2023:	300 fb^{-1}
HL-LHC (~2035):	3000 fb^{-1}

see also https://indico.cern.ch/event/539266

Monophoton + MET

- Large brem from beam halo muon or cosmic muon
- Anomalous signal in ECAL barrel photosensors

- Multijet events with MET
- Jet fakes photon

- Gamma + jet – gamma escapes, jet fakes photon/ jet mismeasured

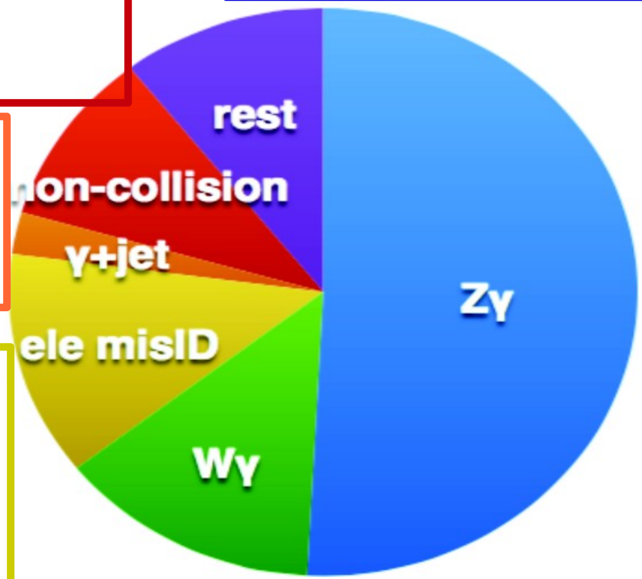

- Z(vv) + gamma irreducible.
- Z is invisible recoiling against high pT photon
- MC NNLO QCD (DYRES) + NLO EWK

- Single electron + MET (mostly single W)
- Electron misses pixel hit, identified as photon

- W(lv) + gamma
- MET from W decay + lepton escaping
- MC NNLO QCD (DYRES) + NLO EWK

monophoton @ 13 TeV

ATLAS, arXiv:1704.03848, Eur. Phys. J. C 77 (2017) 393

- Analysis probes simplified model parameters and EFT vertex qq$\chi\chi$
- Dominant backgrounds from Z($\nu\nu$)/W(lν)γ,γ+jets
- Analysis requires a photon with ET > 150 GeV, dϕ(γ,MET) > 0.4
- Veto >1 jets, no leptons
- several signal regions in ranges of MET, starting from MET > 150 GeV
- Normalisation of Z/Wγ,γ+jets combined profile likelihood fit of control regions (1μ, 2μ, 2e,γ+jets)
- Dominant systematics from jet->γ fake factor (1-5%) , e->γ fake factor (1.5%), jet energy scale (6-1%)

ATLAS monophoton @ 13 TeV

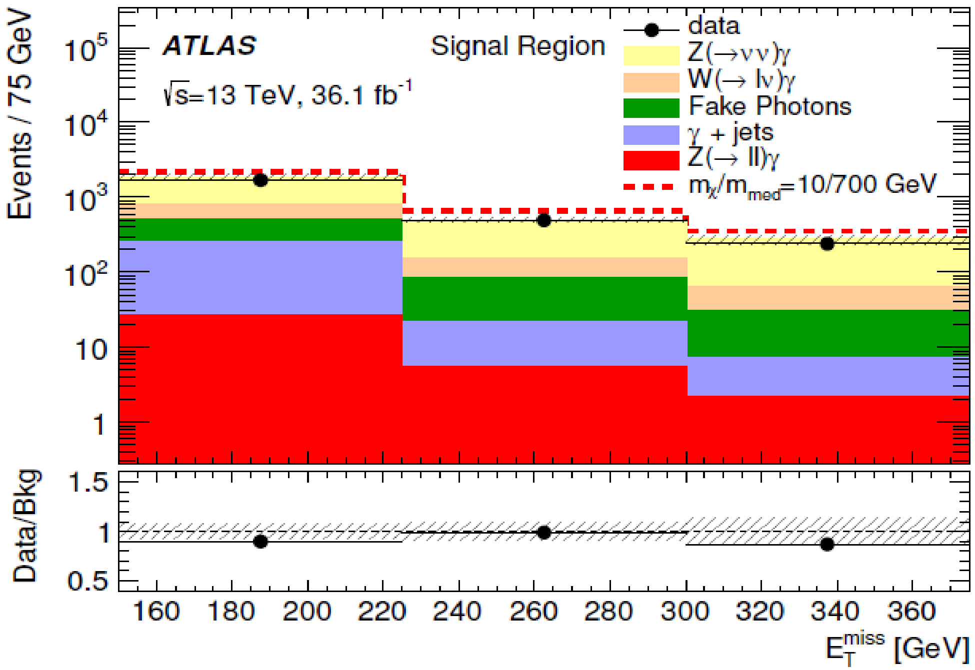

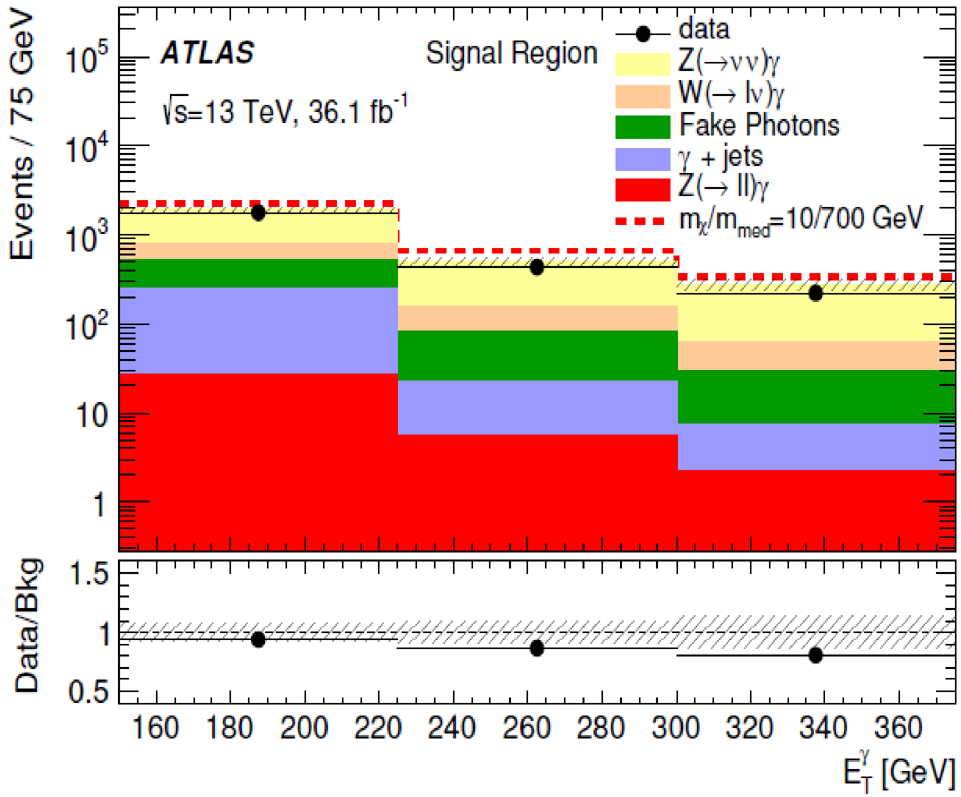

CMS monophoton @ 13 TeV

12.9 fb^{-1}

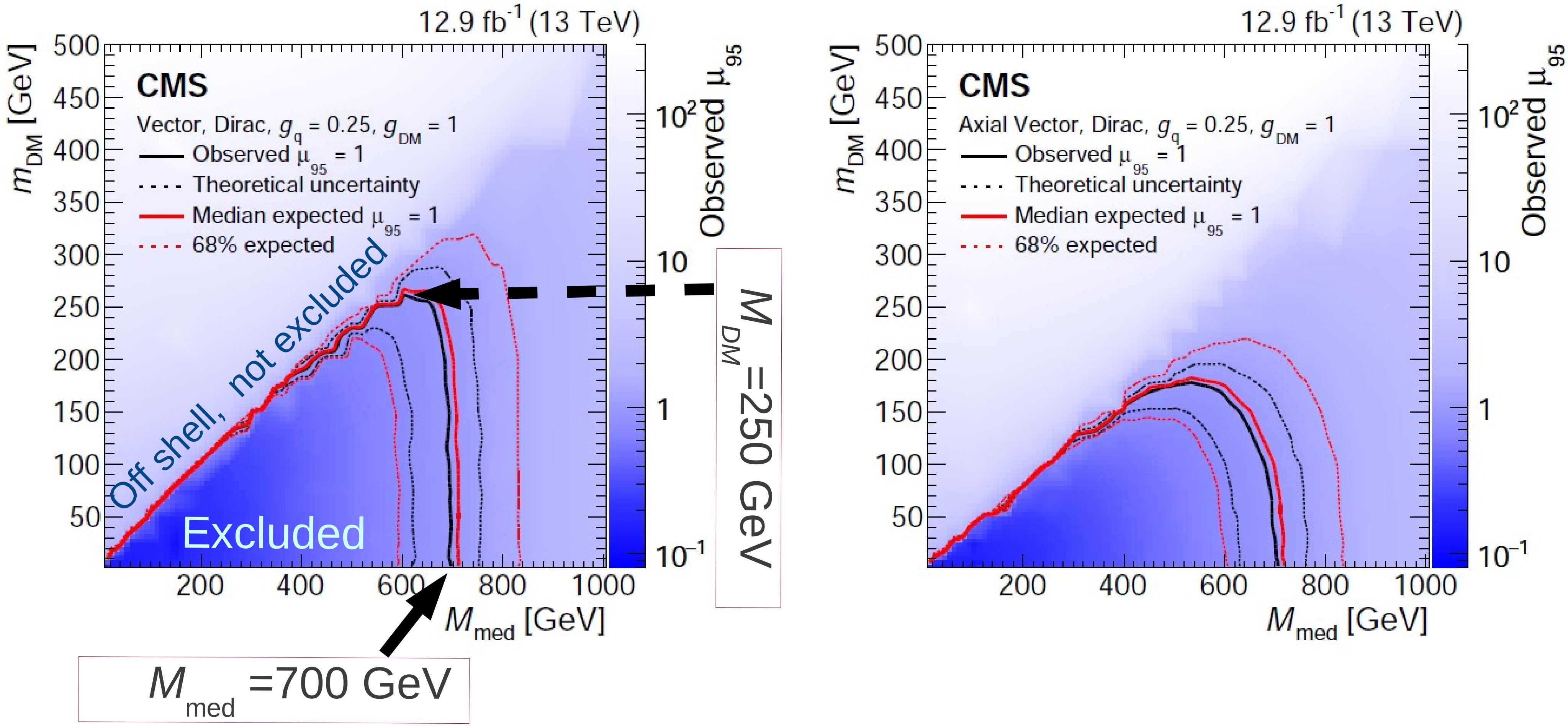

ATLAS Monophoton @ 13 TeV

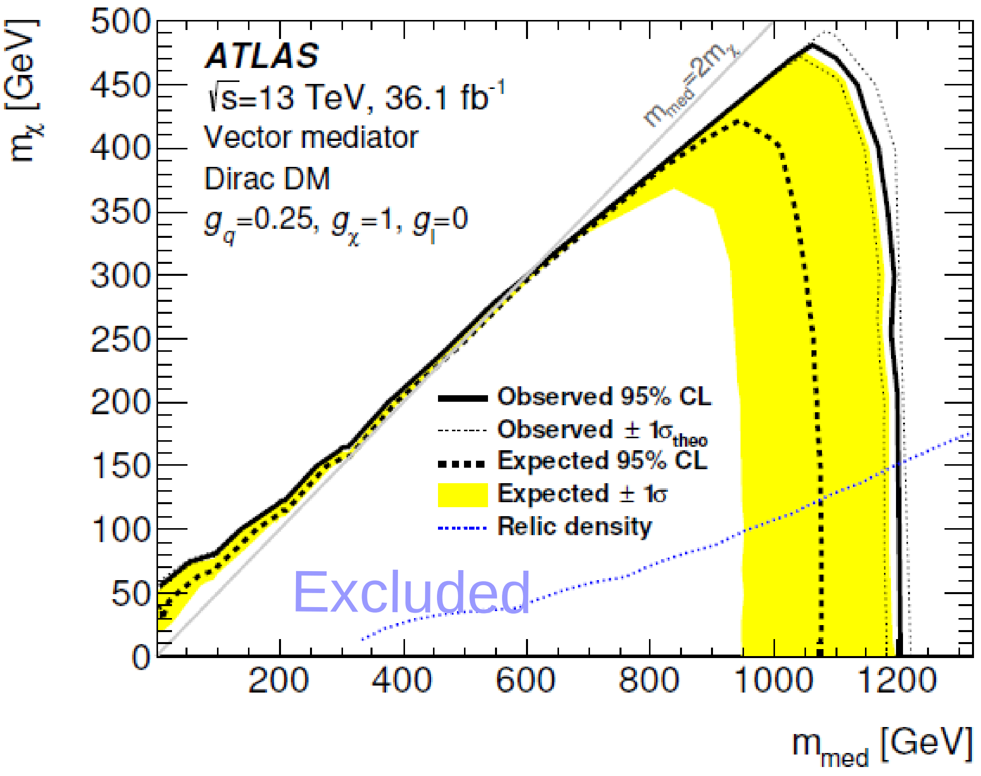

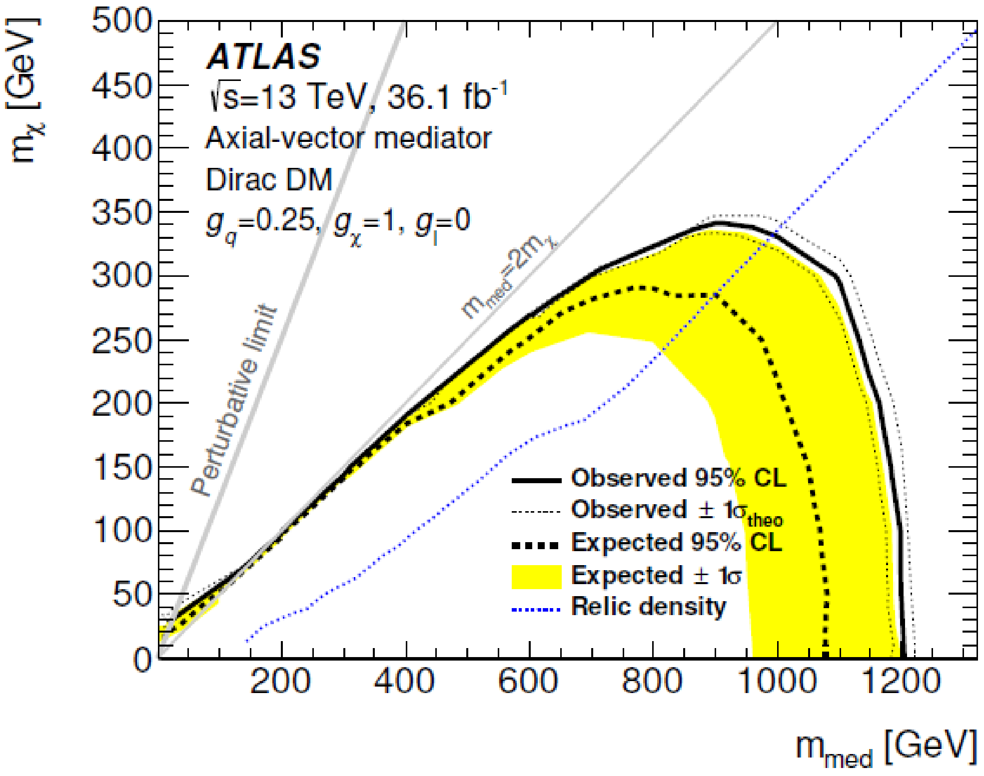

ATLAS monophoton @ 13 TeV

$$\sigma_{\mathrm{SI}}^{\mathrm{vector}} \simeq 6.9\times10^{-41}\,\mathrm{cm}^2 \left(\frac{g_q g_{\mathrm{DM}}}{0.25}\right)^2 \left(\frac{1\ \mathrm{TeV}}{M_{\mathrm{med}}}\right)^4 \left(\frac{\mu_{n\chi}}{1\ \mathrm{GeV}}\right)^2$$

$$\sigma_{\mathrm{SD}}^{\mathrm{axial}} \simeq 2.4\times10^{-42}\,\mathrm{cm}^2 \left(\frac{g_q g_{\mathrm{DM}}}{0.25}\right)^2 \left(\frac{1\ \mathrm{TeV}}{M_{\mathrm{med}}}\right)^4 \left(\frac{\mu_{n\chi}}{1\ \mathrm{GeV}}\right)^2$$

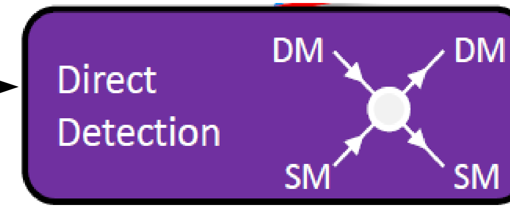

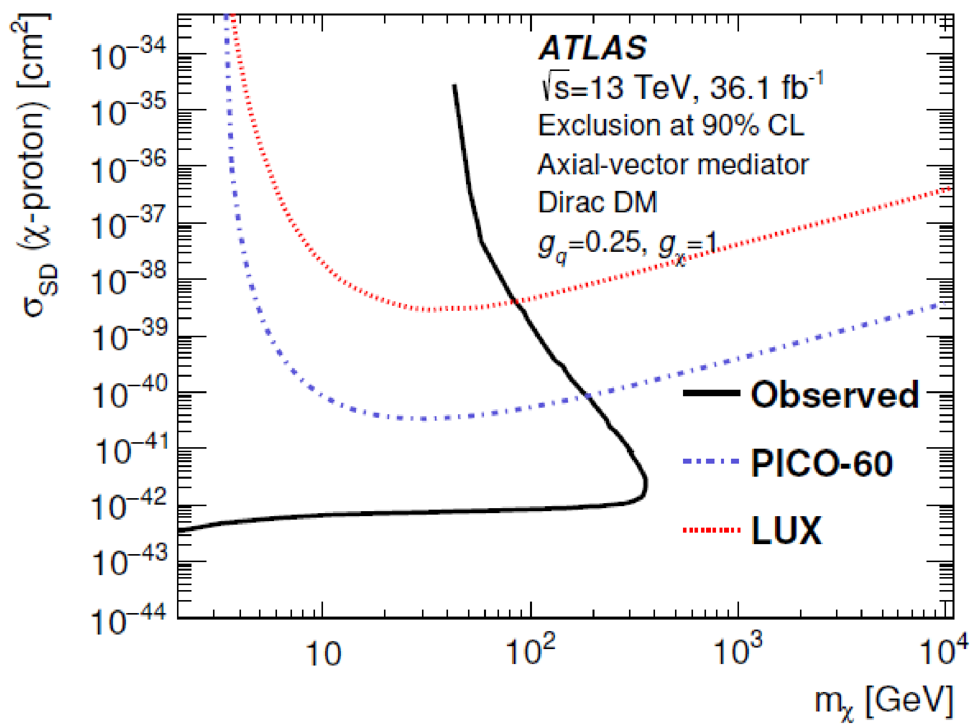

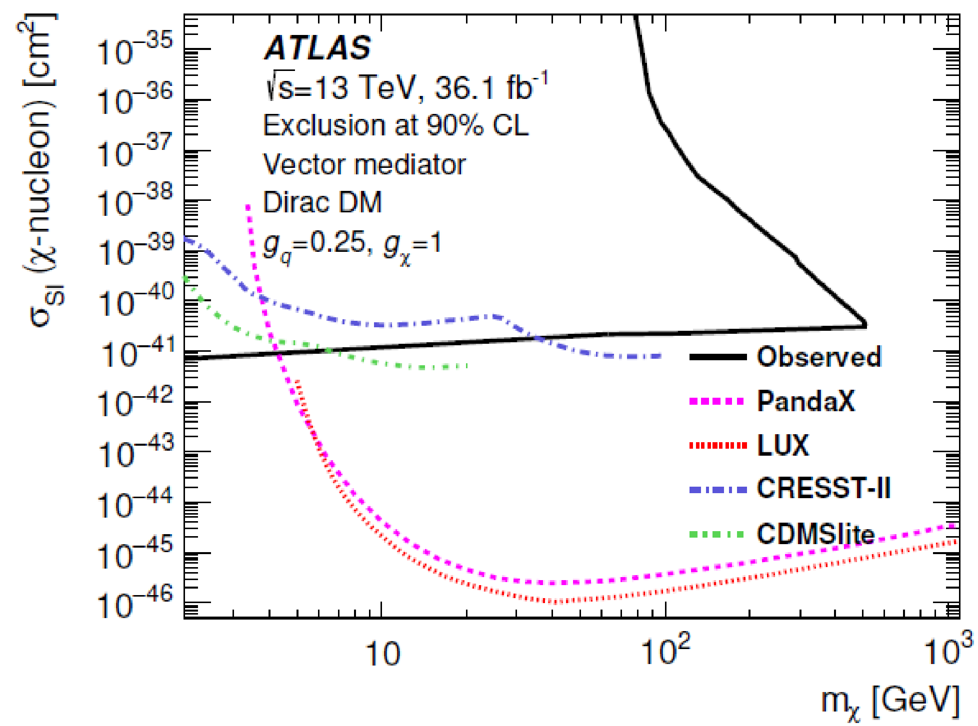

CMS monophoton @ 13 TeV

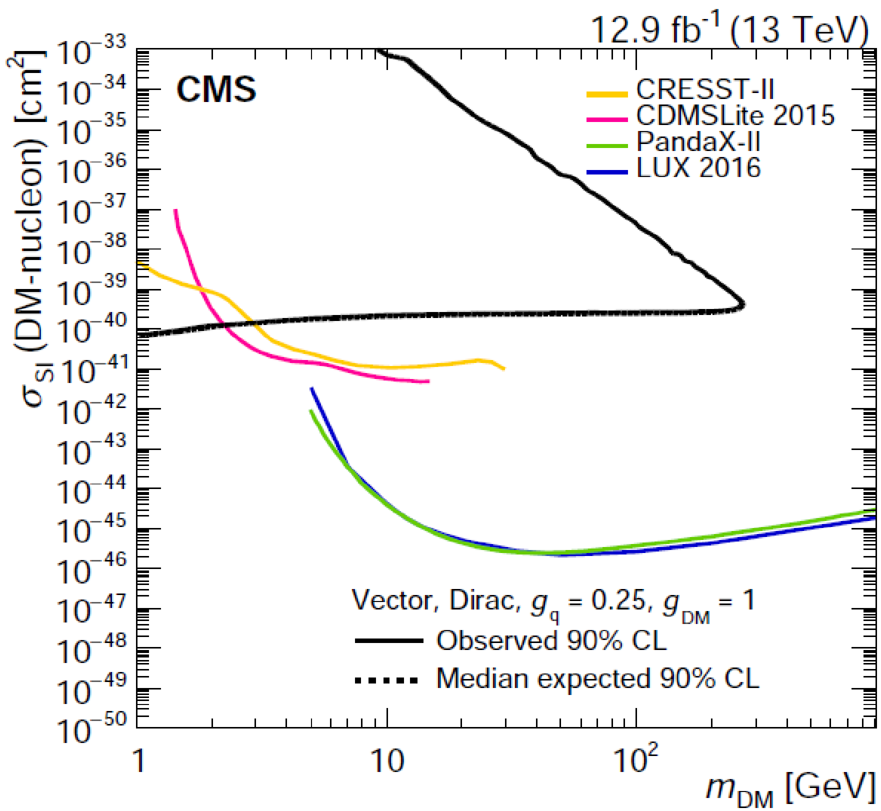

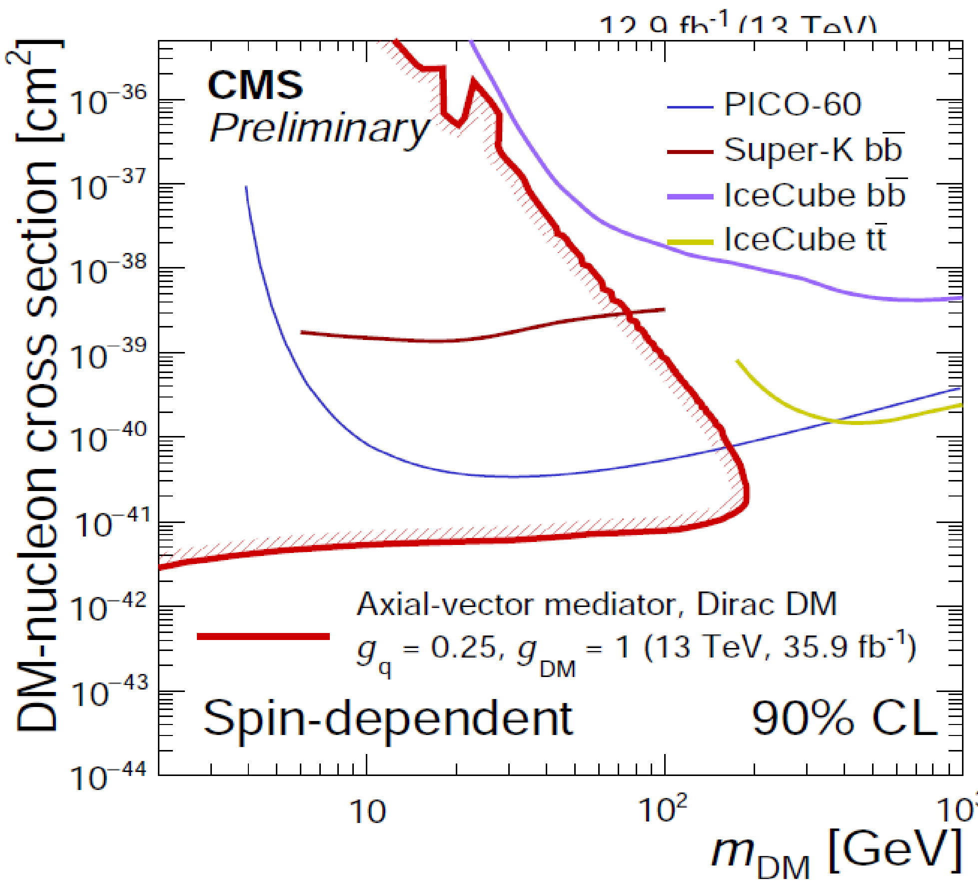

Monojet : topologies and interpretations

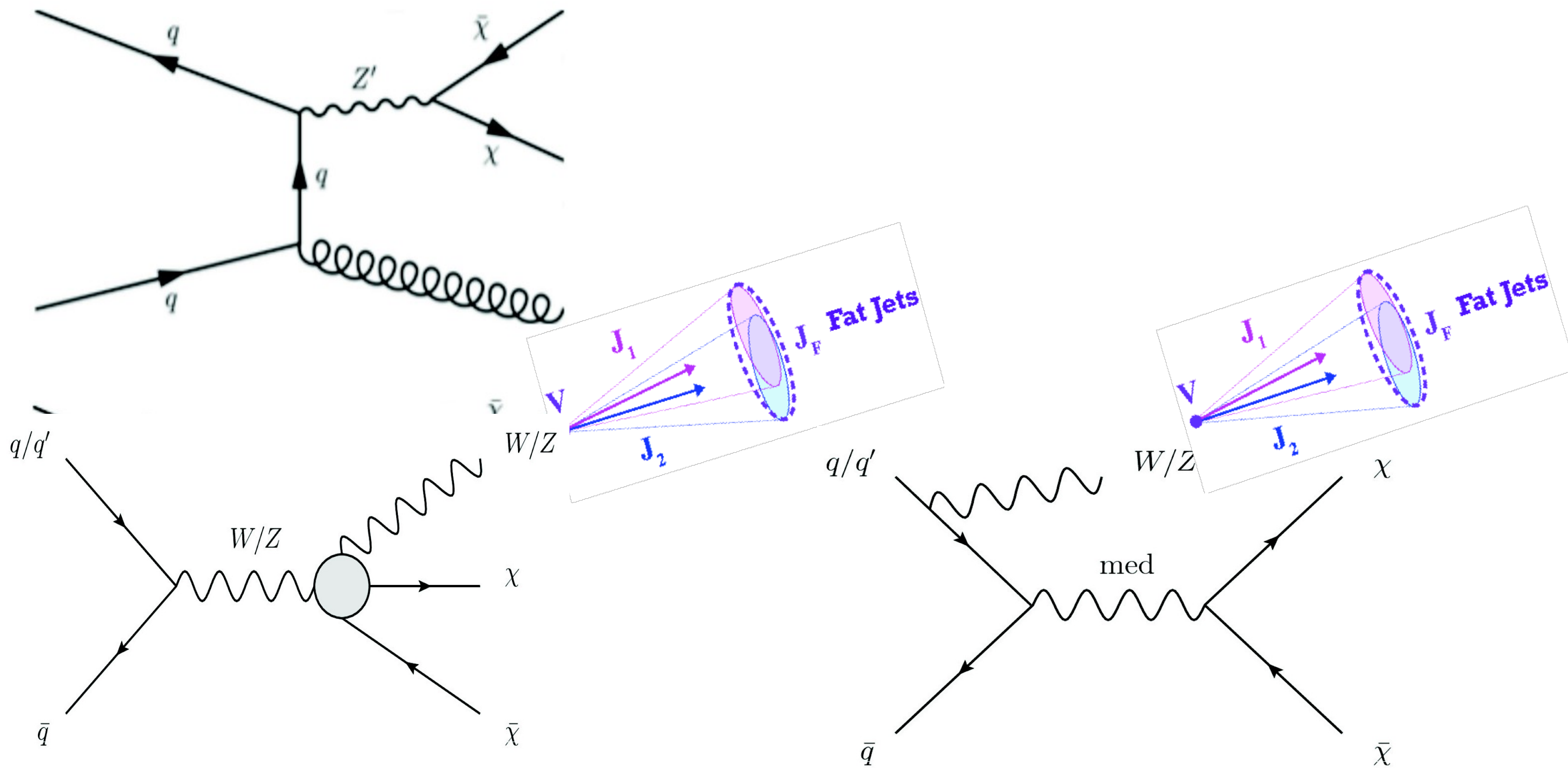

- Monojet can be mono-V with a fat jet
- Use the jet substructure machinary

CMS monojet @ 13 TeV

- Monojet p_T of AK4 jet > 100 GeV, $|\eta| < 2.5$
- Mono V: AK8 jet p_T > 250 GeV, $|\eta| < 2.4$
- V tagging: pruned jet mass in {65,105} GeV + n subjettiness $\tau 2/\tau 1$ < 0.6

- Veto:
- E/μ with p_T > 10 GeV, τ with p_T > 18 GeV, photon with p_T > 15 GeV

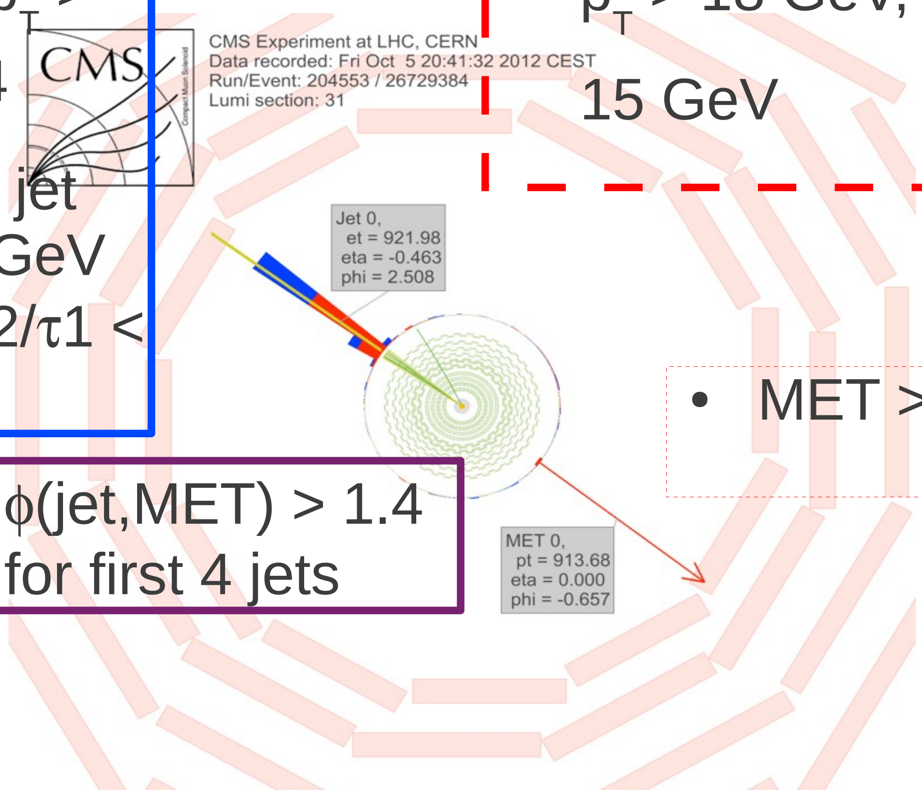

- MET > 250 GeV

- ϕ(jet,MET) > 1.4 for first 4 jets

CMS monojet/mono-V @ 13 TeV

- Dominant background Z (νν) + jets, W(lν) + jets
- Control regions(CR), with pT of hadron recoil system as proxy for MET
- Constrain electroweak backgrounds
- Binned likelihood fit of hadronic recoil to estimate Zjets and Wjets spectra in signal region
- Bin by bin transfer factors (TF) to extrapolate to signal region(SR)
  - PT dependent NLO k-factors

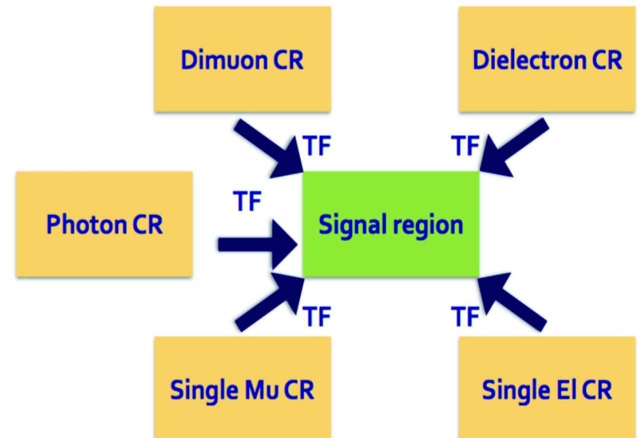

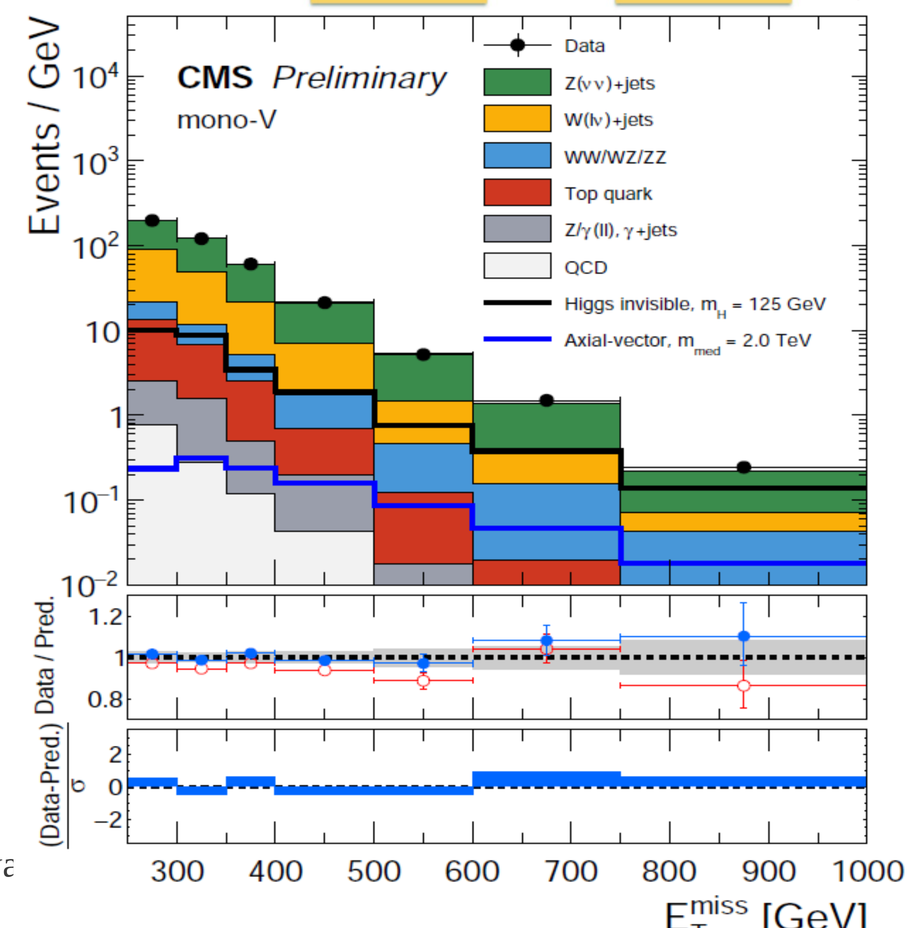

Monojet/V bounds CMS @ 13 TeV

Combined binned profile likelihood fit of MET spectrum in SR and CR, to extract upper limit on signal strength

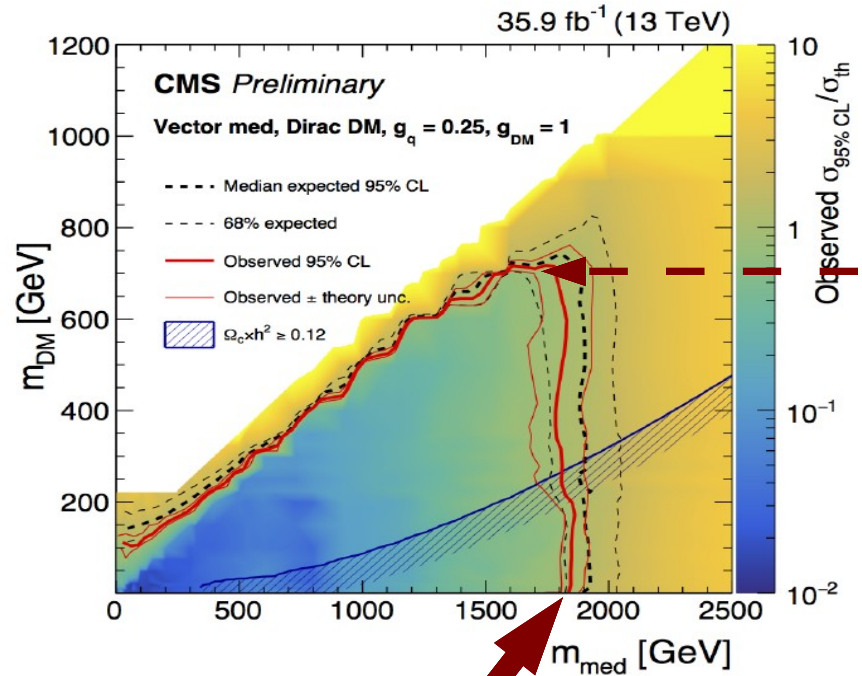

M_{DM} =700 GeV

1.8 TeV

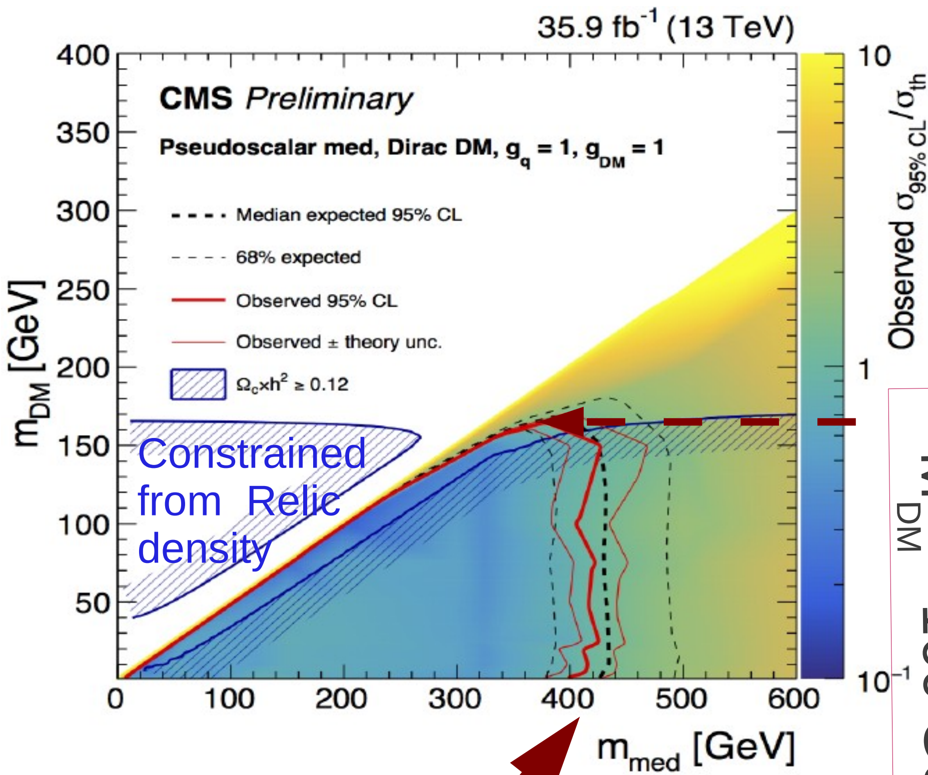

M_{DM} =160 GeV

M_{med} = 400 GeV

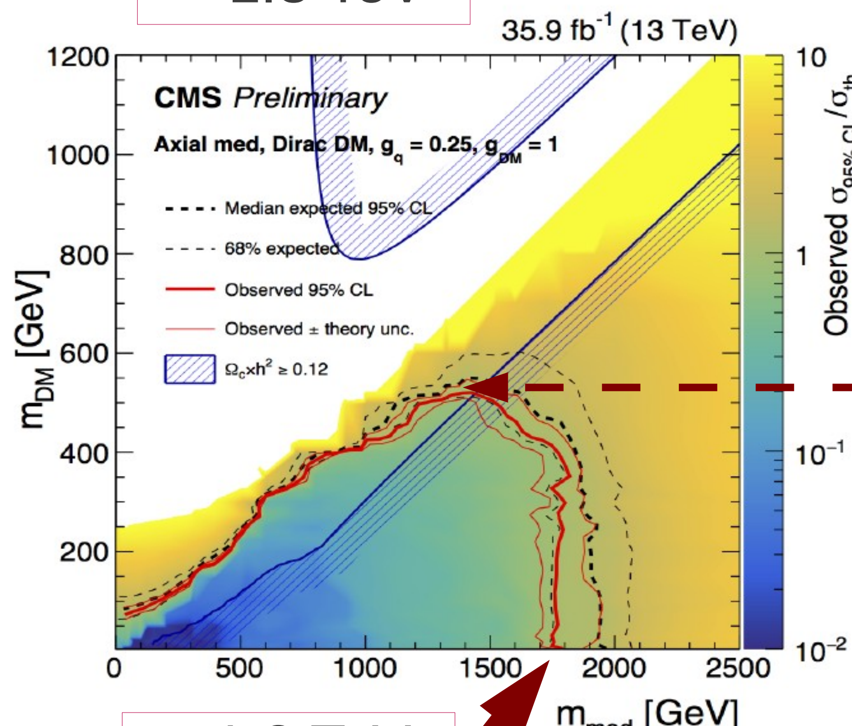

M_{DM} =500 GeV

1.8 TeV

CMS monojet/V @ 13 TeV

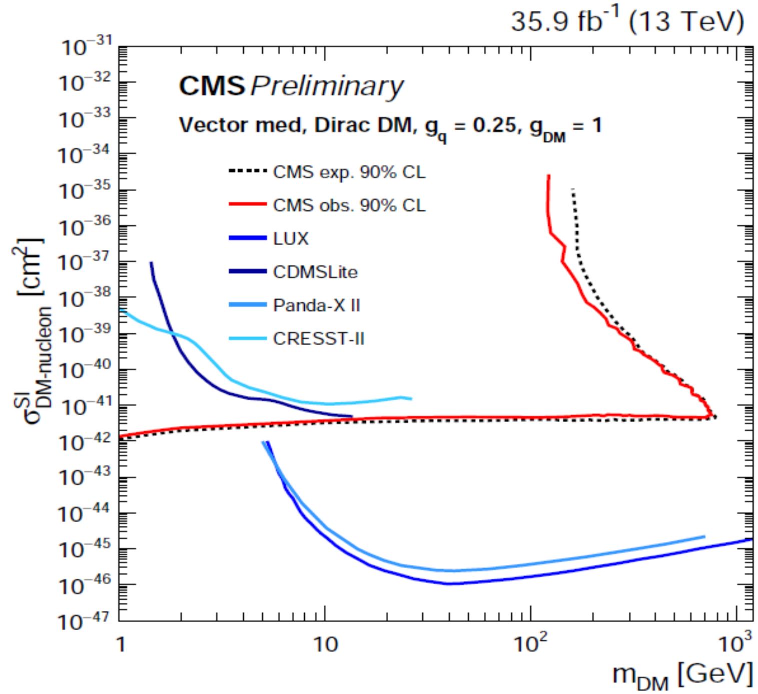

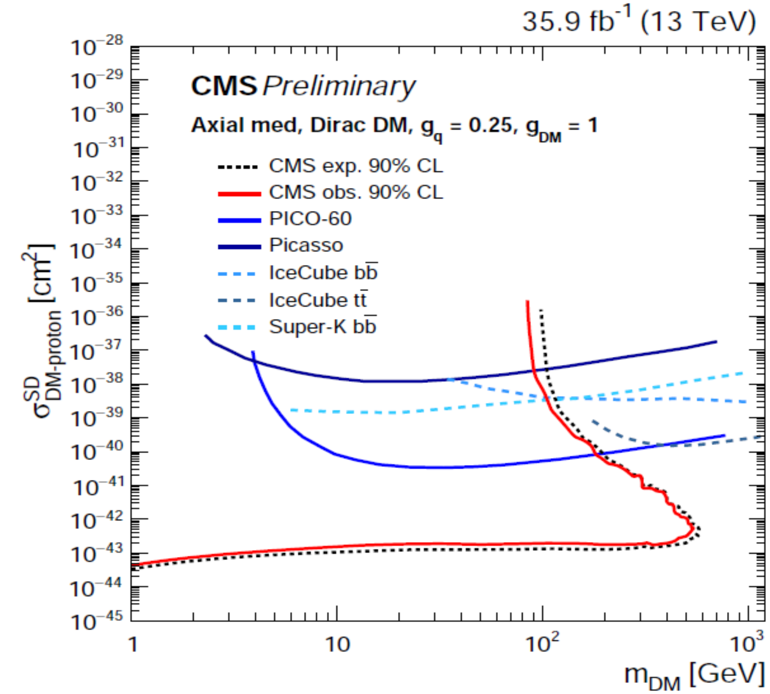

- For pseudoscalar mediator bound is on velocity averaged DM annihilation cross section
- Quark scattering suppressed at low velocities
- Compared with FermiLAT
- SD bounds better than PICO 60 for M_{DM} < 500 GeV

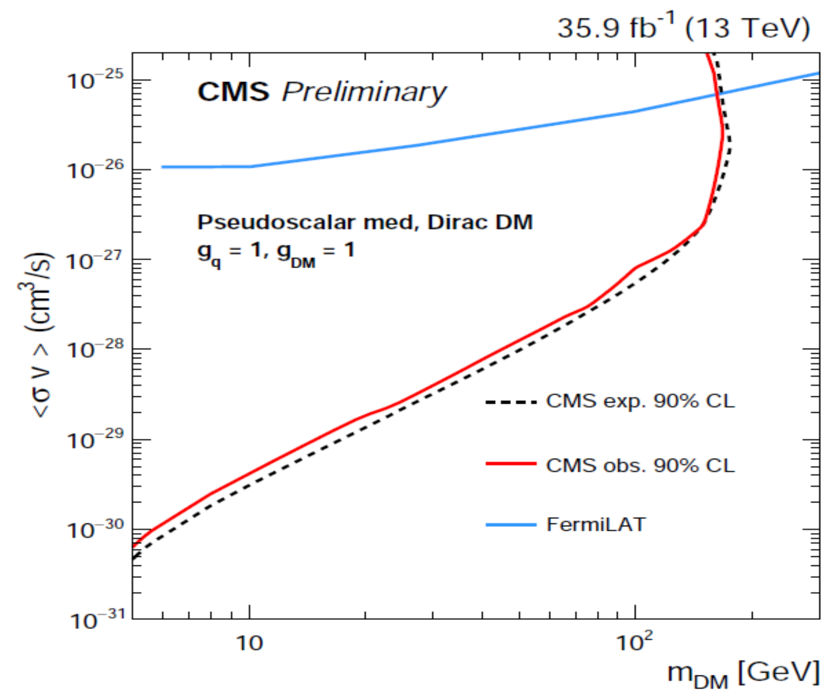

Z(ll) + MET

ATLAS-CONF-2017-040,
CMS EXO-16-052

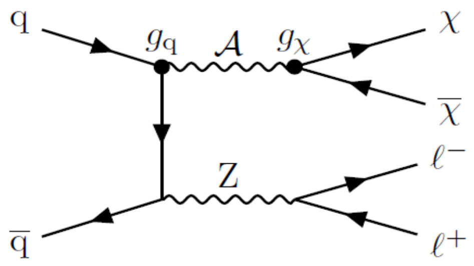

(a)

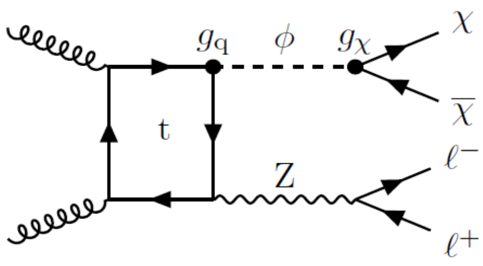

(b)

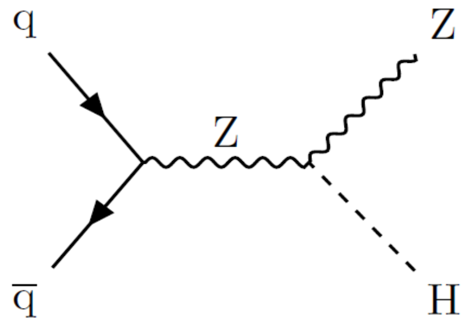

(c)

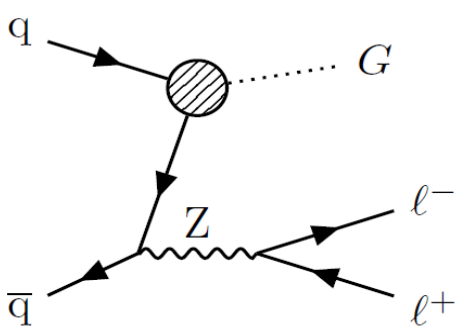

(d)

CMS Z(ll) + MET

- MET > 100 GeV,
- Dilepton pT > 60 GeV
- MET, pTll balance
- No additional lepton, tau events with more than 1 jets above pT 30 GeV

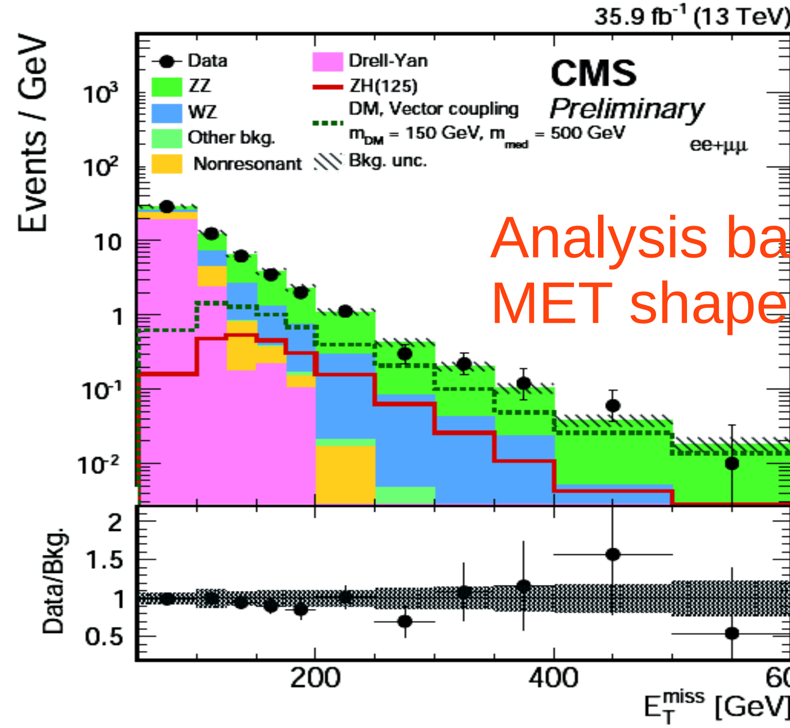

Analysis based on MET shape

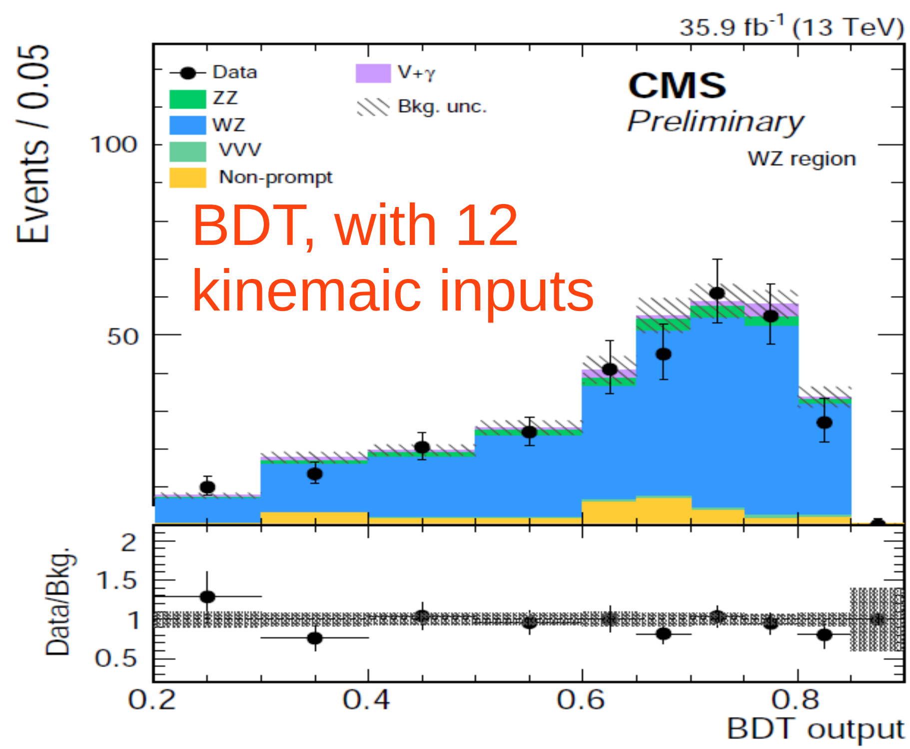

BDT, with 12 kinemaic inputs

15%,
WW, W, tt, tW,Z to taus.
From data

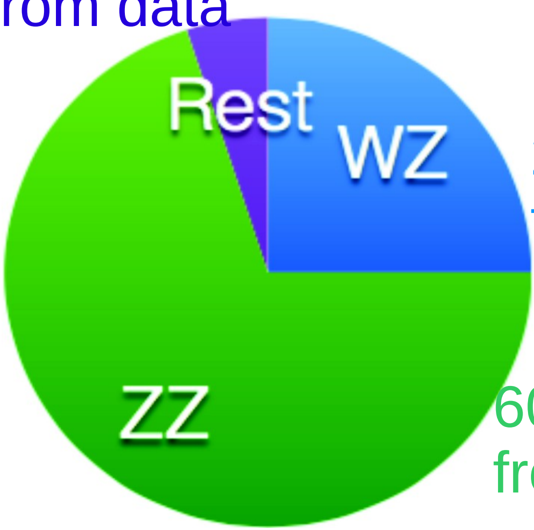

25%,
from MC

60%,
from MC

CMS Z(ll) + MET @ 13 TeV

- Vector mediator mass upto ~650 GeV excluded @ 95% CL for DM mass below ~200 GeV
- Axial vector mediator mass exclusion lies between 500 - 700 GeV @ 95% CL, for DM mass below ~ 150 GeV

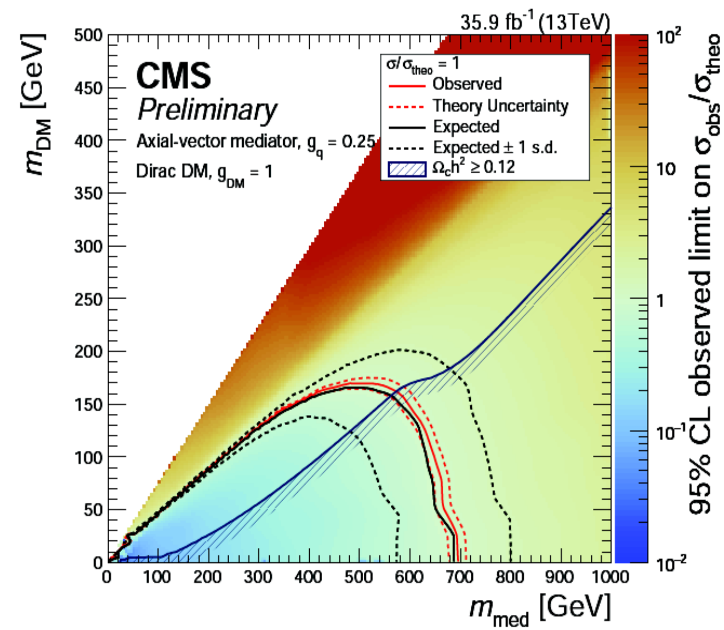

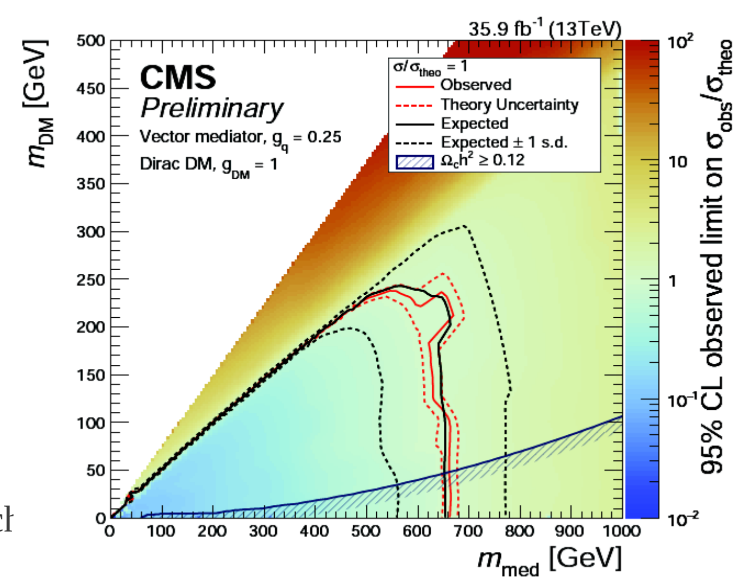

CMS bounds on DM-nucleon scattering cross section from Z (ll) + MET

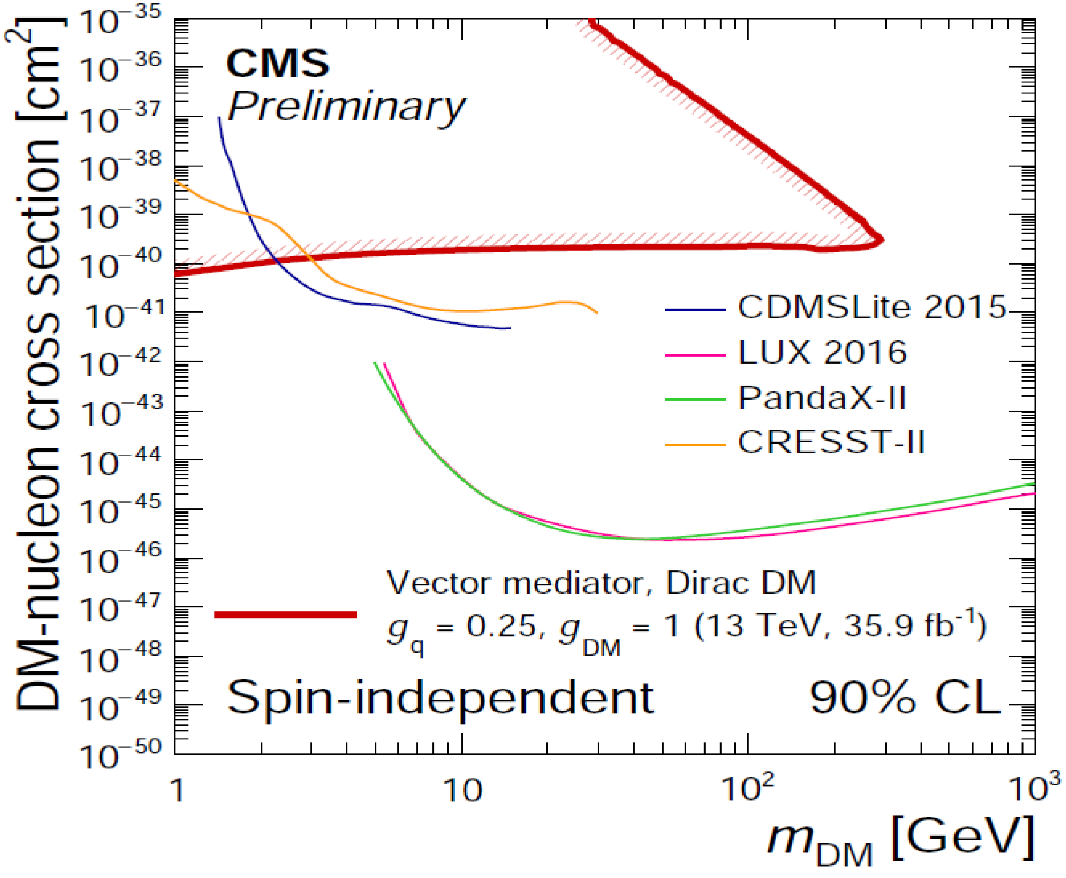

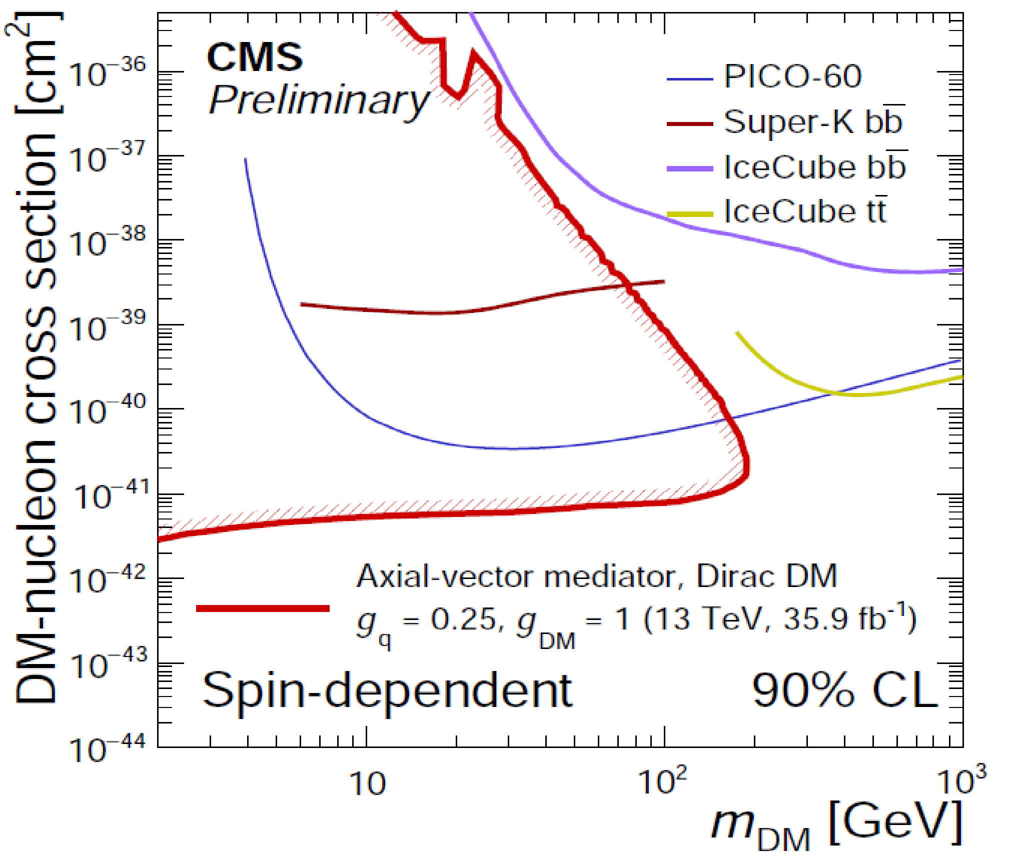

CMS bound on invisible higgs BR from Z (ll) + MET

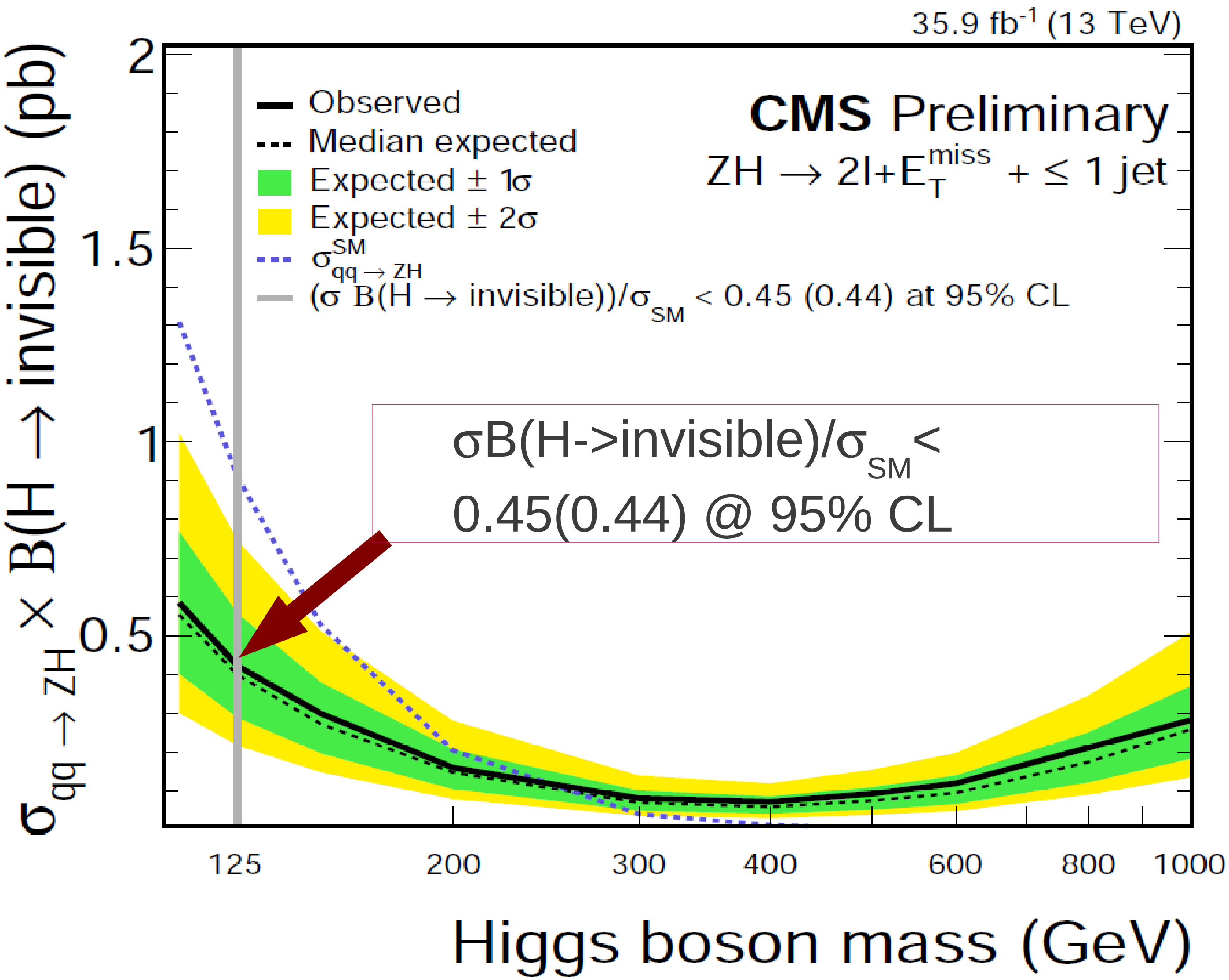

$\sigma B(H\text{->}invisible)/\sigma_{SM} <$ 0.45(0.44) @ 95% CL

ATLAS Z(ll) + MET summary

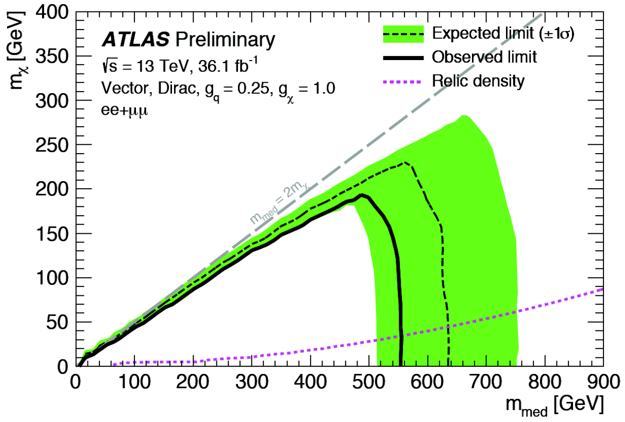

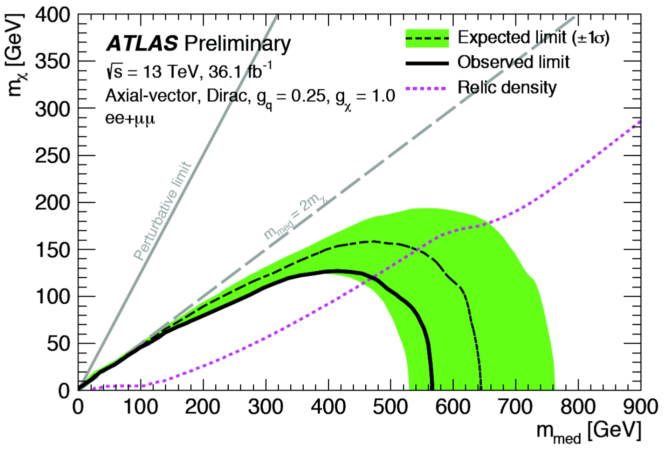

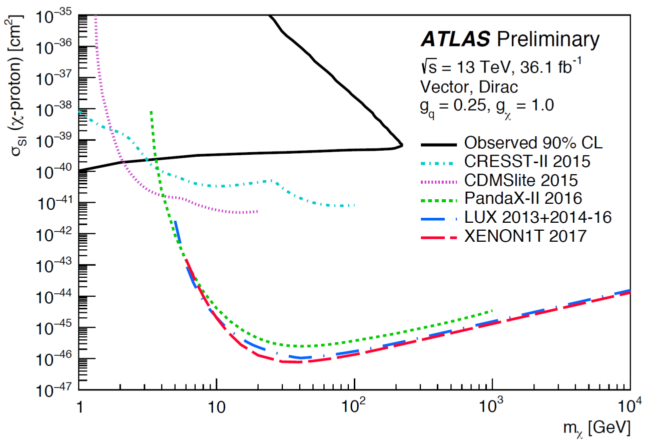

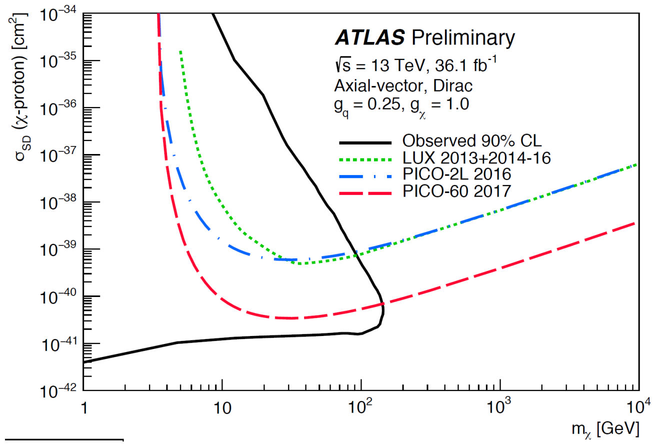

CMS Bounds on DM-Nucleon scattering (SI)

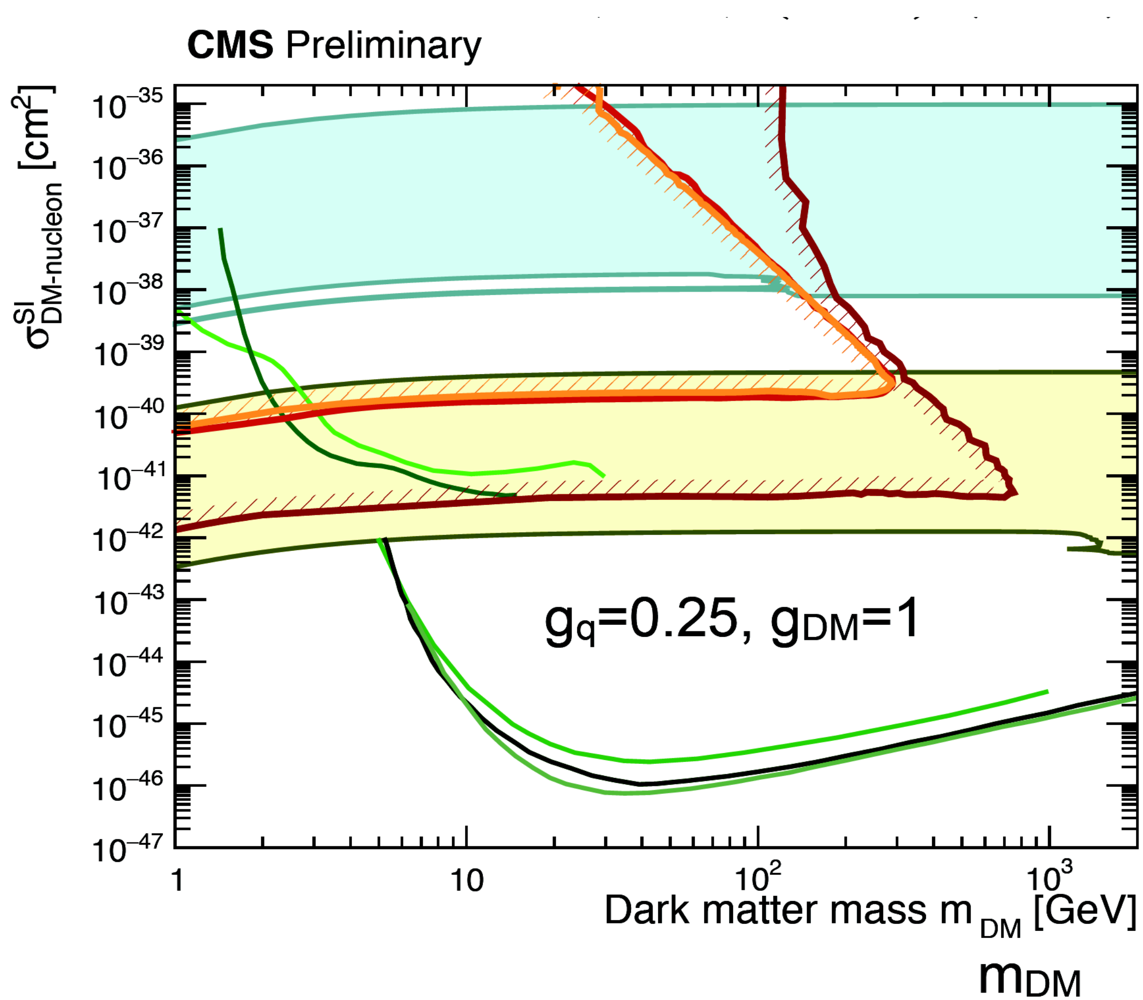

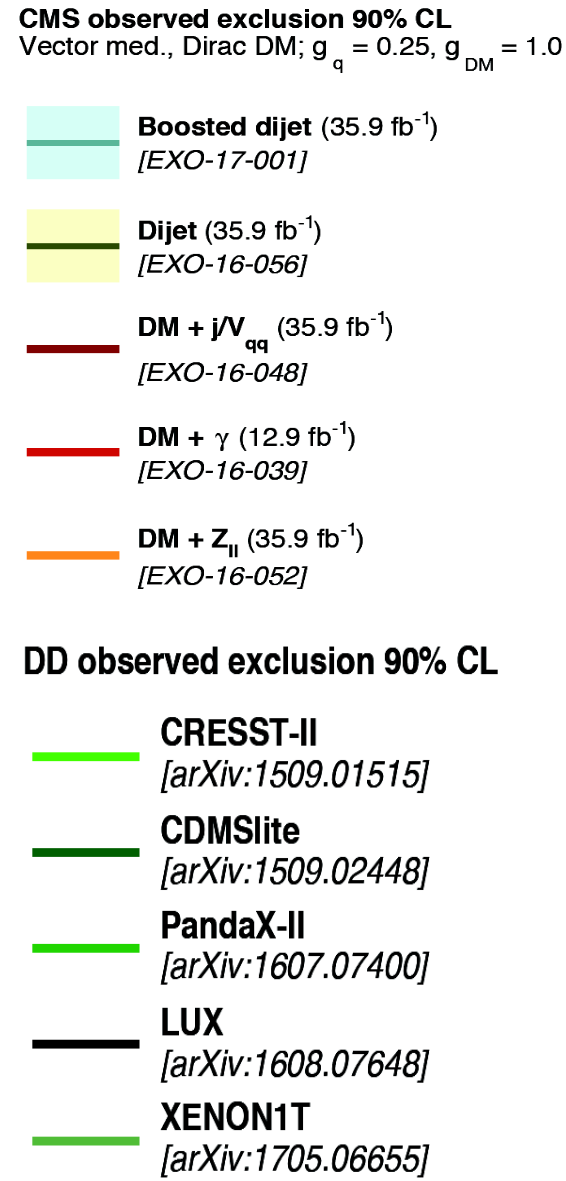

$$\sigma_{SI}^{vector} \simeq 6.9\times10^{-41}\,\mathrm{cm}^2 \left(\frac{g_q g_{DM}}{0.25}\right)^2 \left(\frac{1\ \mathrm{TeV}}{M_{med}}\right)^4 \left(\frac{\mu_{n\chi}}{1\ \mathrm{GeV}}\right)^2$$

CMS Bounds on DM-Nucleon scattering (SI)

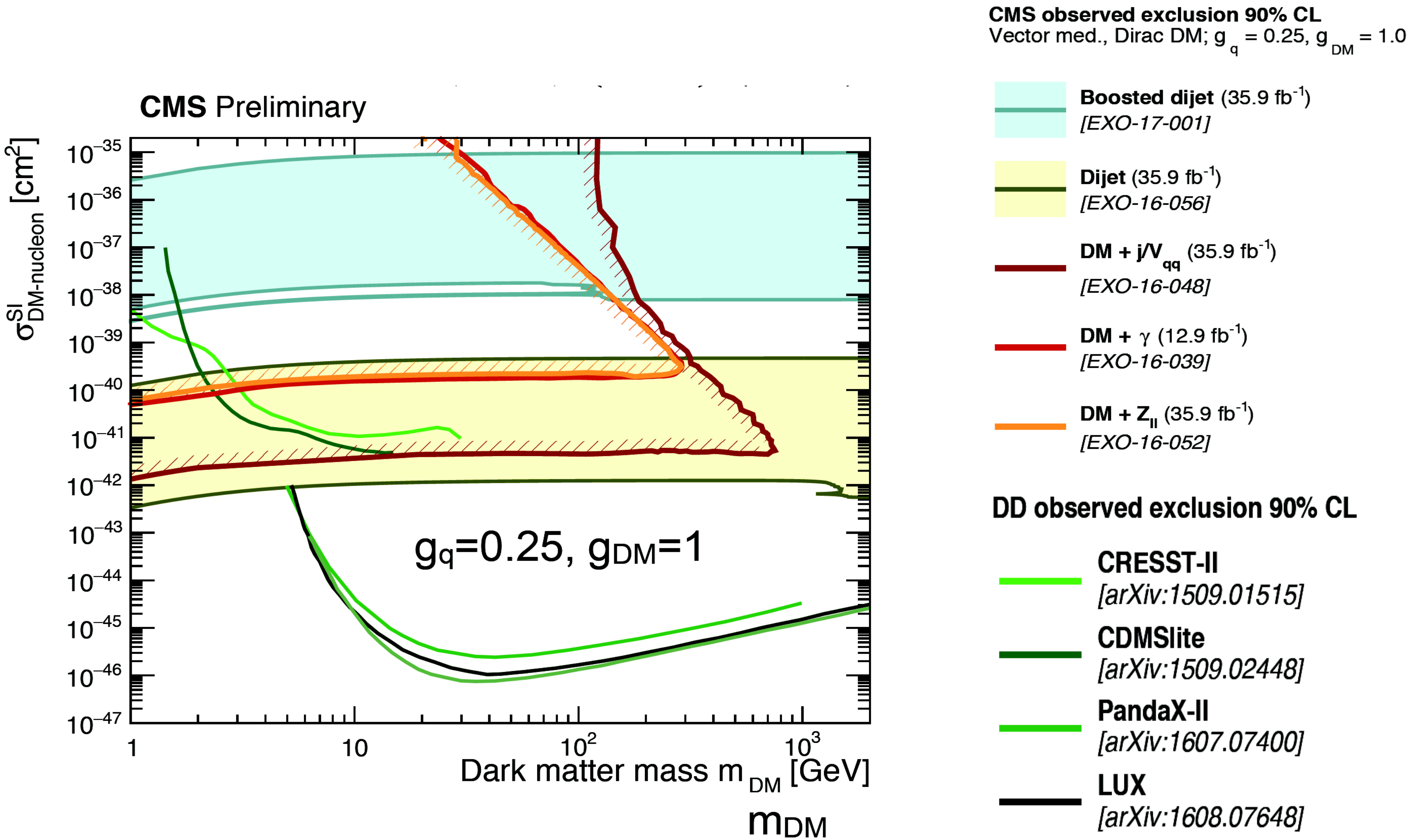

$$\sigma_{SI}^{\text{vector}} \simeq 6.9\times10^{-41}\,\text{cm}^2\left(\frac{g_q g_{DM}}{0.25}\right)^2\left(\frac{1\ \text{TeV}}{M_{\text{med}}}\right)^4\left(\frac{\mu_{n\chi}}{1\ \text{GeV}}\right)^2$$

ATLAS bounds on DM-nucleon scattering (SI)

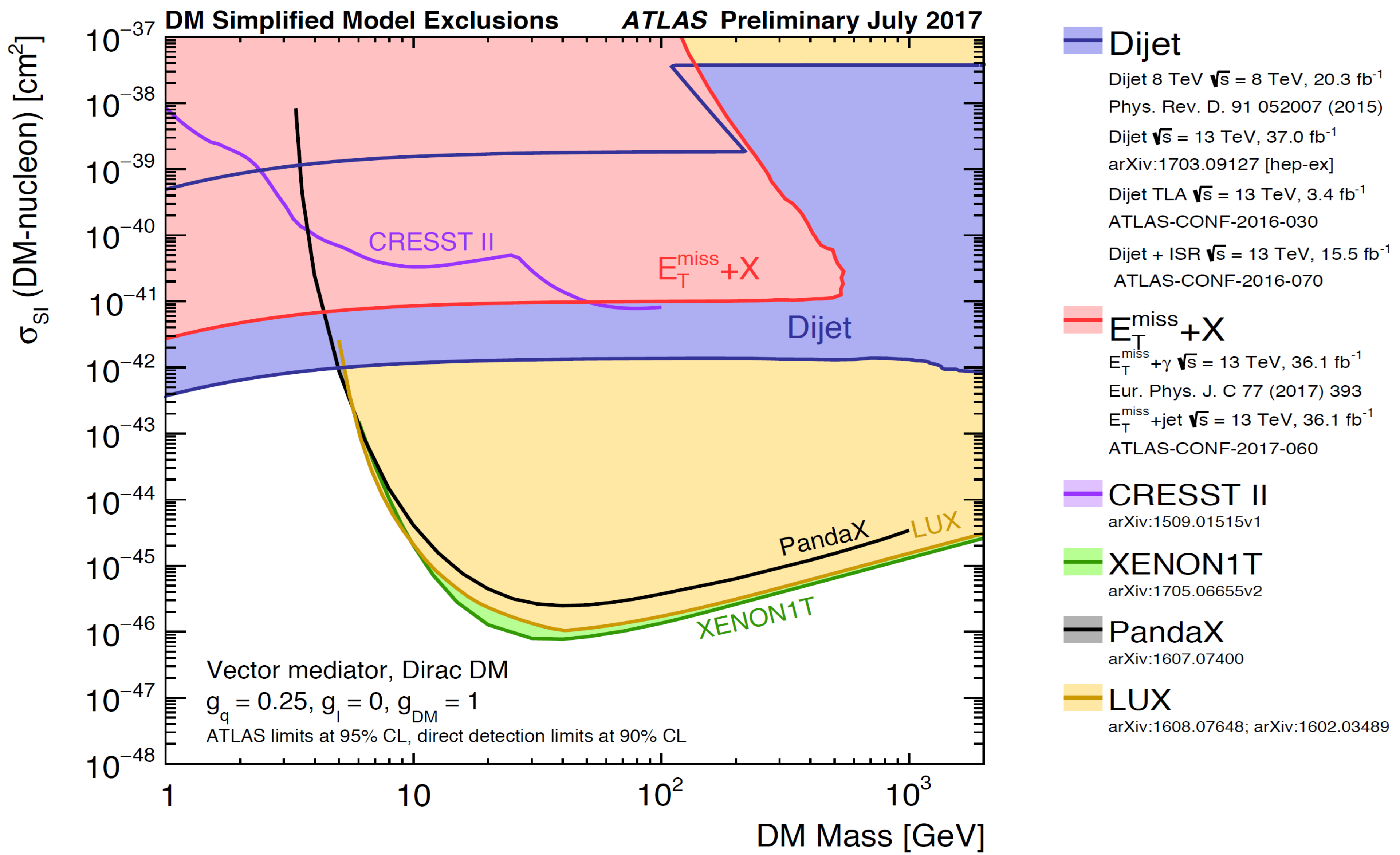

CMS bounds on DM-nucleon scattering (SD)

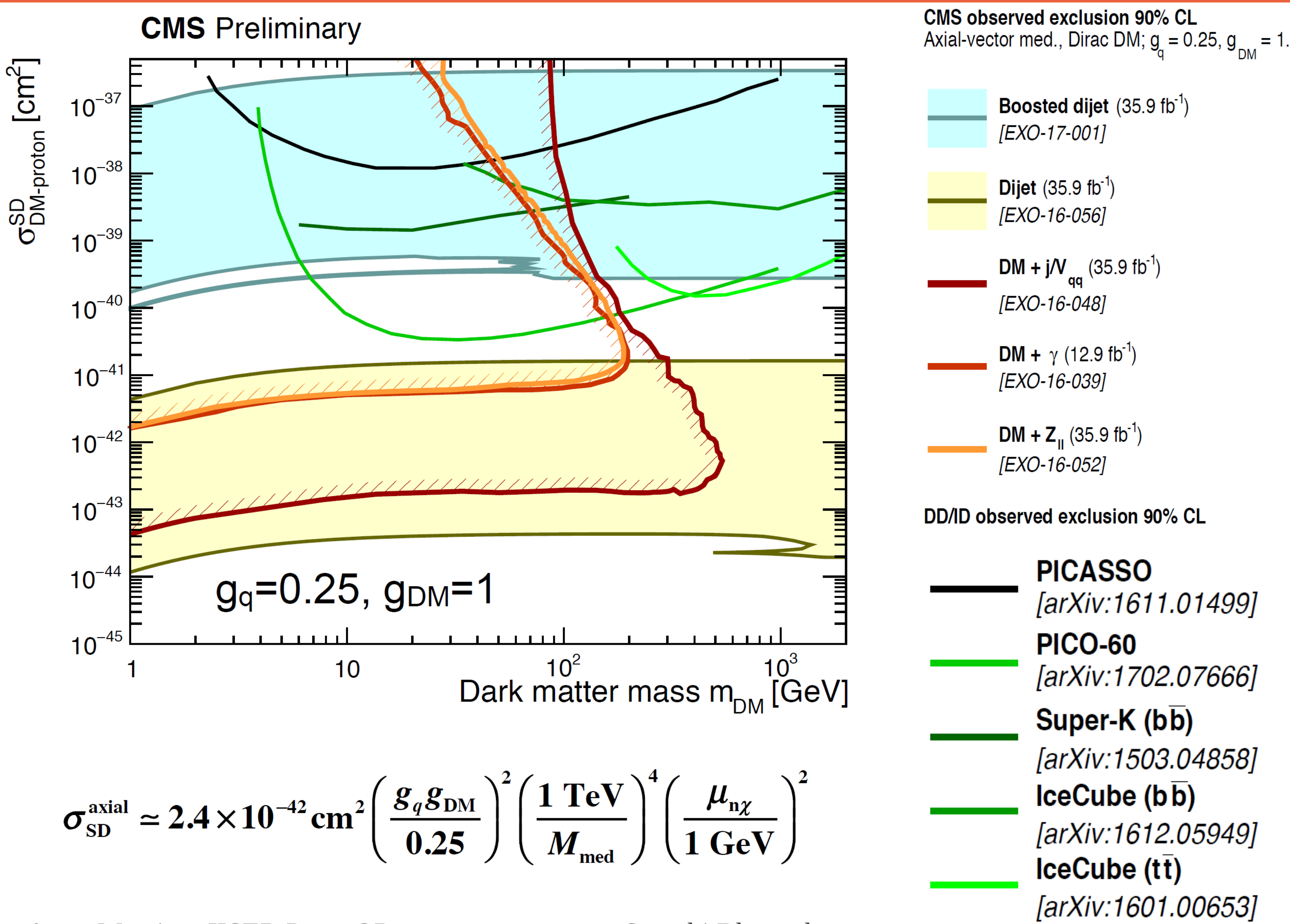

$$\sigma_{SD}^{axial} \simeq 2.4\times10^{-42}\,\mathrm{cm}^2 \left(\frac{g_q g_{DM}}{0.25}\right)^2 \left(\frac{1\,\mathrm{TeV}}{M_{med}}\right)^4 \left(\frac{\mu_{n\chi}}{1\,\mathrm{GeV}}\right)^2$$

ATLAS bounds on DM-nucleon scattering (SD)

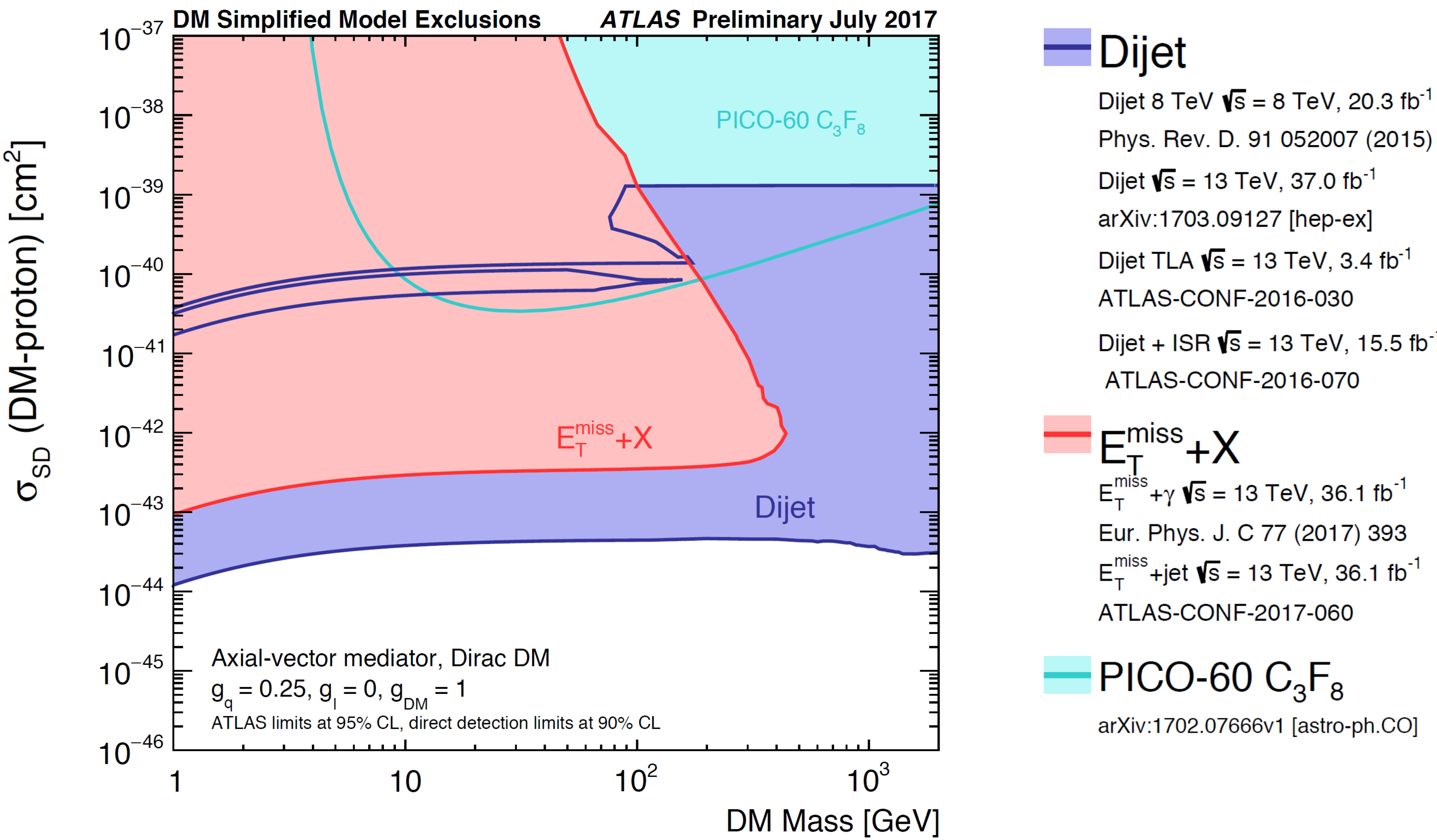

Conclusion

- Direct searches have some interesting excesses which are not confirmed by other experiments
- New experiments are looking at larger volumes and lower thresholds
- From LHC many new results @ 13 TeV
- No evidence (so far!)
- Translated to bounds on DM-Nucleon scattering cross sections
- Complements direct searches, specially in lower mass region of SD scattering
- Next decade will be of interest

backup

Searches with scalar/pseudo-scalar

Shin-Shan Eiko Yu, EPS 2017

- For the mono-V channel, pseudo-scalar/Scalar limits include ggZH diagrams only because VH generators do not yet include mixing with SM Higgs
- ttbar is the best at low-mass

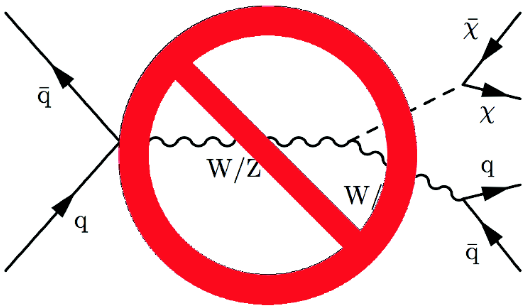

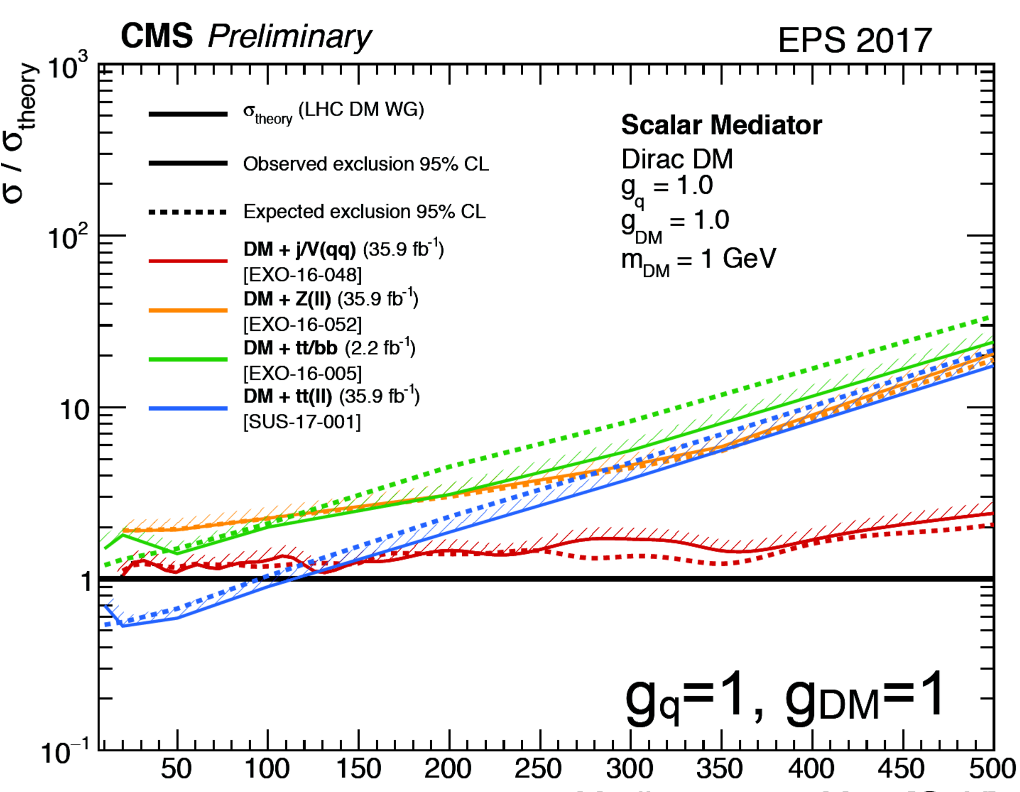

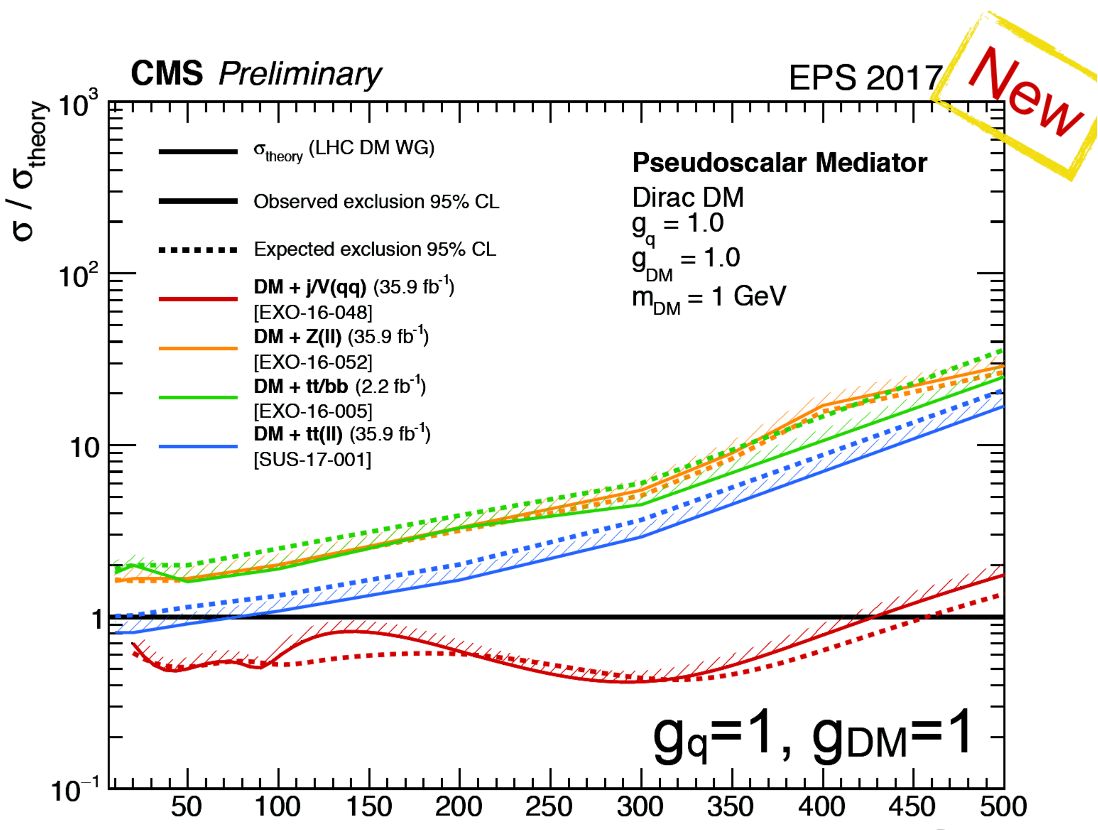

ATLAS Mono h (bb) + MET @ 13 TeV, 36 fb^{-1}

ArXiv 1707.01302

- Both small R and large R jets used (large R jets must be > 200 GeV)
- Analysis with merged jets in the highest MET bin (> 500 GeV)
- Trimming and jet substructure variables used

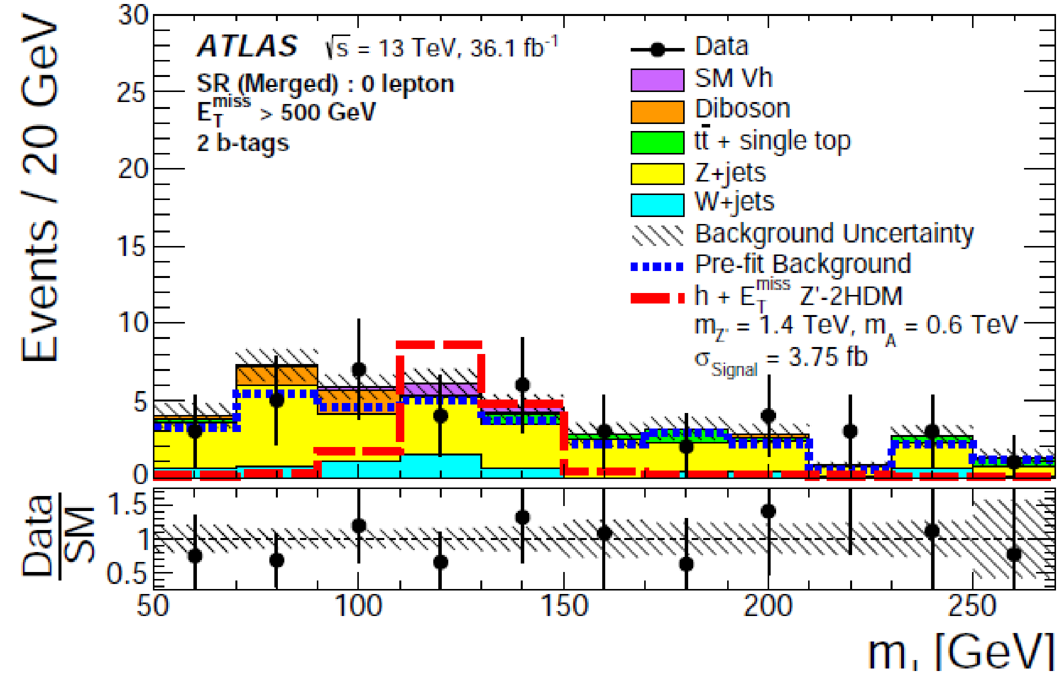

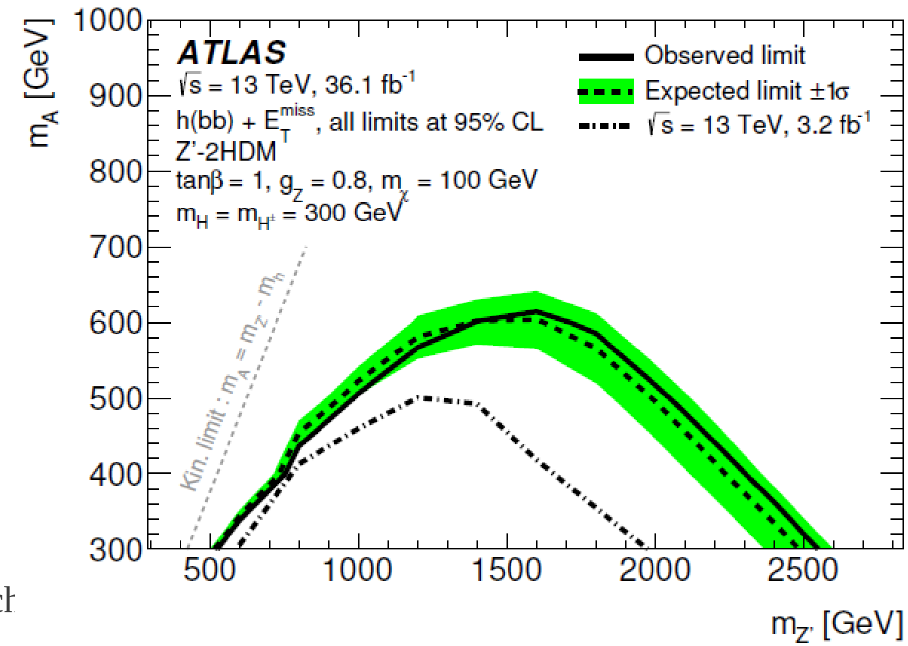

Status of LHC

- First stable beams are were produced in May
- 145 days of physics expected
- 2017 is a production year. Some challenges are to be faced to move towards HL-LHC era

~90 fb^{-1} in 2017+18

See Matteo Solfaroli, LHCC 10 May, 2017, for details

LHC schedule Q1 + Q2

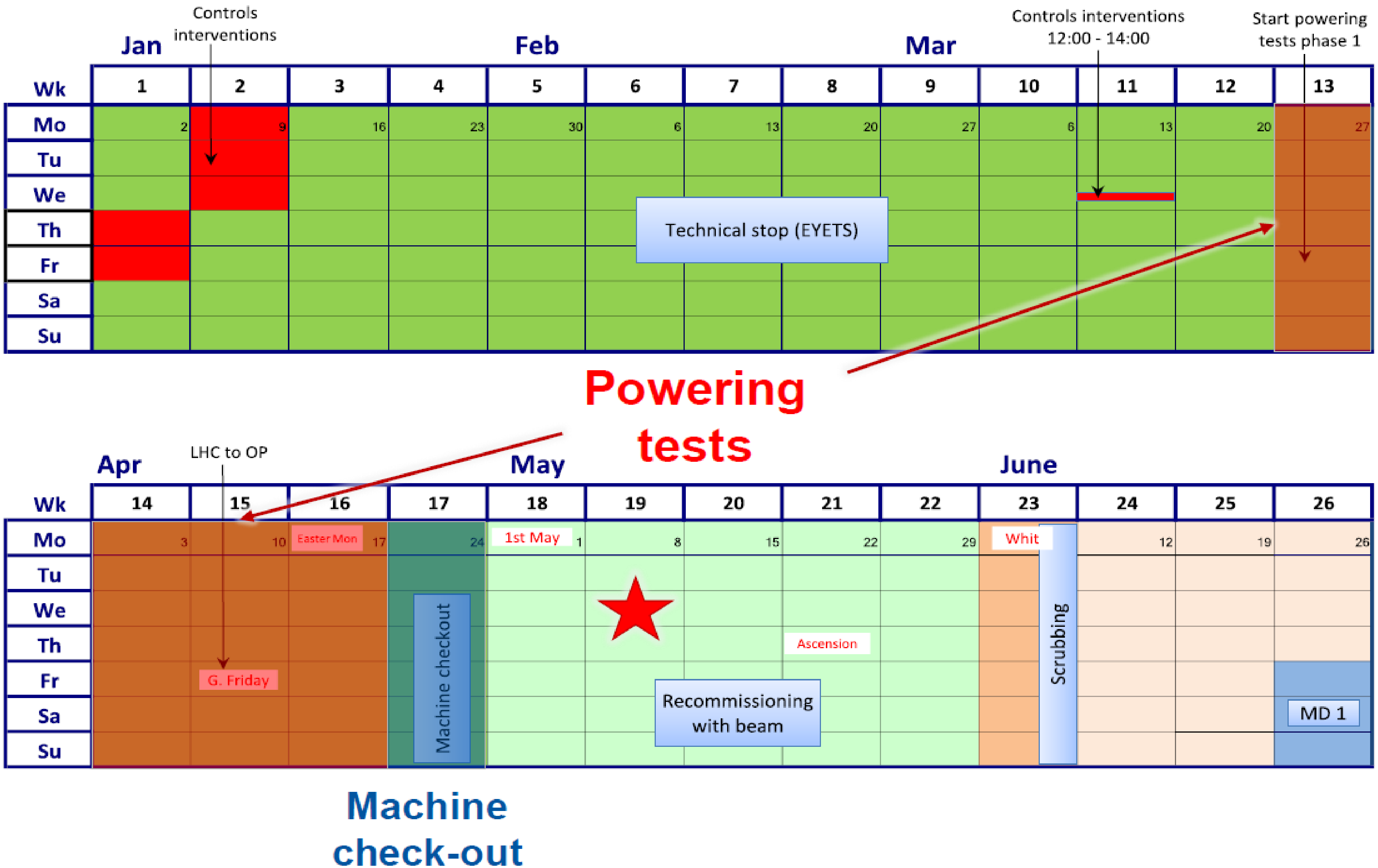

LHC Schedule Q3 + Q4

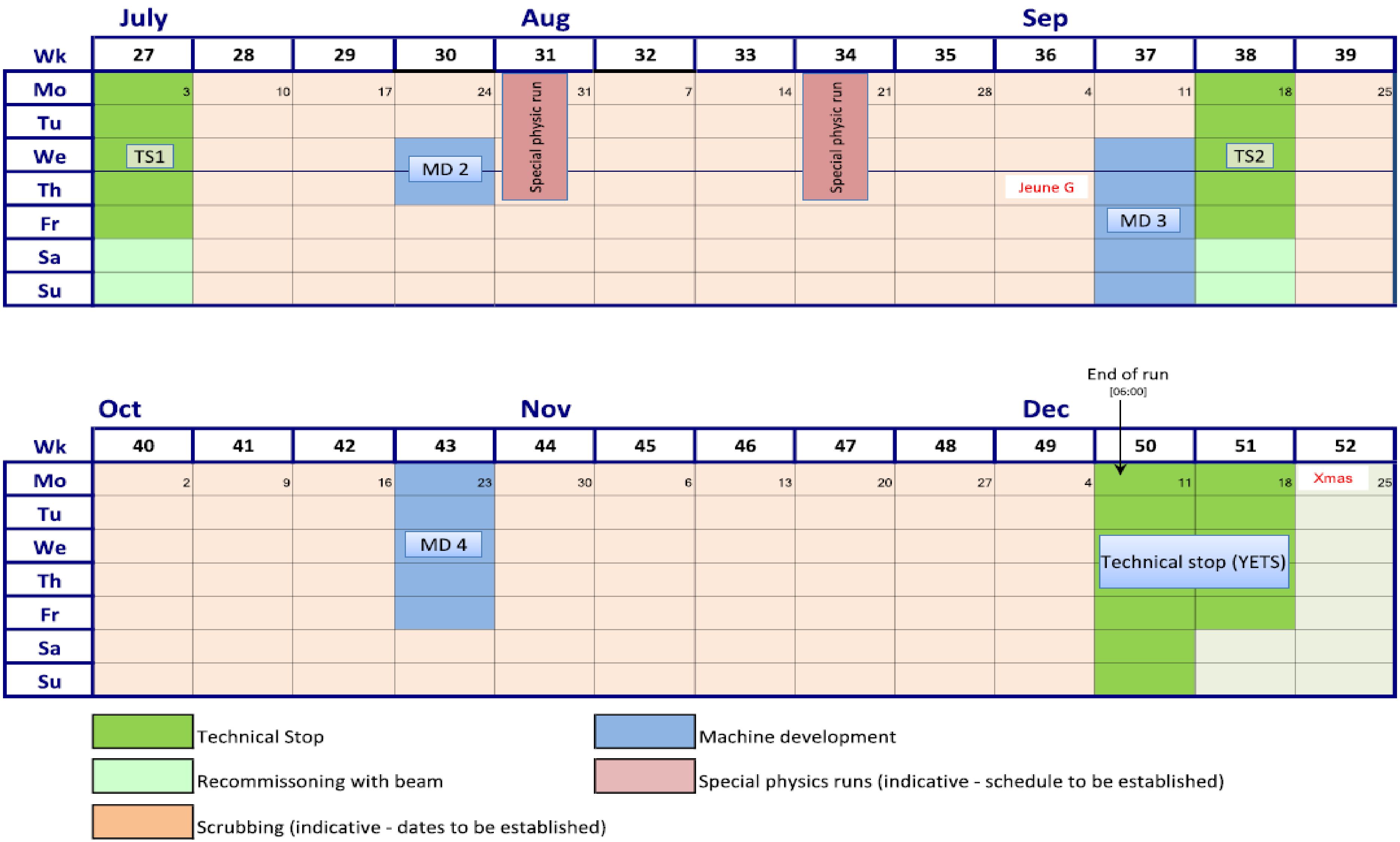

Electrons and photons

- Photon identification efficiency ~ 90%
- Photon energy resolution ~ 1% from Z to ee data

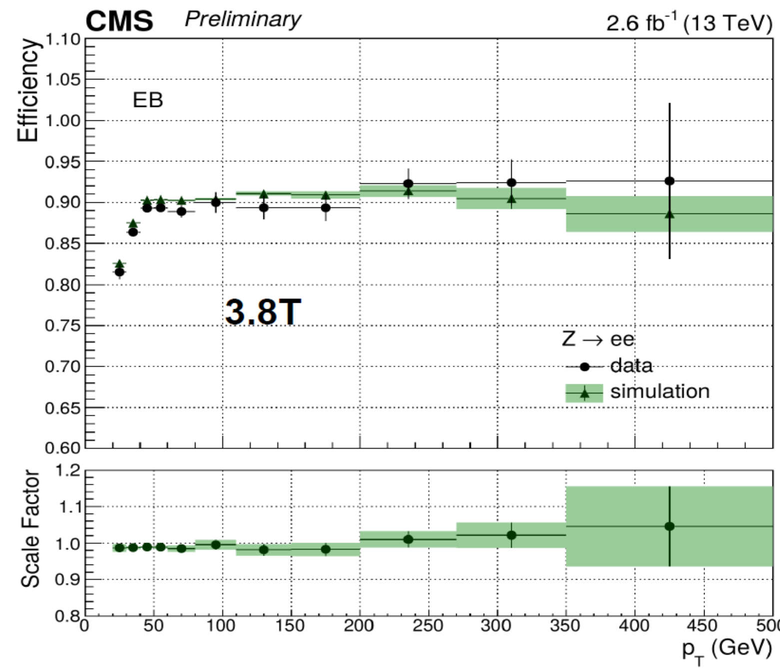

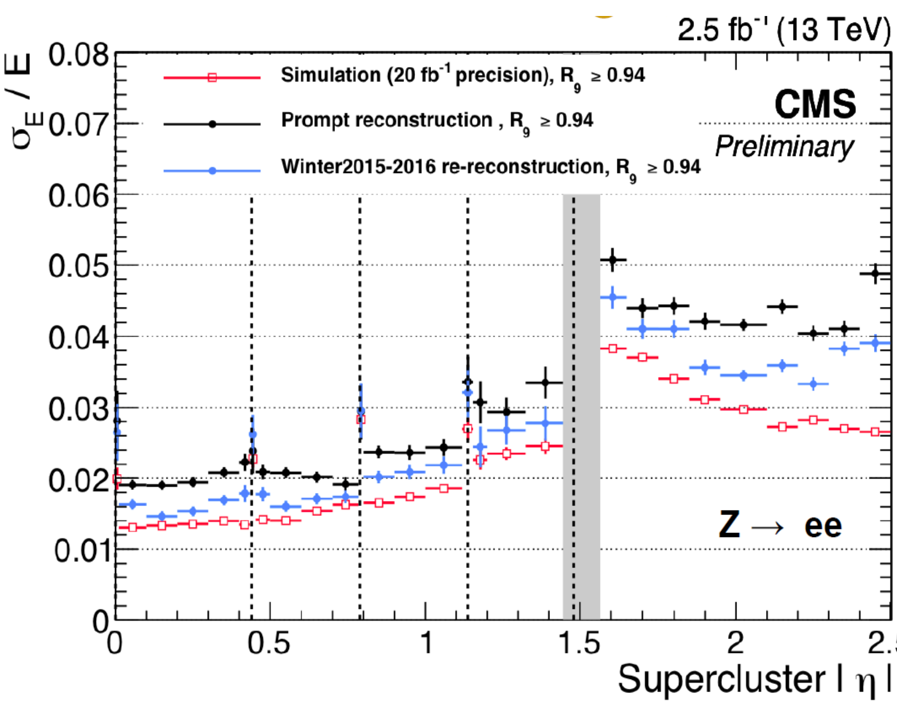

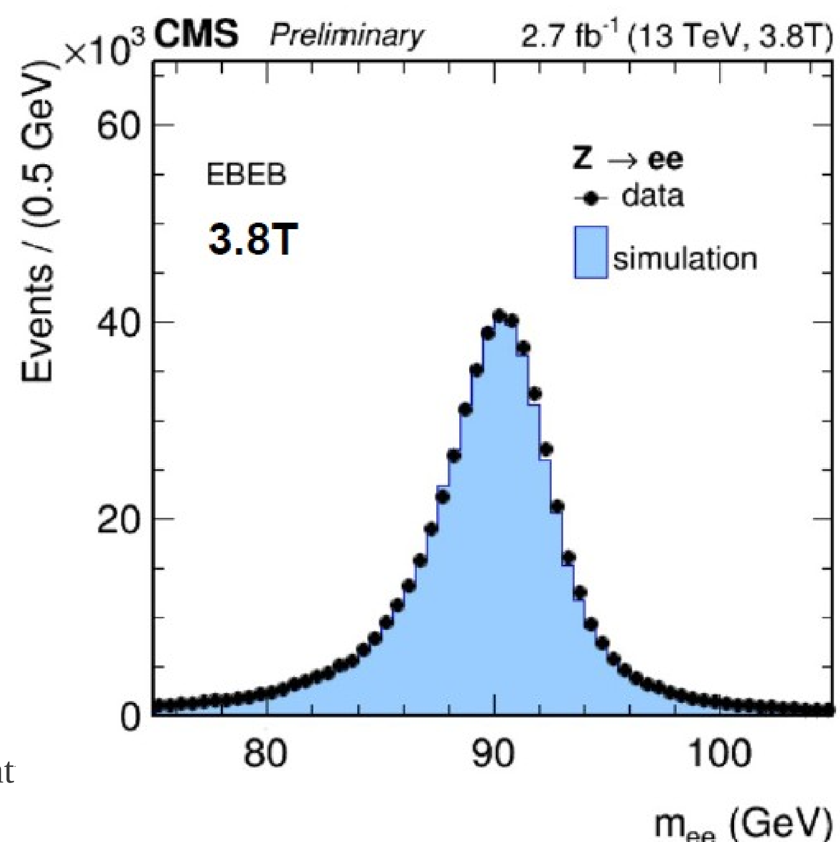

Jets

- Anti-KT with distance parameter 0.5
- CALO, JPT, PF
- PF jets clustered from PF candidate particles
- Resolution measured from MC and various energy balancing methods

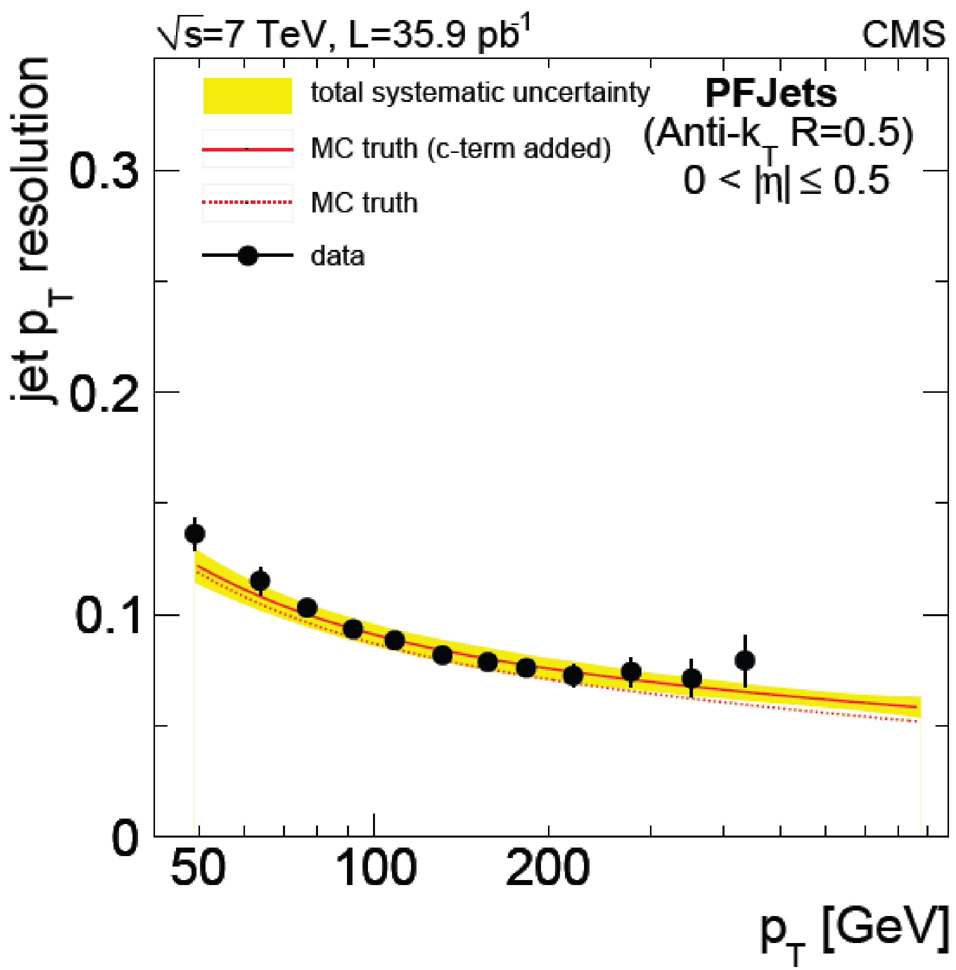

2011 JINST 6 P11002

MET ($\not{E}_T$)

- Constructed from PF candidates
- Correted for various detector effects
- Dominated by jet enrgy resolution

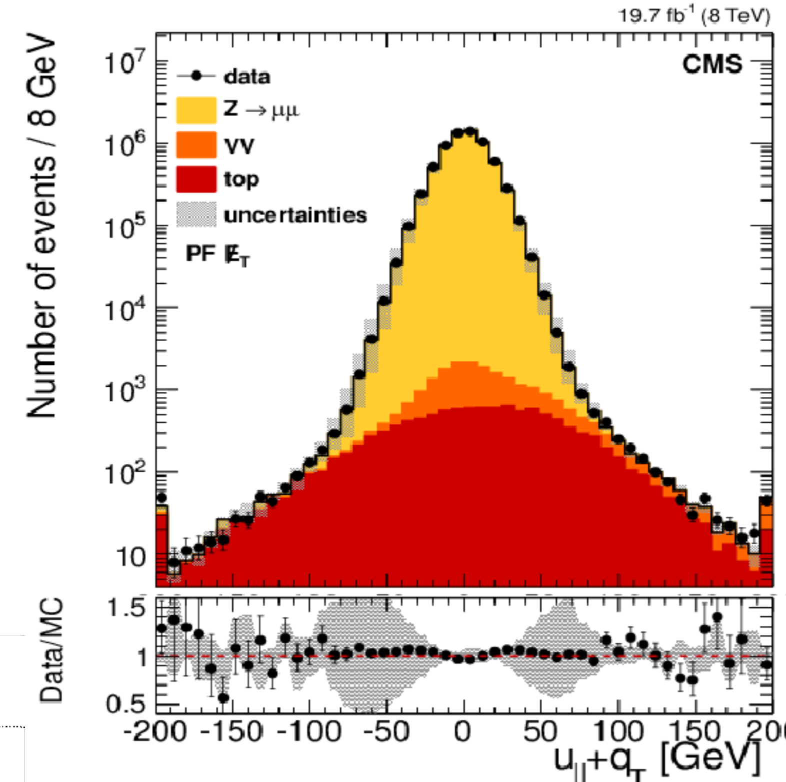

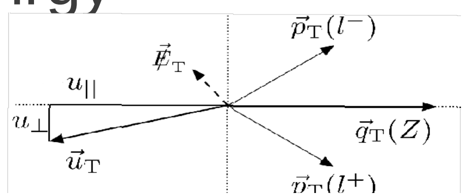

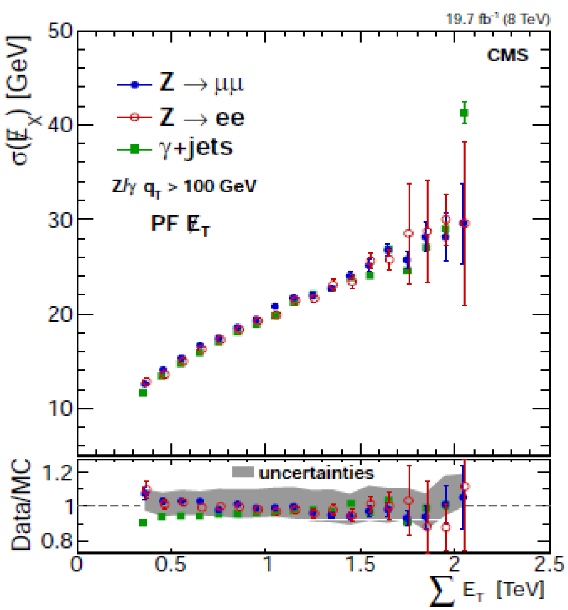

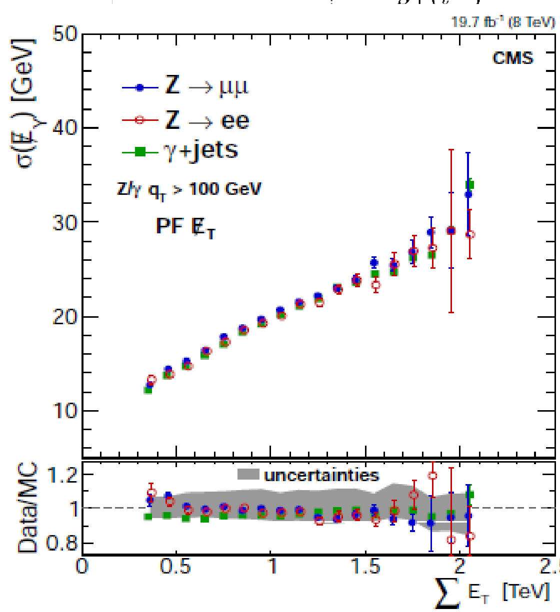

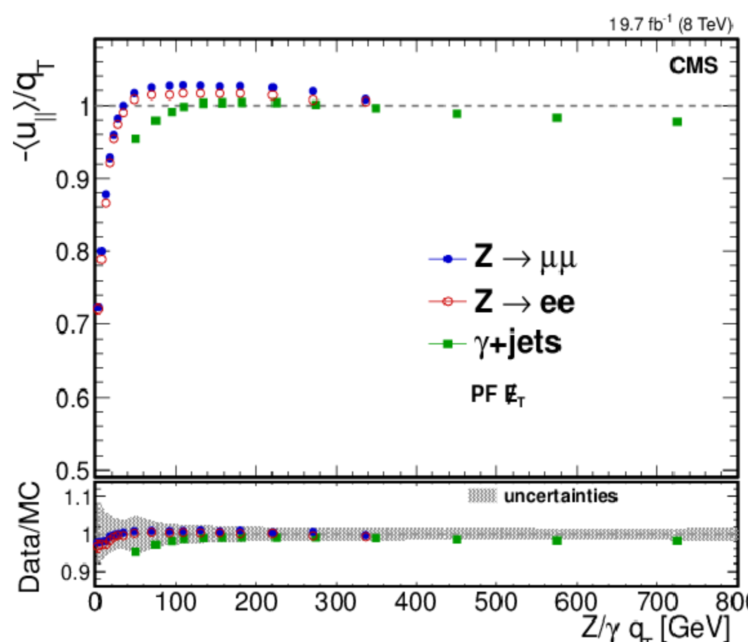

Muons

- 1-6% relative momentum resolution for pT<100GeV
- > 10% at a TeV
- > 1% hadron to muon fake probability
- Single muon trigger rates (much) better than 90% above a few GeV

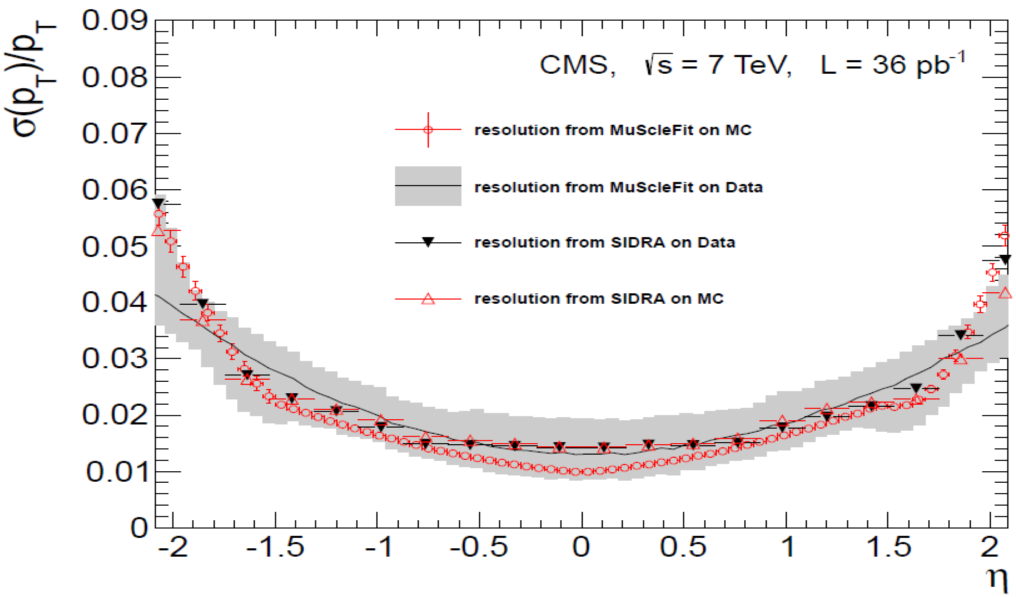

Tau efficiency

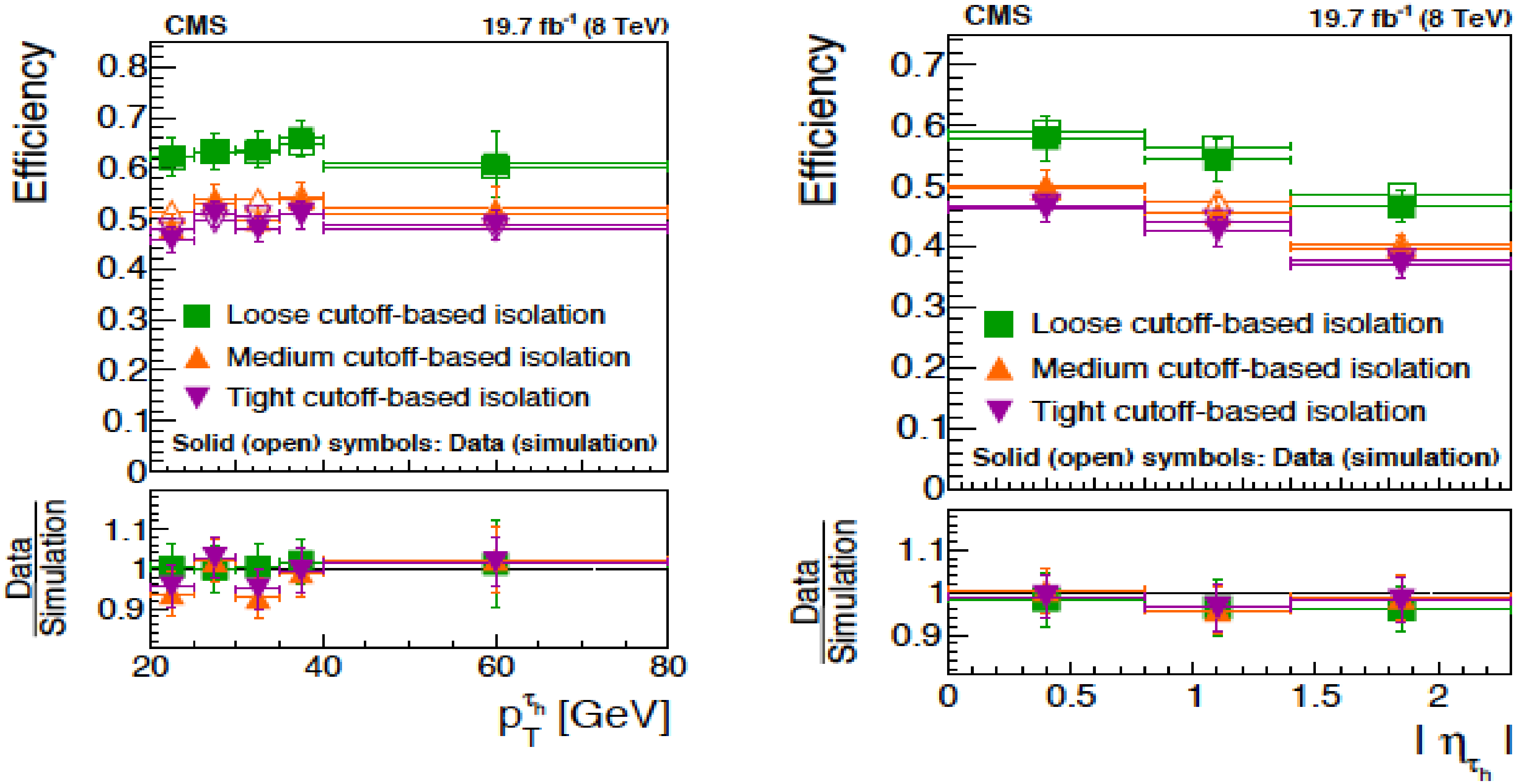

Particle Flow

- Reconstruct all stable particles in CMS detector by linking responses of subdetectors
  - Photon, electron, muon, charged and neutral hadrons
  - Resulting list of particles can be used as if they came from a MC generator
  - Composite objects like jets, taus, MET can be reconstructed from the “PF candidates”

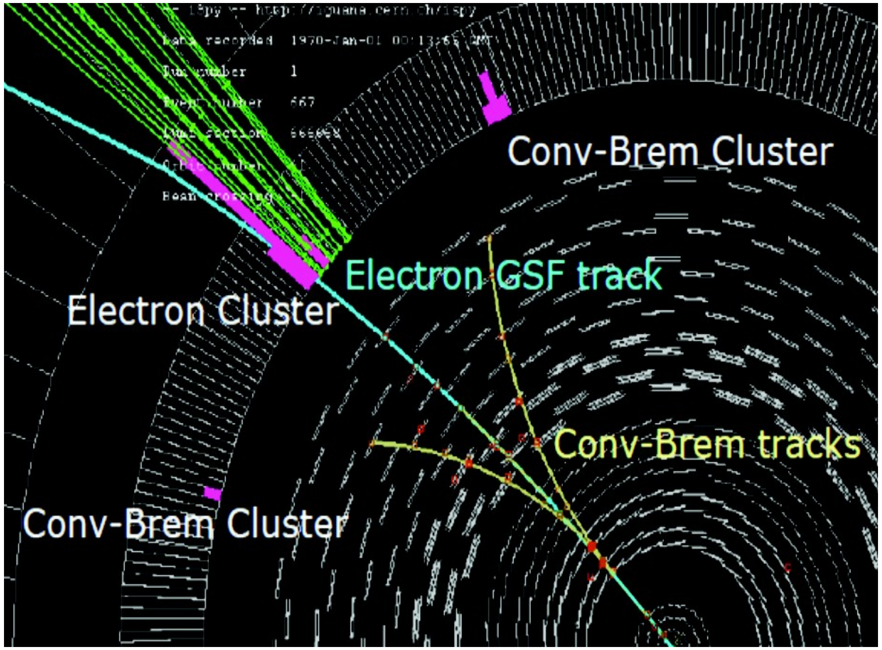

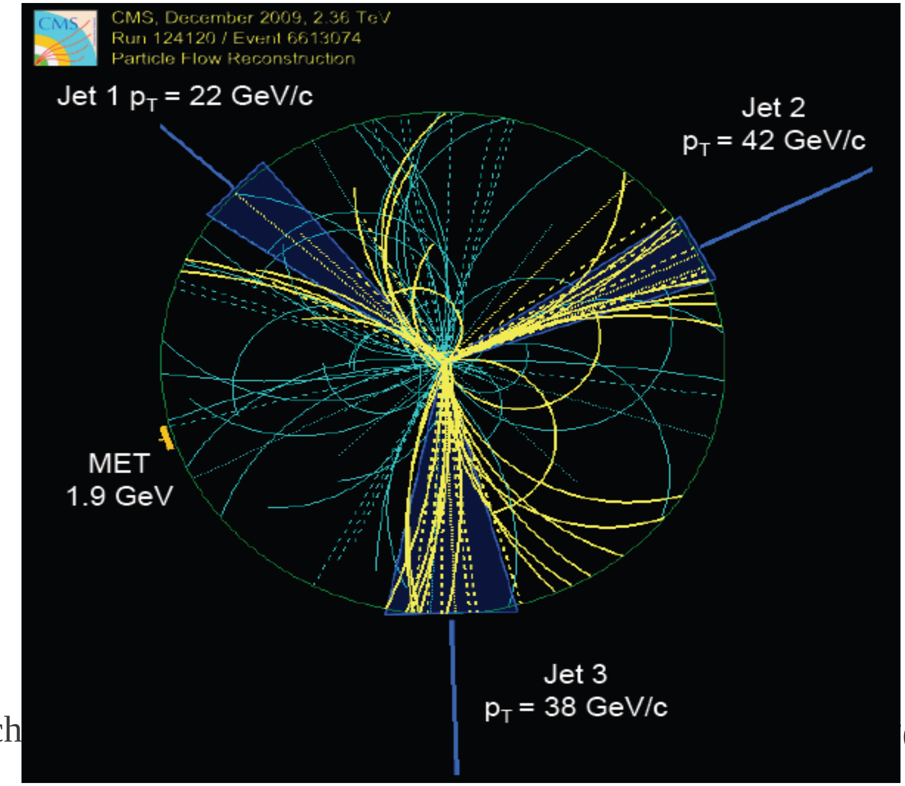

Taus: The HPS algorithm

- charged hadrons reconstructed using PF algorithm
  - π0's are reconstructed in ECAL as strips
- Strips:
  - $\pi^0 \to \gamma\gamma$
  - Photon conversion in the tracker material
  - electron tracks bending in the magnetic field: broadening of the signal in the azimuthal direction
  - A strip of 0.05 in η and 0.2 in φ is built
  - Mass is required to be consistent with π0

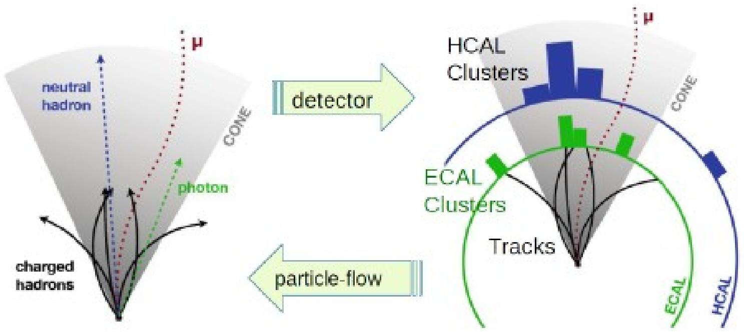

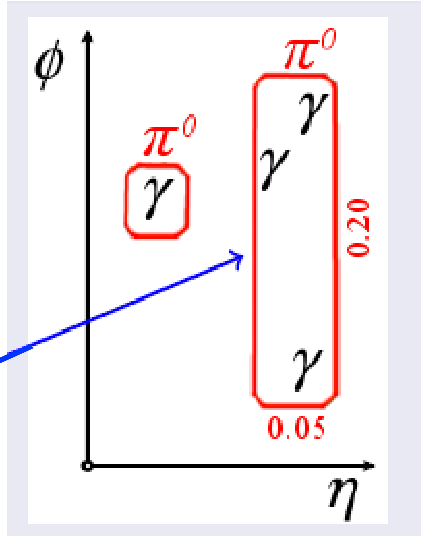

b-tagging efficiency

- The impact parameter (IP) of the track wrt the primary vertex is used to distinguish the decay product of the b hadron from the prompt tracks
- Algorithms:
  - Track counting: sorts tracks in a jet by decreasing value of IP significance
  - Jet probability (JP): uses estimate of the likelihood that all the tracks associated to the jet come from primary vertex
  - Jet B probability (JBP): same as JP, in addition, it gives more weight to the tracks with high IP significance

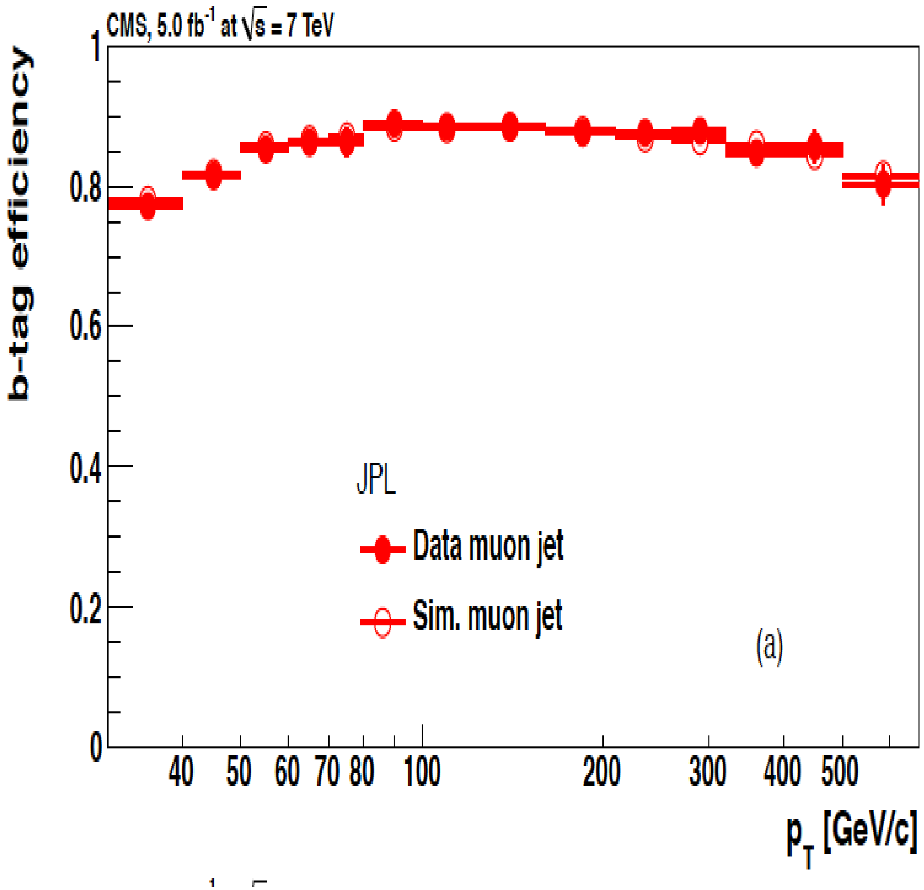

SUSY searches @ 13 TeV after 35 fb^{-1}

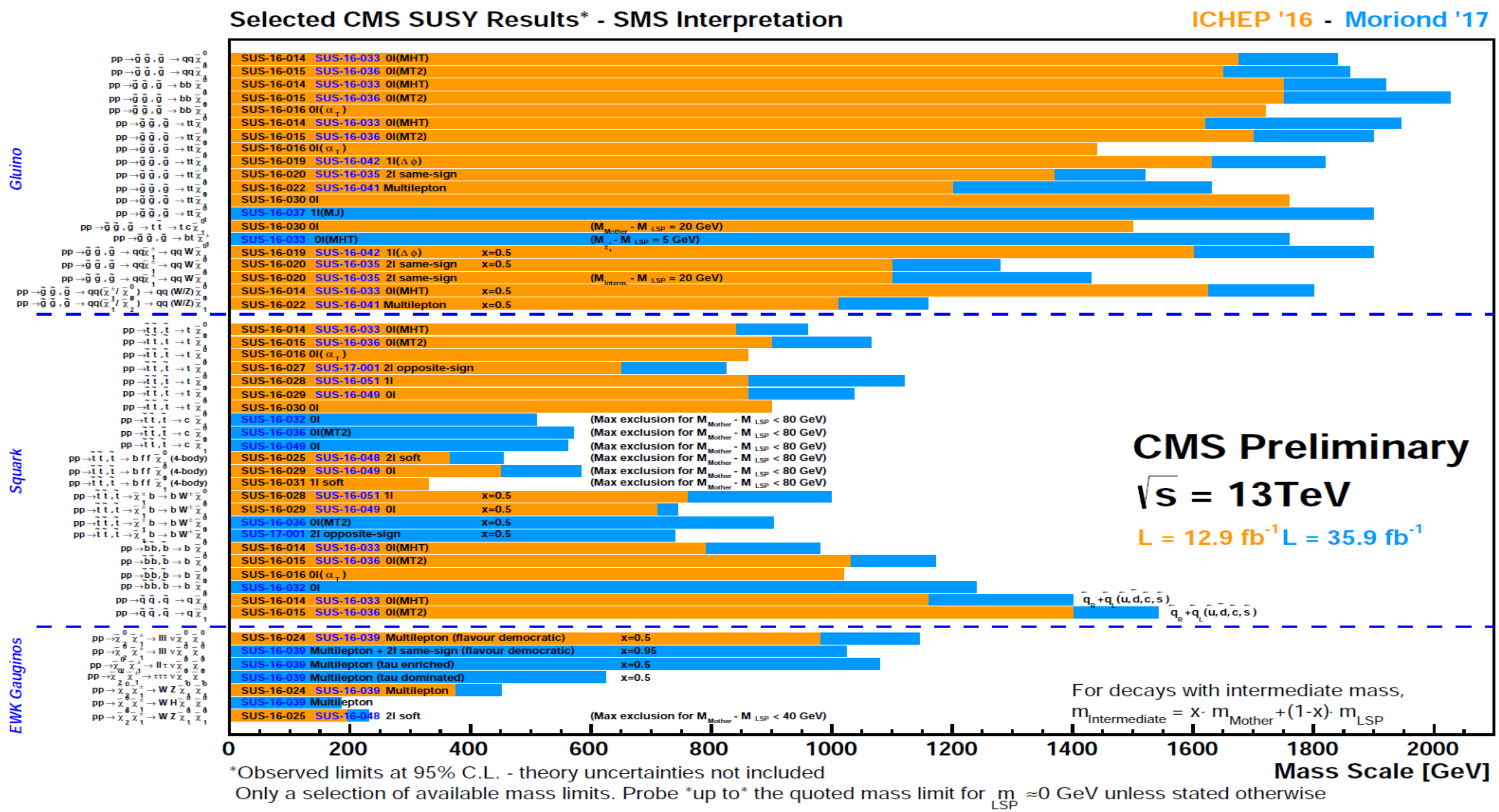

CMS Z (ll) backup 1

- Inputs to BDT

- $|m_{\ell\ell} - m_Z|$ (dilepton mass);
- $p_T^{\ell 1}$ (leading lepton transverse momentum);
- $p_T^{\ell 2}$ (subleading lepton transverse momentum);
- $p_T^{\ell\ell}$ (dilepton transverse momentum);
- $|\eta^{\ell 1}|$ (leading lepton pseudorapidity);
- $|\eta^{\ell 2}|$ (subleading lepton pseudorapidity);
- E_T^{miss} (missing transverse energy);
- $m_T(p_T^{\ell 1}, E_T^{miss})$ (leading lepton transverse mass);
- $m_T(p_T^{\ell 2}, E_T^{miss})$ (subleading lepton transverse mass);
- $\Delta\phi(\vec{p_T}^{\ell\ell}, \vec{p_T}^{miss})$ (azimuthal separation between dilepton and missing energy);
- $\Delta R_{\ell\ell}$ (separation between leptons); and
- $|\cos\theta_{\ell 1}^{CS}|$ (cosine of Collins–Soper angle for leading lepton).

CMS mono-photon @ 13 TeV

arXiv:1706.03794

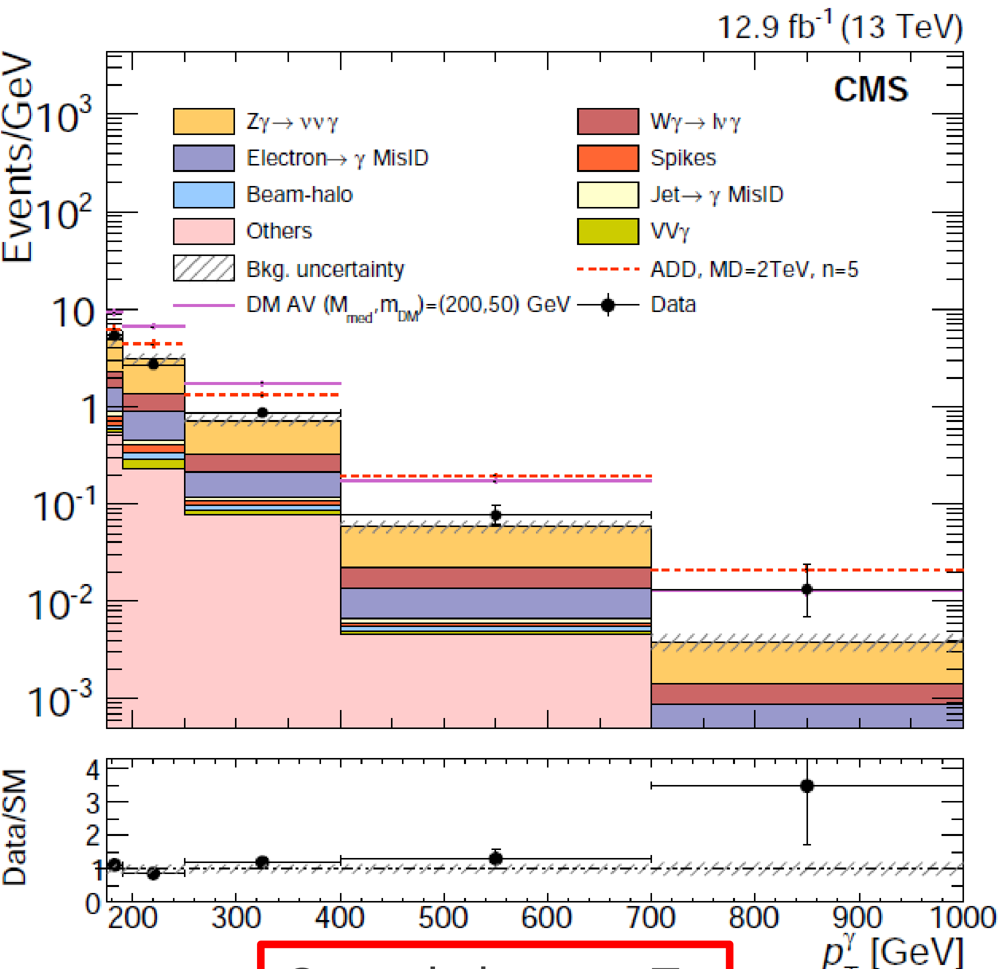

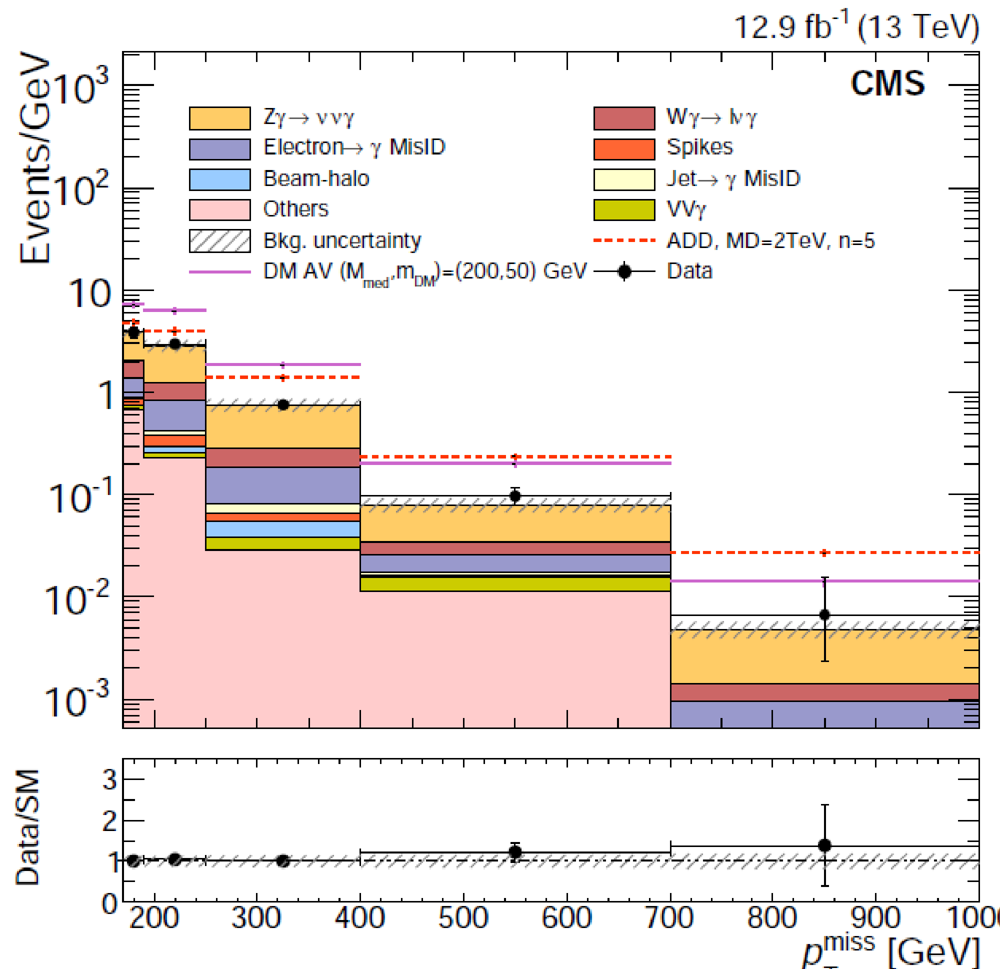

Central photon, pT > 175 GeV

MET > 170 GeV

Backgrounds to monophoton

- Large brem from beam halo muon or cosmic muon
- Anomalous signal in ECAL barrel photosensors

- Multijet events with MET
- Jet fakes photon

- Gamma + jet – gamma escapes, jet fakes photon/ jet mismeasured

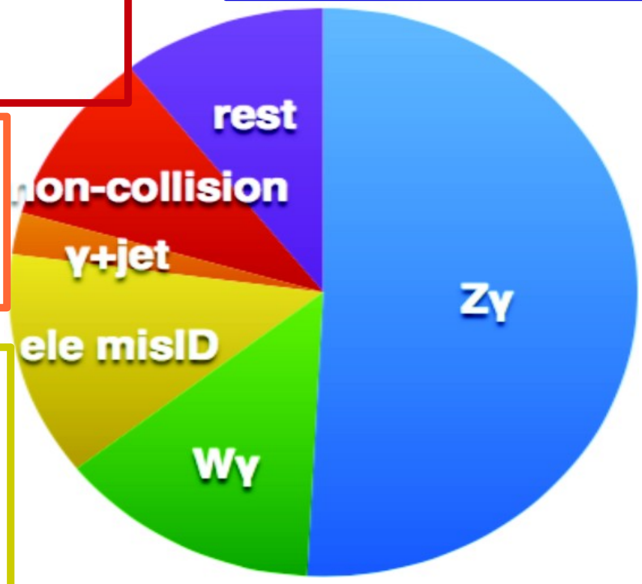

- Z(νν) + gamma irreducible.
- Z is invisible recoiling against high pT photon
- MC NNLO QCD (DYRES) + NLO EWK

- Single electron + MET (mostly single W)
- Electron misses pixel hit, identified as photon

- W(lν) + gamma
- MET from W decay + lepton escaping
- MC NNLO QCD (DYRES) + NLO EWK

ATLAS Monophoton @ 13 TeV backup

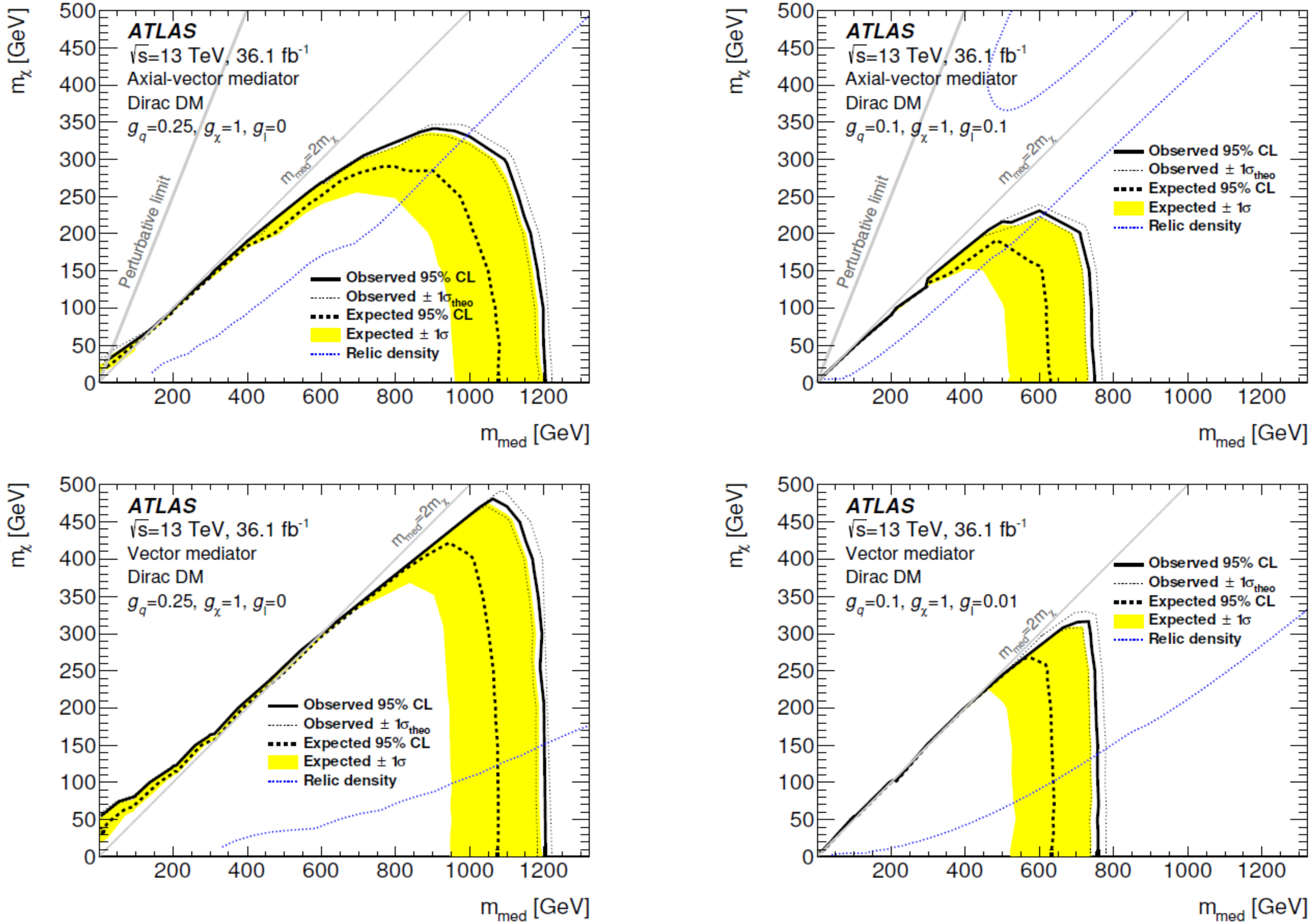

ATLAS monophoton backup

Table 2: Criteria for selecting events in the SRs and the numbers of events selected in data.

Event cleaning	Quality and Primary vertex				
Leading photon	$E_T^\gamma > 150$ GeV, $\|\eta\| < 1.37$ or $1.52 < \|\eta\| < 2.37$, tight, isolated, $\|z\| < 0.25$ m, $\Delta\phi(\gamma, E_T^{miss}) > 0.4$				
$E_T^{miss} / \sqrt{\Sigma E_T}$	> 8.5 GeV$^{1/2}$				
Jets	0 or 1 with $p_T > 30$ GeV, $\|\eta\| < 4.5$ and $\Delta\phi(\text{jets}, E_T^{miss}) > 0.4$				
Lepton	veto on e and μ				
	SRI1	SRI2	SRI3	SRE1	SRE2
E_T^{miss} [GeV]	> 150	> 225	> 300	150–225	225–300
Selected events in data	2400	729	236	1671	493
Events with 0 jets	1559	379	116	1180	263

	SRI1	1muCR	2muCR	2eleCR	PhJetCR
Observed events	2400	1083	254	181	5064
Fitted Background	2600±160	1083±33	243±13	193±10	5064±80
$Z(\to \nu\nu)\gamma$	1600±110	1.7±0.2	–	–	81±6
$W(\to \ell\nu)\gamma$	390±24	866±40	1.1±0.3	0.7±0.1	163±9
$Z(\to \ell\ell)\gamma$	35±3	77±5	233±13	180±10	13±1
γ + jets	248±80	33±8	–	–	4451±80
Fake photons from electrons	199±40	17±3	0.50±0.13	0.09±0.04	72±14
Fake photons from jets	152±22	88±19	7.9±3.8	12±5	284±28
Pre-fit background	2400±200	1025±72	218±15	181±13	4800±1000

ATLAS Z(ll) backup

Final State	ee	$\mu\mu$
Observed Data	437	497
Signal		
$ZH \to \ell\ell + inv$ ($BR_{H\to inv} = 30\%$)	32±1±3	34±1±3
DM ($m_{\text{med}} = 500$ GeV, $m_\chi = 100$ GeV) $\times$ 0.27	10.8±0.3±0.8	11.1±0.3±0.8
Backgrounds		
$qqZZ$	212±3±15	221±3±17
$ggZZ$	18.9±0.3±11.2	19.3±0.3±11.4
WZ	106±2±6	113±3±5
Z + jets	30±1±28	37±1±19
Non-resonant-$\ell\ell$	30±4±2	33±4±2
Others	1.4±0.1±0.2	2.5±2.0±0.8
Total Background	399±6±34	426±6±28

Table 3: 95% CL upper limits on $BR_{H\to inv}$ for $m_H = 125$ GeV from the ee, $\mu\mu$, and combined $ee + \mu\mu$ channels. Both the observed and expected limits are given, and the 1σ and 2σ uncertainties on the expected limits are also presented.

	Exp. $BR_{H\to inv}$ Limit $\pm 1\sigma \pm 2\sigma$	Obs. $BR_{H\to inv}$ Limit
$ee + \mu\mu$	$39\%\,^{+17\%}_{-11\%}\,^{+38\%}_{-18\%}$	67%
ee	$51\%\,^{+21\%}_{-15\%}\,^{+49\%}_{-24\%}$	59%
$\mu\mu$	$48\%\,^{+20\%}_{-14\%}\,^{+46\%}_{-22\%}$	97%

As
201

CMS Higgs + DM

CMS-EXO-16-054

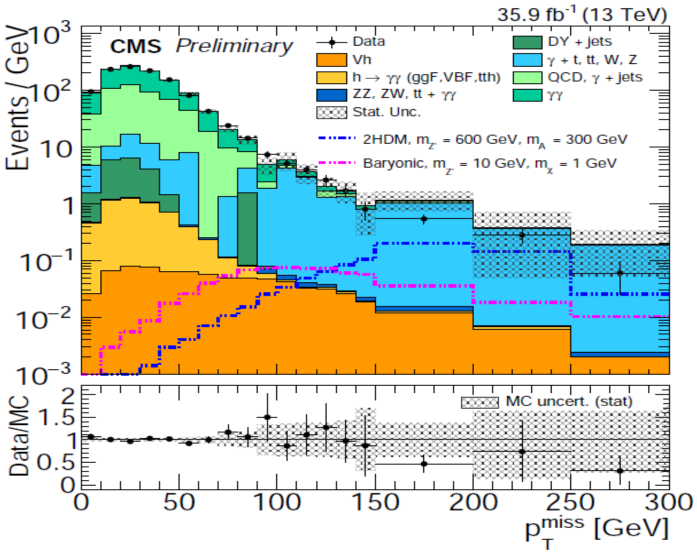

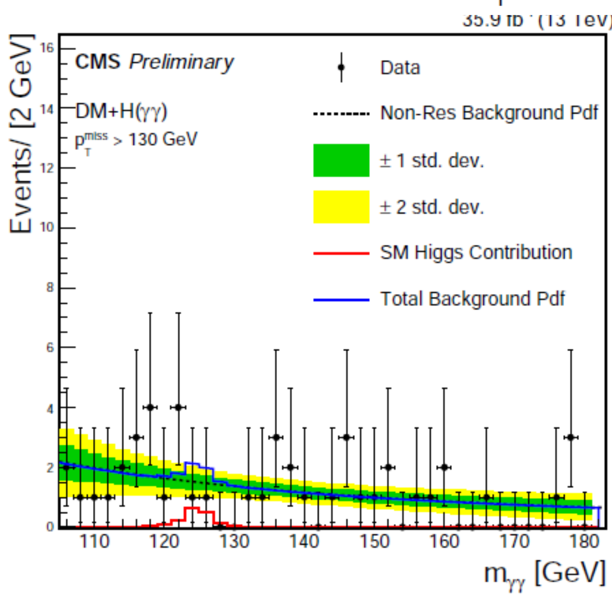

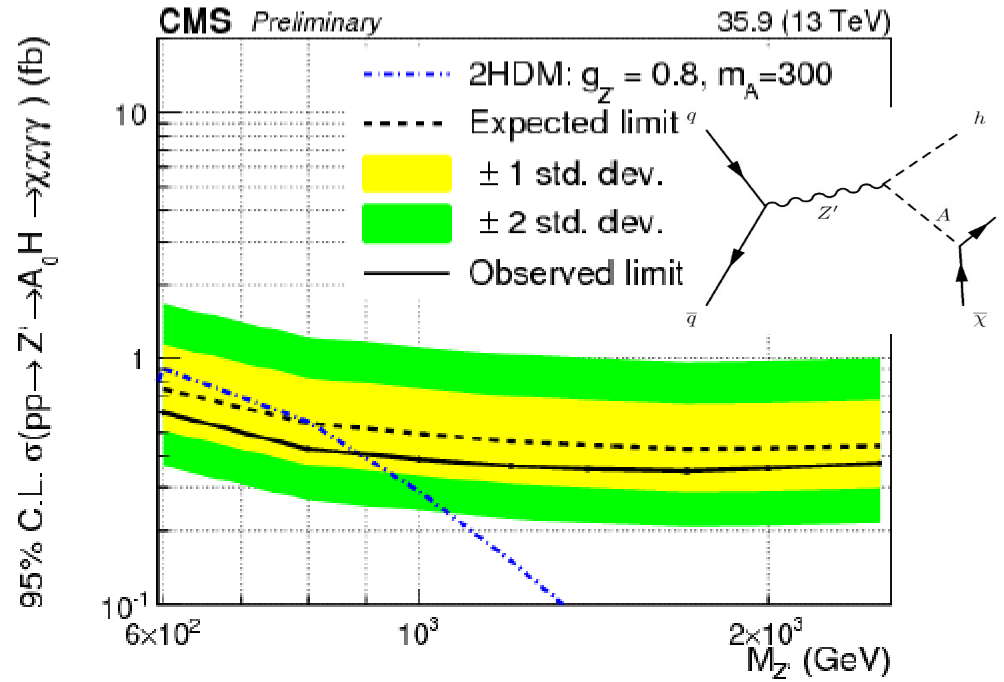

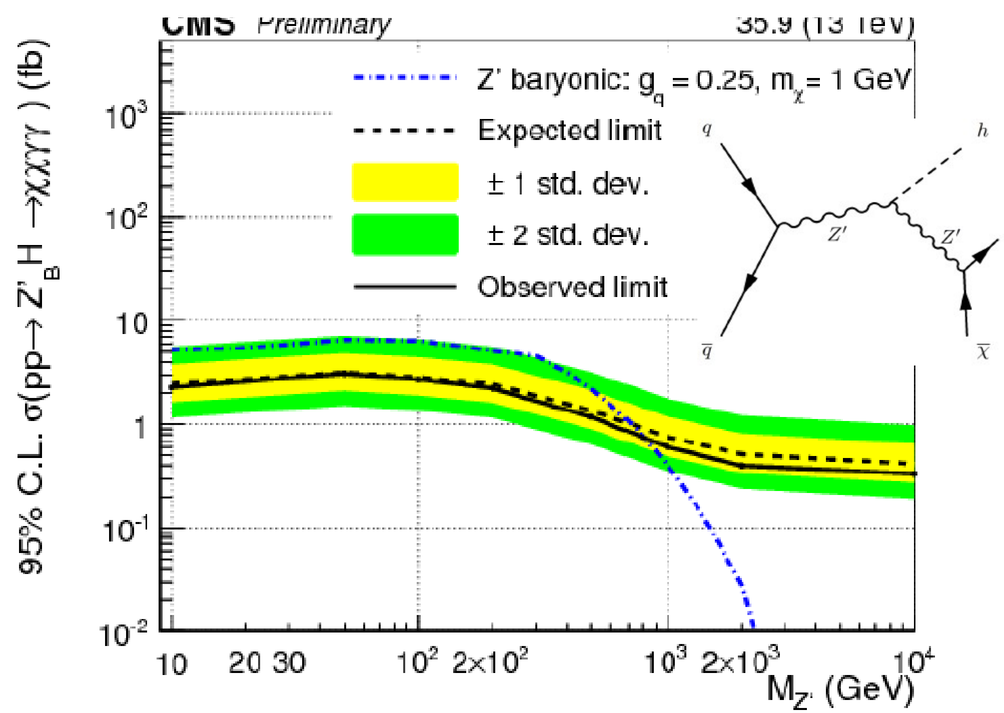

H to γγ (peak at 125 GeV)+ large MET

ATLAS older papers

Photons	http://arxiv.org/abs/1604.01306 (13 TeV) Phys. Rev. D 91, 012008 (8 TeV)	
Heavy flavour quarks	Eur. Phys. J. C (2015) 75:92 (8 TeV)	
W and Z bosons	Hadronic decays: ATLAS-CONF-2015-080 (13 TeV) Phys. Rev. Lett 112, 041802 (8 TeV)	Leptonic W decays: JHEP09 (2014) 037 (8 TeV) Leptonic Z decays: PRD 90, 012004 (8 TeV)
Higgs bosons	H→bb: ATLAS-CONF-2016-019 (13 TeV) Phys. Rev. D 93, 072007 (8 TeV)	H→γγ: ATLAS-CONF-2016-011 (13 TeV) Phys. Rev. Lett. 115, 131801 (8 TeV)

ATLAS reference for V(hadronic) + MET (Xuanhong Lou, EPS 2017)

[1] ATL-PHYS-PUB-2015-033

[2] arXiv:1007.1727

[3] arXiv:1212.3352

[4] arXiv:1507.00966

[5] J. Phys. G 28 (2002) 2693–2704

More details about the search for dark matter produced in association with a hadronically decaying vector boson at $\sqrt{s}$ =13 TeV with the ATLAS detector can be found at Phys. Lett. B 763 (2016) 251

ATLAS reference for V(hadronic) + MET (Xuanhong Lou, EPS 2017)

[1] ATL-PHYS-PUB-2015-033
[2] arXiv:1007.1727
[3] arXiv:1212.3352
[4] arXiv:1507.00966
[5] J. Phys. G 28 (2002) 2693–2704

More details about the search for dark matter produced in association with a hadronically decaying vector boson at $\sqrt{s}$ =13 TeV with the ATLAS detector can be found at Phys. Lett. B 763 (2016) 251

LHC DM models

- Two models of vector mediator
- Minimum Flavor violation

$$\mathcal{L}_{\text{vector}} = -g_{\text{DM}} Z'_\mu \bar{\chi}\gamma^\mu \chi - g_q \sum_{q=u,d,s,c,b,t} Z'_\mu \bar{q}\gamma^\mu q\,,$$

$$\mathcal{L}_{\text{axial-vector}} = -g_{\text{DM}} Z'_\mu \bar{\chi}\gamma^\mu \gamma_5 \chi - g_q \sum_{q=u,d,s,c,b,t} Z'_\mu \bar{q}\gamma^\mu \gamma_5 q\,.$$

Mediator decay widths

$$\Gamma^{\chi\bar{\chi}}_{\text{vector}} = \frac{g_{\text{DM}}^2 M_{\text{med}}}{12\pi} \left(1 - 4 z_{\text{DM}}\right)^{1/2} \left(1 + 2 z_{\text{DM}}\right) , \tag{2.3}$$

$$\Gamma^{q\bar{q}}_{\text{vector}} = \frac{g_q^2 M_{\text{med}}}{4\pi} \left(1 - 4 z_q\right)^{1/2} \left(1 + 2 z_q\right) , \tag{2.4}$$

where $z_{\text{DM},q} = m^2_{\text{DM},q}/M^2_{\text{med}}$ and the two different types of contribution to the width vanish for $M_{\text{med}} < 2m_{\text{DM},q}$. The corresponding expressions for the axial-vector mediator are

$$\Gamma^{\chi\bar{\chi}}_{\text{axial-vector}} = \frac{g_{\text{DM}}^2 M_{\text{med}}}{12\pi} \left(1 - 4 z_{\text{DM}}\right)^{3/2} , \tag{2.5}$$

$$\Gamma^{q\bar{q}}_{\text{axial-vector}} = \frac{g_q^2 M_{\text{med}}}{4\pi} \left(1 - 4 z_q\right)^{3/2} . \tag{2.6}$$

The two models with a spin-0 mediator ϕ are described by

$$\mathcal{L}_{\text{scalar}} = -g_{\text{DM}} \phi \bar{\chi}\chi - g_q \frac{\phi}{\sqrt{2}} \sum_{q=u,d,s,c,b,t} y_q \bar{q} q , \tag{2.7}$$

$$\mathcal{L}_{\text{pseudo-scalar}} = -i g_{\text{DM}} \phi \bar{\chi}\gamma_5\chi - i g_q \frac{\phi}{\sqrt{2}} \sum_{q=u,d,s,c,b,t} y_q \bar{q}\gamma_5 q , \tag{2.8}$$

where $y_q = \sqrt{2} m_q / v$ are the SM quark Yukawa couplings with $v \simeq 246$ GeV the Higgs vac-

Loop induced decays to gluons

$$\Gamma^{\chi\bar{\chi}}_{\text{scalar}} = \frac{g^2_{\text{DM}} M_{\text{med}}}{8\pi} \left(1 - 4 z^2_{\text{DM}}\right)^{3/2}$$

$$\Gamma^{q\bar{q}}_{\text{scalar}} = \frac{3 g^2_q y^2_q M_{\text{med}}}{16\pi} \left(1 - 4 z^2_q\right)^{3/2}$$

$$\Gamma^{gg}_{\text{scalar}} = \frac{\alpha^2_s g^2_q M^3_{\text{med}}}{32\pi^3 v^2} \left| f_{\text{scalar}}(4 z_t)\right|^2$$

$$\Gamma^{\chi\bar{\chi}}_{\text{pseudo-scalar}} = \frac{g^2_{\text{DM}} M_{\text{med}}}{8\pi} \left(1 - 4 z^2_{\text{DM}}\right)^{1/2} ,$$

$$\Gamma^{q\bar{q}}_{\text{pseudo-scalar}} = \frac{3 g^2_q y^2_q M_{\text{med}}}{16\pi} \left(1 - 4 z^2_q\right)^{1/2} ,$$

$$\Gamma^{gg}_{\text{pseudo-scalar}} = \frac{\alpha^2_s g^2_q M^3_{\text{med}}}{32\pi^3 v^2} \left| f_{\text{pseudo-scalar}}(4 z_t)\right|^2$$

$$f_{\text{scalar}}(\tau) = \tau \left[1 + (1-\tau)\arctan^2\left(\frac{1}{\sqrt{\tau - 1}}\right)\right]$$

$$f_{\text{pseudo-scalar}}(\tau) = \tau \arctan^2\left(\frac{1}{\sqrt{\tau - 1}}\right) .$$

LHC results presentation

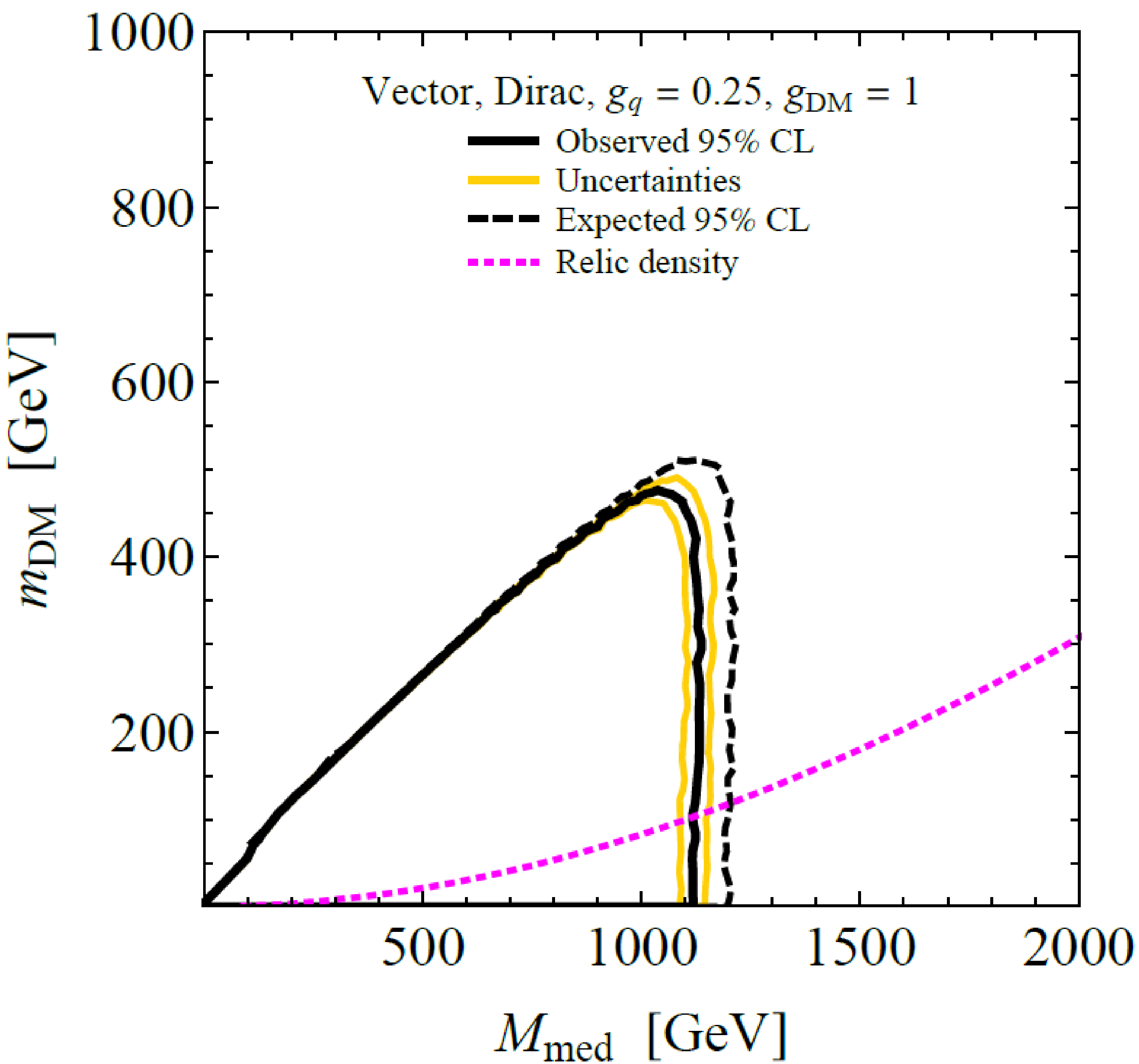

M_{DM}-M_{med} plane

LHC results presentation

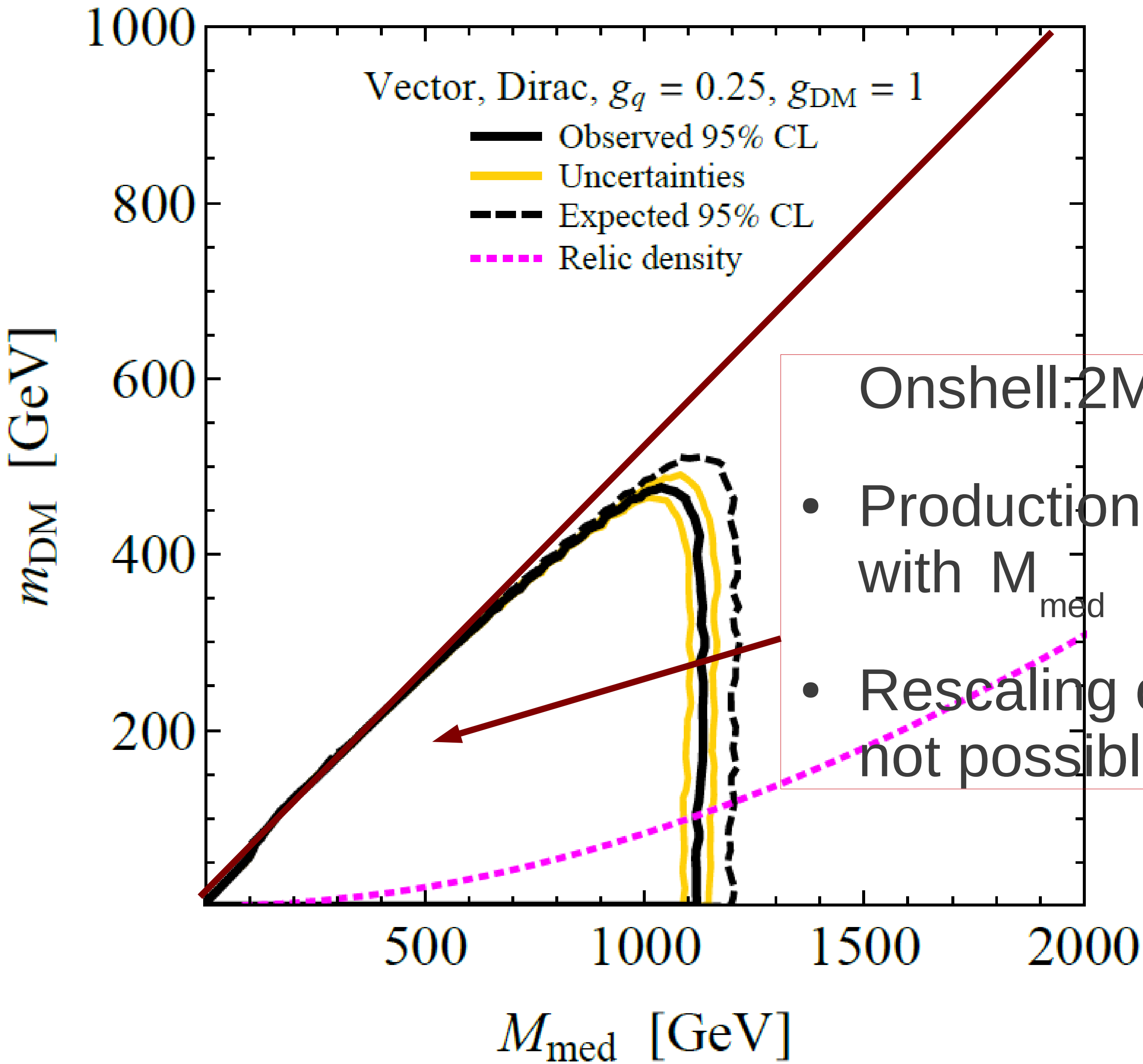

M_{DM}-M_{med} plane

Onshell: $2M_{DM} < M_{med}$

- Production rate of med. Falls with M_{med}
- Rescaling of limit with coupling not possible

LHC results presentation

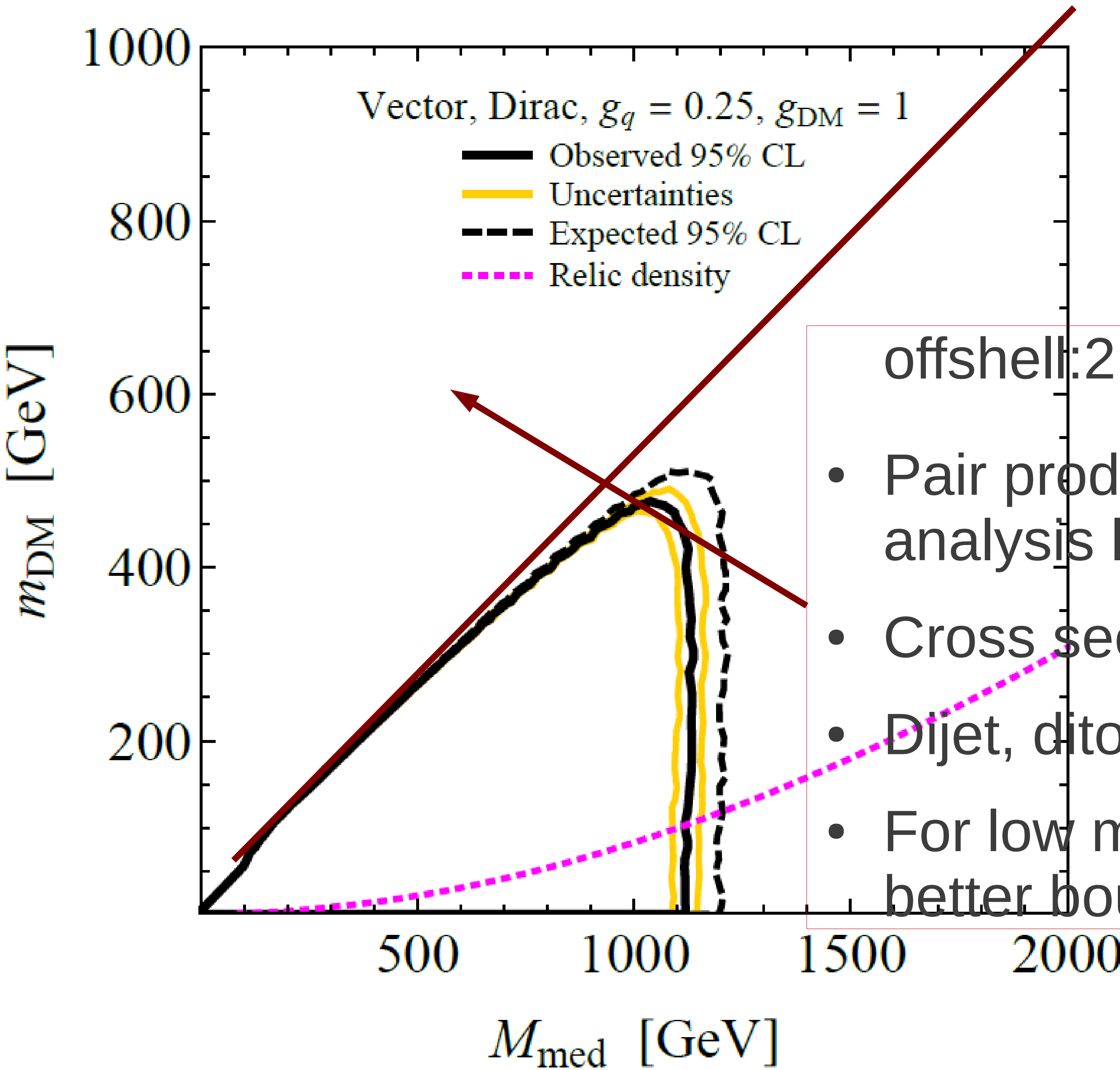

M_{DM}-M_{med} plane

offshell:$2M_{DM}$>M_{med}

- Pair production turns off, MET analysis loses power.
- Cross section ~ $g_q^2 \, g_{DM}^2$
- Dijet, ditop searches
- For low med mass DD, ID give better bounds

LHC results presentation

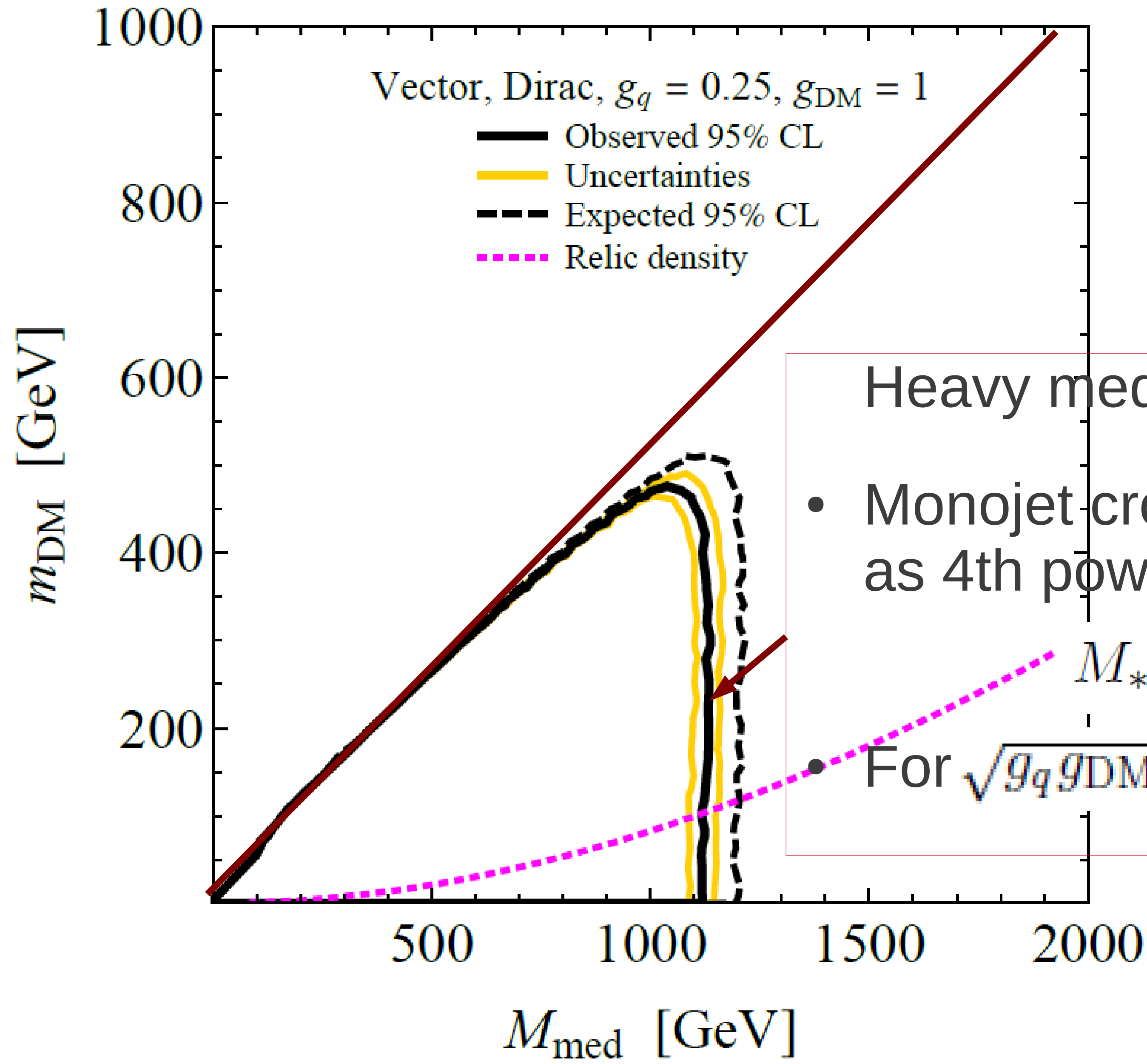

M_{DM}-M_{med} plane

Heavy mediator: M_{med} large

- Monojet cross section falls off as 4th power of

$$M_* = M_{med}/\sqrt{g_q g_{DM}}$$

- For $\sqrt{g_q g_{DM}} \ll 4\pi$ EFT applies

Direct detection: Rescaling

- Collider searches simplified model - relic density calculation changes in mass-mass plane
- DD – assumes relic density from one species saturates the cosmological density
- In case of multiple species rescaling of DD results needed to compare with mass-mass plots from LHC – not recommended.

Direct detection: Rescaling

- Collider searches simplified model - relic density calculation changes in mass-mass plane
- DD – assumes relic density from one species saturates the cosmological density
- In case of multiple species rescaling of DD results needed to compare with mass-mass plots from LHC – not recommended by LHC DM WG.

Mono Higgs

Indirect detection

AMS